UNIVERSITÀ DEGLI STUDI DI UDINE

Beyond necroptosis: alternative pathways in necrotic cell death

PhD student: Andrea Tomasella

Cellular Biology section

Department of Medical and Biological Sciences

University of Udine

PhD course in Biomedical and Biotechnological Sciences

XXVI cycle

Supervisor: Professor Claudio Brancolini

Dedicata a:

quel bimbo che sogna di volare.

Indossa le sue ali di cartone, il cappello e gli occhiali da aviatore

e inizia correre in un campo di grano.

Il vento soffia sul suo viso, ma non è quello che lo sostiene e lui lo sa.

La sua forza risiede in quegli sguardi rivolti verso il cielo,

negli occhi di coloro cha sanno che lui ci riuscirà.

Da lassù....lui dedicherà e regalerà il suo sorriso a tutti loro.

Table of contents

Abstract

Regulation of the necrotic cell death is a highly debated issue and several questions are still open about mechanisms, genes and pathways involved. The aim of this PhD thesis was to explore the necrotic response by comparing two different stimuli: DMNQ, a generator of oxidative stress, and G5, an isopeptidases inhibitor and inducer of alterations in cell adhesion and of actin cytoskeleton. We took advantage of U87MG glioblastoma cells expressing Bcl-xL, as model of human cells that die through necrosis. Our results show that necrosis can be governed by completely different signaling pathways. DMNQ necrotic cell death relies on the RIP1 kinase activity, whereas G5-necrosis is RIP1-independent. Mitochondria play crucial role in energy metabolism and cell survival; furthermore alterations in mitochondrial bio-energetic activity and morphology have been observed during necrosis. Analysis of mitochondrial fragmentation in U87MG cells revealed that both necrotic insults triggered mitochondrial fragmentation. This fragmentation was not accompanied by MOMP, as verified by Smac release. G5 mitochondrial fragmentation occurred before the appearance of cytoplasmic vacuolization, thus representing an early marker of the necrotic response. To understand the role of mitochondrial fragmentation, we used Mdivi-1, an inhibitor of the mitochondrial fission protein Drp-1. Drp-1 inhibition reduced the necrotic death induced by DMNQ, but was unable to counteract the necrotic effect of G5. In fact, U87MG/Bcl-xL cells overexpressing the dominant negative mutant (K38A) of Drp1 showed that only DMNQ necrotic effect depends on Drp1 activity. Moreover, the inhibition of RIP1, using necrostatin-1, demonstrated that two distinct necrotic pathways were activated by DMNQ and G5. Indeed, Nec-1 efficiently rescued only DMNQ-induced cell death. To gain insight into necrotic effect elicited by G5, we analyzed different stress or pro-survival signaling pathways. p38, ERKs and Akt were transiently activated but only Akt dephosphorylation status was paired with the necrotic outcome. Next, we simultaneously evaluated PP2A, which can dephosphorylate and inactivate Akt. Interestingly, we showed an increase of its catalytic subunit amount and of its activity in response to G5. This led us to identify PP2A as a regulator of necrotic cell death. In fact, siRNA mediated down-regulation of PP2Ac reduced G5 cell death while increased DMNQ necrotic effect. Necrotic response induced by G5 provoked a re-localization of PP2Ac, with a reduced nuclear localization and increased cytoplasmatic shuttling. This was paired with the release of HMGB1 from the nucleus, a well-established necrotic marker. Finally, we investigated the link between the dramatic reorganization of the actin cytoskeleton induced by G5 and a possible role of PP2A in this context. For this purpose, we used U87MG/Bcl-xL cells overexpressing phospho mutants of cofilin, an actin de-polymerizing protein substrate of PP2A. Our results demonstrated that phosho-mimetic mutant (S3D) of cofilin slightly decreased G5 induced cell death, so defining a connection in this necrotic mechanism. In conclusion, these results describe alternative necrotic program beyond the actually well defined “programmed necrosis” (necroptoptic) pathways. DMNQ necrotic cell death is dependent on the canonical necroptotic elements while G5 relies on different players. We finally proved for the first time a connection between PP2A, actin cytoskeleton remodeling and necrotic outcome.

Theoretical Background

Programmed cell death: evolution of the concept over the time

*"**Nascimur uno modo, multis morimu: "in one way we are born, in many ways we die",** and certainly there is not a unique form of programmed cell death (adapted from [1])*. This field of research gave rise to a great implementation of knowledge about cellular demise. "Apoptosis: the programmed form of cell death": this concept has been the groundbreaking and most defined sentence, between 1970 and 1990s [2]. The notion of apoptosis, as the tightly organized mechanism evolved to govern development and homeostasis of the multi-cellular organisms, is still one of the milestone of the biological research [3]. Since the beginning, the role of apoptosis has been clearly associated with disease especially with cancer progression and chemoresistance [3-5].

However, the surprise was at least comparable when knockout mice models of fundamental apoptotic players revealed no overall deficit in the development [6], raising the question: is this the unique mode of programmed cell death? In other words, has the evolution ensured other backup systems for tissue homeostasis? From this starting point, researchers began to define and characterize alternative physiological and pathological mechanisms of cell death, revisiting the concept of programmed cell death as the synonym of apoptosis.

Surprisingly, the answer came from an uncontrollable and unwanted mechanism, with pro-inflammatory effects, not manageable and generally elicited by uncontrollable stress, which causes cell and tissue destruction: the necrotic cell death. Forty years ago necrosis was the term to describe all the types of cell death [7]. Nevertheless, today apoptotic cell death is the best-understood and characterized form of cellular demise while necrosis and, in particular, its regulated form still needs to be molecularly defined and physiologically elucidated. Actually, necrosis is considered a programmed type of cell death (PCD) [7, 8].

Programmed Cell Death: a concept for three main actors

PCD appears with multicellular organisms and can be defined as an ordered schedule of events aimed to drive the cellular demise. Many evidences demonstrated the importance of PCD in all tissues that compose an organism. Cell death is therefore one of the major tools of multi-cellular organisms to modulate tissue homeostasis through the lifespan. In other words, PCD is a key

instrument to manoeuvre development, to remove damaged cells and to protect against disease. At least tree forms of PCD have been characterized in eukaryotic cells: type I cell death, the apoptotic cell death; type II cell death, autophagy that can be considered both a form of survival response and a death outcome generally linked to nutrient deprivation; type III cell death known as *necrotic cell death* [8].

Apoptosis: the cellular suicide

The *groundbreaking* paper of Kerr, Currie and Wyllie [9] gave the first description of apoptosis as a regulated way to govern cell death. This work, published in a cancer journal, predicted immediately the fundamental role of cell death defects during tumorigenesis.

Apoptosis is a multi step and highly regulated mechanism, responsible for cell death during development but also in adult organisms, essential to regulate cell number and tissue homeostasis. Kerr described cells undergoing apoptotic cell death through specific and still accepted morphological features. Cell shrinkage, chromatin condensation and fragmentation of the organelles are hallmarks of this cell suicide. The generation of the apoptotic bodies is the goal of the process. Cell fragmentation facilitates the engulfment by macrophages and neighbouring cells, which ensures a death without tissue damage and without inflammatory response [2]. The molecular determinant sustaining this complex rearrangement of the cell's architecture is a class of cysteine proteases called caspases. Synthesized as zymogens and activated by proteolytical processing or assembling into multiproteins complexes, caspases are the effector enzymes, which dictate the dismantling of the cells. They are classified in *initiator* caspases and *executioner* caspases. *Initiators* mainly cleave and activate *executioner* caspases. The *executioners* process many different substrates destabilizing all cellular structures [2, 10]. Apoptosis is induced by different stimuli: DNA damage, ligand-receptor specific interactions, nutrient and growth factors deprivation, altered ions homeostasis, viral infections and various cellular stresses. Signalling events controlling apoptotic cell death can be distinguished in the extrinsic and intrinsic pathways.

Extrinsic apoptotic pathway

The extrinsic apoptotic pathway is engaged by extracellular signals, which are recognised and propagated by specific transmembrane receptors. Ligands such as FASL/CD95L, TNF-α, TNFSF10 (APO1/CD95/TRAIL) are well-characterized stimuli that bind their specific receptors and induce the formation of multiproteins complexes, which recruit and activate caspases (Fig. 1). The interaction

between the ligands and the receptors, which are trimerics, stabilizes the complex, favouring the aggregation of several ligand/receptor complexes. Engagement of *Death Receptors* guarantees the recruitment of adaptors proteins, such as FADD, which in turn recruit and aggregate several molecules of caspase-8 and caspase-10, thereby promoting their auto-processing and activation. This platform, called DISC (Death Inducing Signalling Complex), is the main player of extrinsic apoptotic pathway [11]. Regulatory mechanisms of extrinsic apoptosis have been characterized, such as the FLIP proteins, which compete for *initiator* caspases recruitment, or the expression of decoy receptors on plasma membrane, which do not transmit ligands death stimulus [11].

Noteworthy, the composition of DISC determines not only the apoptotic outcome but, based on the elements recruited, many different biological processes: such as NF-kB activation, pro-survival programs or non-apoptotic cell death [7, 12, 13].

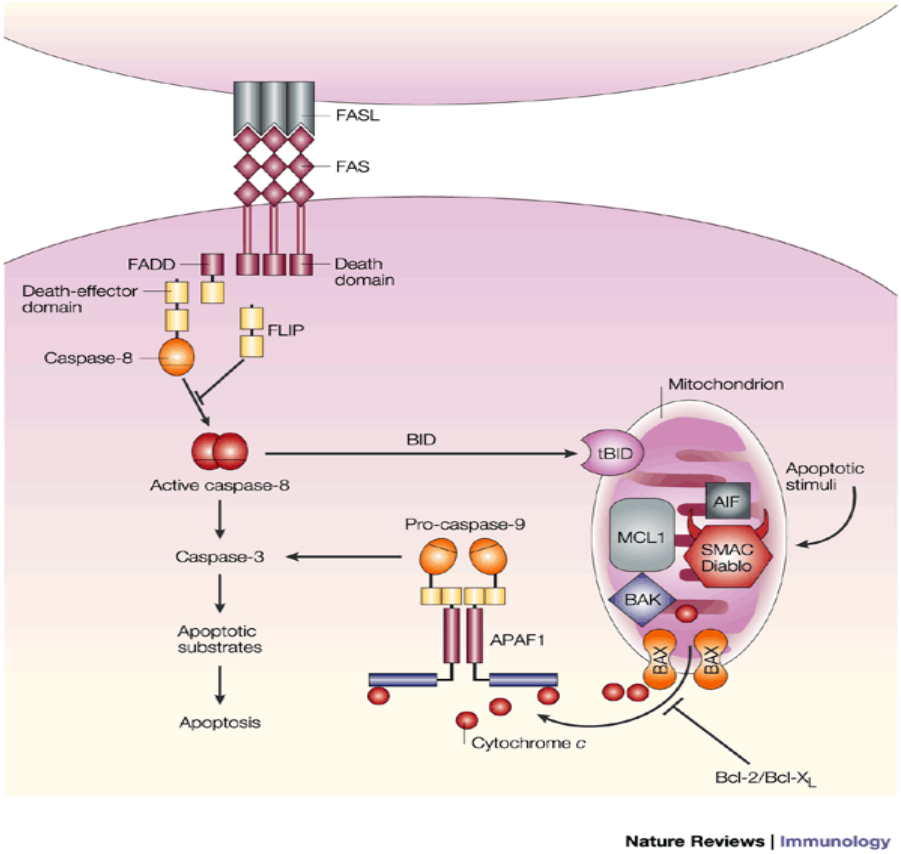

***Figure 1: Simplified representation of apoptotic process*.** Extrinsic and intrinsic apoptotic cell death are the two distinct but interconnected pathways activated in response to different stimuli that are involved in cellular suicide.

A short guide to the Intrinsic apoptotic pathway

The cellular demise could be dictated also by internal stimuli, which represent the self-control mechanisms to govern lifespan and tissue homeostasis. DNA damages, altered metabolism, organelles dysfunction, oxidative stress and intracellular pathogens activate specific pathways which trigger caspases activation [14] [2]. Intrinsic apoptotic process relies on the surveillance role elicited by mitochondria, whose integrity and functionality mirror the cell survival or cell death commitment. The maintenance of mitochondrial integrity and the choice between the survival/death fates are guaranteed by Bcl-2 family members, which operate at the mitochondrial outer membrane (MOM). Mitochondria control the compartmentalization of pro- and anti-apoptotic factors; while lethal signals alter MOM permeability favouring the release of such molecules in the cytoplasm, thus leading to the activation of *initiator* caspases. Members of the Bcl-2 family of proteins are the guardians of mitochondrial integrity and the modulators of the cell suicide. This family is divided into pro- and anti-apoptotic factors: the regulation of their mutual interactions dictate survival or commitment to apoptosis [15]. Anti-apoptotic Bcl-2 proteins contain four BH homology domains (BH1-4), localize generally to MOM and are named Bcl-2, Bcl-xL, Bcl-w, A1 and Mcl-1. Pro-apoptotic factors can be subdivided in *multidomains pro-apoptotic members,* containing BH1, BH2 and BH3 domains and *BH3-only* proteins. BAX and BAK belong to the first class and their property consists in the ability to oligomerize on the surface of the MOM, thus generating a channel that allows the release of mitochondrial pro-apoptotic factors into the cytoplasm. This process is defined MOM permeabilization (MOMP). On the other hand, BH3-only proteins are responsible for the binding of anti-apoptotic members in order to block their inhibitory effect on BAX and BAK. Certain BH3-only members can also interact with Bax and Bak to promote their oligomerization. The final event of intrinsic pathway is the translocation into the cytosol of pro-apoptotic factors such as cytochrome C and SMAC/Diablo, with the subsequent activation of caspases. MOMP is considered the *point of no return* in the apoptotic process: it leads to the formation of the *apoptosome*, a multiproteins complex composed by APAF-1, caspase-9 and cytochrome C. Concomitantly, the release of SMAC/Diablo removes the block performed by caspases inhibitors (IAPs). MOMP often coincides with mitochondria fragmentation, underscoring the tight relationship between Bcl-2 family and the dynamics of this organelle. However BAX and BAK can promote mitochondrial fission without MOMP execution, especially in presence of Bcl-xL antagonistic activity [16].

Necrosis: not a merely accidental cell death

In 1971, Kerr defined the morphological aspects of an unusual form of cell death which he called "shrinkage necrosis" [3], without any further characterization. However, this type of cell death has been renamed apoptosis. Consequently, the term necrosis has been used to describe pathological and unregulated forms of cell death. Since that moment, necrosis remained the less defined type of cell death. Until recent years, it was restrained as a merely outcome of excessive stress or physico-chemical injuries and therefore defined as uncontrolled and purely accidental process [7]. Although the description of necrosis evolved during the last decade, acquiring also precise morphological features, its experimental definition still begin with the exclusion of the apoptotic features. The involvement of caspases remains the first and the principal read-out to distinguish between Type I and Type III cell death.

Morphological representation

Morphologically, a necrotic cell is defined by cellular and organelle swelling, translucent cytoplasm and membrane rupture with cytoplasmic content leakage in the extracellular *milieu* (Fig. 2B). All these features perfectly depicted a cellular explosion; however, this phenomenon is not always uncontrolled and not merely accidental. Necrosis can rely on a complex network of interconnected players involving several signalling pathways and different organelles (Fig. 8).

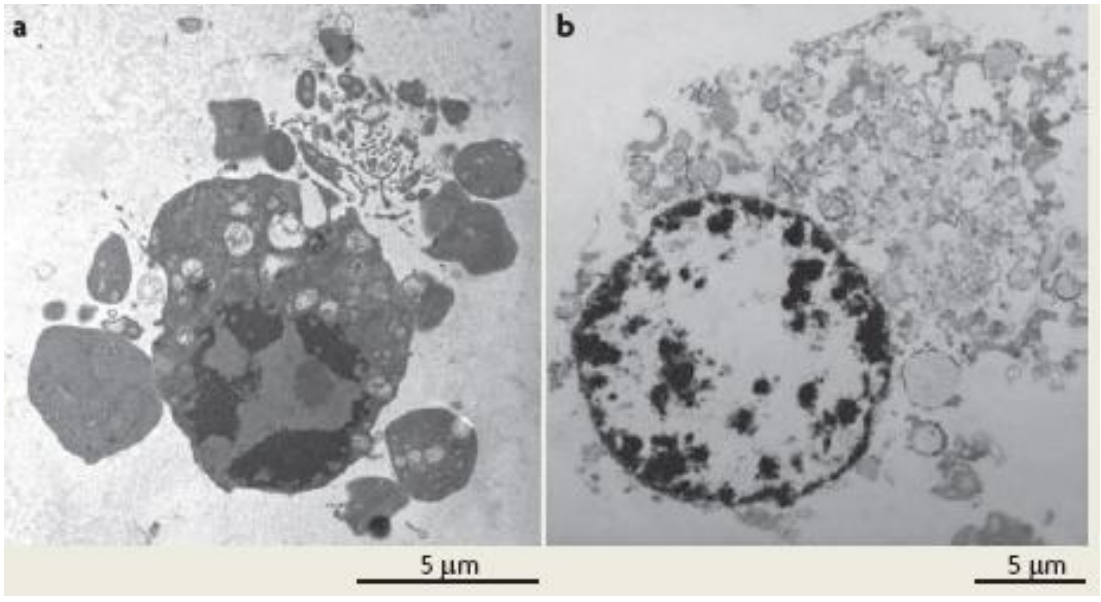

***Figure 2: Morphological features that distinguish apoptotosis and necrosis*.** Electron microscopy picture, on the left (part a) apoptotic cell: cell shrinkage and condensation with formation of apoptotic bodies; on the right (part b) necrotic cell: swelling of the cell and organelles, with plasma membrane permeabilization

and condensation of nuclear membrane with chromatin condensation in defined patches. Adapted from [7].

The "roots" of necrosis as PCD: reasons for investigation

Chautan and colleagues in 1999 [6], for the first time showed that a non-apoptotic cell death can ensure a correct organism development, a backup system when apoptosis is deficient. Indeed, using Hammertoe mutant, or mice homozygous for a mutation in the gene encoding APAF-1, interdigital cell death still occurred. This cell death was negative for the terminal-deoxynucleotidyl-mediated dUTP nick end-labelling (TUNEL) assay and there was no overall cell condensation. The electron microscopy analysis revealed typical signs of classical necrotic cell death, such as no cell condensation, chromatin alterations and marked mitochondrial and membrane lesions. Thus, in this developmental context, although caspase activity confers cell death with an apoptotic phenotype, a caspase-independent mechanism can also ensure cell death, but with a necrotic phenotype. Another groundbreaking step in necrosis was the discovery of necrostatins, as inhibitors of non-apoptotic cell death elicited under specific circumstances by TNF-α stimulation or *in vivo* using brain ischemic models [17-19]. After these evidences, many other scientific reports confirmed physiological roles of necrosis in intestinal shaping [20], longitudinal bones formation [21], as well as the pathological consequences of its alteration. Activation or dysfunction of necrotic processes have been documented in ischemia-reperfusion injury [19], neurodegenerative disease [22], myopaties [23], in response to pathogen infection [24] and in cancer [25]. The identification of the molecular players, which are involved in the transduction of necrotic signals fostered new interest in the comprehension of this form of cell death.

Summarizing, two main aspects justify the study of the necrotic cell death:

1) ***The Novelty***. The discovery of the fundamental genes and regulators of necrotic cell death, forced people to consider it as a PCD, but many aspects of the mechanism are still obscures and only few elements of the necrotic signalling pathways have been identified [7, 8];

2) ***Clinical Applications.*** Failure of anti-cancer agents to induce apoptosis, due to acquired resistance, has driven the research toward the determination of the molecular mechanisms governing necrosis. The hope is to develop new drugs that can engage necrotic forms of cell death for alternative anticancer therapies. On the other hand, neurodegenerative disorders, ischemia-

reperfusion injuries and myopathies, are characterized for the excessive cell loss by necrosis. Hence, the development of anti-necrotic drugs could result in a clinical benefit [17, 18].

In 1995 [26], Majno and Jolis presented the image below (Fig.3), describing necrosis as a merely consequence and a secondary effect of cell death. They exactly wrote "*Necrosis should not be used to define a mode of cell death…..In other words cells die long time before any necrotic changes can be seen by light microscopy. To say cell death by necrosis implies that the cell dies when they become necrotic, which is patently untrue.*". Nowadays, in 2014, the concept of necrotic cell death has been totally revolutionized.

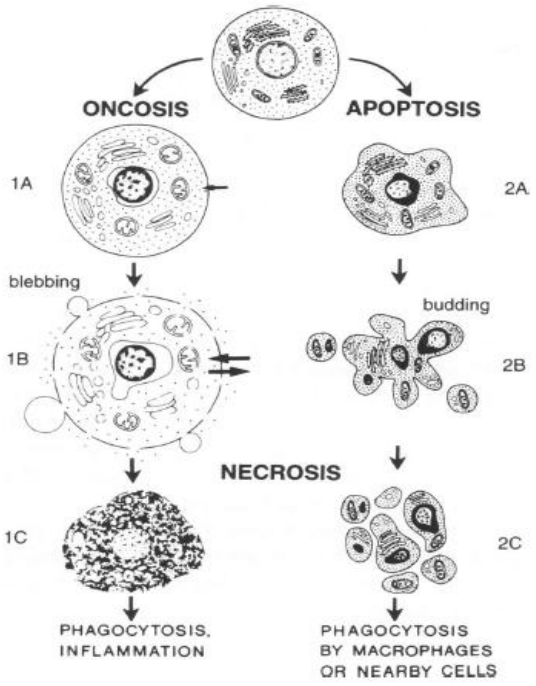

***Figure 3: The oversimplification of cell death concept in 1990s by Majno e Jolis*.**

In 2011, Welz, Zhang [27, 28] and Bonnet [29] separately gave three of the most convincing evidences of the role of the necrotic death in tissue development and homeostasis and highlighted an interconnection between the scaffold protein (FADD), fundamental in apoptosis, and a regulated form of necrosis. These evidences confirmed once more the fundamental role of two serine/threonine kinases during programmed necrosis (RIP1 and RIP3), as it will be described later. Zhang and Welz, separately described the relationship between RIP1 or RIP3 and FADD during

development and tissue homeostasis. FADD$^{-/-}$ embryos have elevated levels of RIP1 and exhibit massive necrosis, while RIP1 deletion in this model rescues embryonic lethality. Moreover, RIP3 has been defined as a key regulator of the necrotic demise in intestinal epithelial cells, underscoring a possible connection between necrosis and inflammatory bowel disease. Finally, Bonnet provided an *in vivo* demonstration that the regulation of programmed necrosis in keratinocytes represents a relevant mechanism to prevent chronic inflammation of the skin and to ensure an immune homeostasis. Indeed, mice with epidermis-specific FADD deficiency develop severe skin inflammation, with an important role of keratinocytes necrotic death (no evidences of caspase-3 activation). This work highlighted that the disease induced by FADD deficiency is provoked by necrotic cell death driven by RIP3, with the involvement of TNFR1 signalling pathway and the de-ubiquitinating activity of CYLD.

In table 1, the early classical signs of cell death in several models of necrosis are shown. Mitochondrial dysfunctions, such as ROS over-production, organelles swelling and peri-nuclear clustering, ATP depletion, altered Ca^{2+} homeostasis and finally activation of different proteases following lysosomal alteration [8], represent the multitude of effects elicited by necrotic insults.

Cells	Inducers	ROS in mitochondria	Swelling of mitochondria	ATP depletion	Cytoplasmic Ca^{2+} increase	Peri-nuclear clustering	Calpain required	Cathepsin required	Lysosomal alteration
L929	TNF	Yes	–	–	–	Yes	–	–	–
Primate neuronal cells	Ischemia	–	Yes	–	–	–	Yes	Yes	Yes
Rabbit kidney cells	AntimycinA	–	–	Yes	Yes	–	Yes	–	–
Human T cell lines	Anti-Fas and others	–	–	Yes		–	–	–	–
C. elegans neuronal cells	*mec-4*(*d*) and other mutants	–	–	–	Yes	–	Yes	Yes	Yes
Dictyostelium discoideum	Developmental signals in *atg*$^-$ mutants	Yes	Yes	Yes	–	Yes	–	–	–

Table 1. Models and morphological aspects analyzed to describe and identify different necrotic processes.

Receptor mediated necrosis: NECROPTOSIS as the first example of regulated necrosis.

Another milestone in the necrotic field was the discovery of the pathway linking death receptors stimulation to necrotic death. In the late 1990s, TNF-α was identified as both an apoptotic and necrotic inducer [13]. In fact, depending on the cell type, TNF-α was shown to kill the cells with an apoptotic or a necrotic phenotype. Subsequent studies demonstrated that other death receptors, such as CD95 [30], TNFR2 [31], TRAILR1 and TRAILR2 [32] can also transmit

necrotic stimuli. Since this mechanism shows a similarity with apoptosis, the term *necroptosis* was coined to describe the merging between the necrotic outcome and the regulated character of the process.

TNF-α is the most used stimulus to study necroptotic cell death. In different cell types, TNFR stimulation can directly cause a necrotic outcome, whereas stimulation of FAS, TRAILR1/2 requires caspases inhibition and the presence of caspase-8 adaptor protein FADD [30]. Fas ligand–induced caspase-independent death is absent in T cells that are deficient in either Fas-associated death domain (FADD) or RIP1; this type of cell death resembles necrotic death [30]. However, *in vivo* experiments performed demonstrated that FADD deletion provokes high epithelial cell necrosis [27, 29]. Such complex *scenario* highlights that the mechanism could differ depending on cell models and contexts.

Hence ligands stimulation induces the formation of multi protein complexes, whose specific composition determine either pro-survival response or cell death, but the mechanism by which this decision between is taken remained unknown till 10 years ago. The elucidation of the mechanism started with the description of the two-step nature of TNFR1 signalling. Ligand stimulation first promotes the formation complex I, a plasma membrane bound complex, which consists of TNFR1, the adaptor TRADD, the kinase RIP1, cIAPs and TRAF2 and leads to a rapid activation of NF-kB pathway. In a second step, TRADD and RIP1 associate with FADD, RIP3 and caspase-8, forming a cytoplasmic complex, complex II. The NF-kB signaling is activated through complex I, here the extrinsic apoptotic regulator $FLIP_L$ block the apoptotic induction by complex II. On the contrary, when the initial signal (via complex I, NF-kB) fails to be activated, using HT1080 fibrosarcoma cell line that is defective in NF-kB activation due to the expression of an proteosomal resistant I-kBα (an inhibitor of NF-kB), complex II ensures a checkpoint to provoke the cellular demise [33]. Moreover, the cytosolic complex II is considered a double edge sword that could determine both apoptotic and necrotic cell death. The platform called "*necrosome*" is essentially the complex II, but this machinery stimulates necroptosis and is dependent on RIP1/RIP3 (Receptor Interacting Kinase 1 and 3) activity, as will be described later.

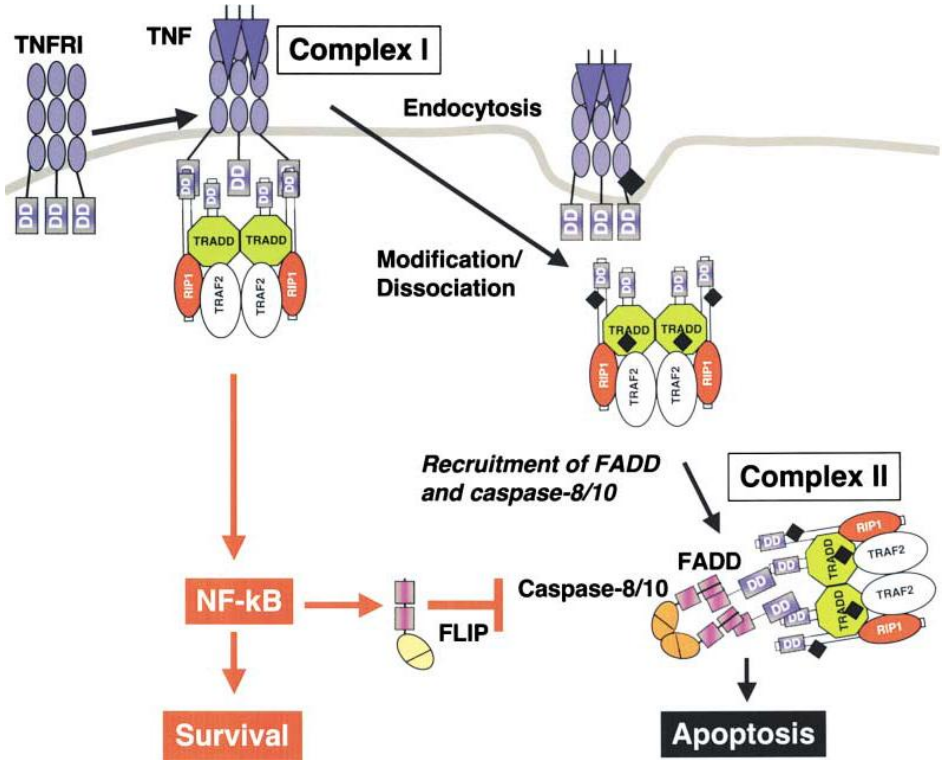

Figure 4. Life or death: the decision depend on complex I and complex II. Description of the dual step of TNFRI signaling pathway as model to understand the basis of programmed necrosis concept evolution [33].

Hence, TNFR1 can switch between different patterns of response, depending on the cell type, cell activation state and microenvironment factors. Complex I is highly regulated, in particular stability, post translational modifications and the kinase activity of RIP1 are strictly regulated depending on the context and on the stimuli. RIP1 Lys-63 poly-ubiquitylation is the fundamental step for the formation of the canonical platform for NF-kB activation (Fig. 5), cIAP1/2 promote RIP1 poly-ubiquitination permitting its interaction with the pro-survival kinase TAK1 [34] [35]. Transcription of cytoprotective genes mediated by NF-kB stimulates cell survival. However, the internalization of complex I, due to limited survival signalling stimulation, changes the composition of the platform and gives up to the formation of complex II [33, 36]. This complex regulates cell death by either apoptosis or necrosis (Fig. 4 and Fig. 5). Inhibition of cIAPs prevents RIP1 ubiquitylation and together with CYLD de-ubiquitinating activity favors the formation of complex II. This complex supports RIP1 association with caspase-8 and stimulates apoptosis. By contrast, when the apoptotic mode is down-regulated complex II triggers necrotic cell death [30, 31]. Nowadays, RIP1 and RIP3 are considered the necroptotic core and their mutual activity governs

the initial steps of programmed necrosis [37] (Fig. 5 and Fig. 6), while during apoptosis they result to be dispensable.

Other receptors can be engaged to trigger necrosis. Two examples are lymphotoxin-β receptor (LTβR) and TWEAK. LTβR induces a caspases independent cell death that requires the kinase activity of ASK1 (Fig. 9). The mechanism is based on the recruitment of TRAF5 and TRAF3, the activation of ASK1 and finally the ROS-mediated, caspase-3 independent cell death [38]. This mechanism can involve RIP1, as it works upstream to ASK1. In the case of TWEAK the necrotic response may be due to an endogenous TNF production; although the mechanism is not so clear, it may rely on RIP1-FADD-caspase-8 complex in presence of caspases inhibition [7].

Necrosome or Ripoptosome: platforms for regulated necrosis

At the moment of the formation of complex II, caspase activity is the determinant of the subsequent mode of cellular demise. Caspase-8 activation leads to apoptotic cell death and, at the same time, to RIP1 and RIP3 cleavage thus abolishing their kinase activity required during necrosis [39, 40]. The caspase cleavage sites are Asp324 and Asp328 residues of RIP1 and RIP3 respectively [39]. On the contrary, without caspase activation, RIP1 and RIP3 kinases trigger multiple downstream effectors provoking necrotic cell death. When caspase activity is blocked, complex II is also called *necrosome* to underscore its pro-necrotic activity.

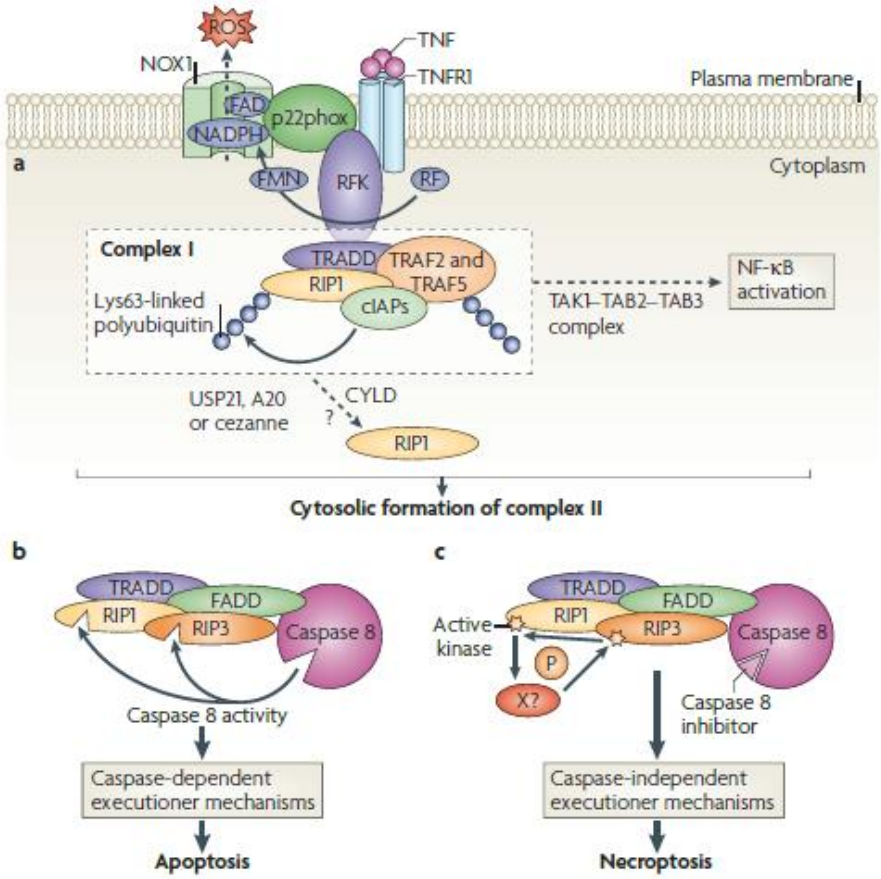

Figure 5: Molecular platforms that govern distinctly apoptotic or necroptotic cascade upon receptor stimulation. The composition of the cytoplasmic structure and the activation of caspases are the determinants of cell demise. RIP1 and RIP3 are considered fundamental actors of the pathway [7].

The K63 polyubiquitination of RIP1 is fundamental to regulate the transition from complex I to complex II; this post-translational modification is carried out by the action of the E3-ligases cIAP1 and cIAP2 (inhibitors of apoptosis proteins) [34, 41]. Deubiquitylating enzymes CYLD and A20 counteract the action of cIPA1 and cIAP2. This process is clearly demonstrated in response to receptors stimulation [34, 42, 43]. The down-regulation of IAPs with Smac mimetics causes the spontaneous formation of a cytosolic complex also in the absence of receptors stimulation [44]: this complex is named "*ripoptosome*" [41] [44], of which RIP1-FADD-caspase 8 are the core elements, and is able to induce either apoptotic or necrotic cell death in different cell lines. The *ripoptosome* activity is determined also by the two isoforms of FLIP. $FLIP_L$ prevents complex formation while $FLIP_S$ promotes its aggregation [41]. Tenev and colleagues demonstrated the

requirement of RIP1 kinase activity in this context, essential to regulate the formation of the *ripoptosome*.

RIP1/RIP3: the blues brothers of necroptosis

In 2000 and 2009 Holler, He and Cho, respectively identified RIP1 and RIP3 as essential modulators of necroptosis, in different cellular models. These proteins are members of Receptor Interacting Protein (RIP) kinases: a family of seven members, all of which contain a kinase domain (KD). RIP1 is composed by N-terminal KD, an intermediate domain containing a RHIM domain that permits the interaction with RIP3 and a C-terminal DD important for the binding with several death receptors [45]. $RIP1^{-/-}$ mice display extensive apoptosis and die 1-3 after birth, while $RIP1^{-/-}$ cultured cells are highly sensitive to TNF-induced cell death, possibly due to limited NF-kB pro-survival pathway activation [46]. However, RIP1 has been identified as a crucial element during FAS-L, TRAIL and TNF induced necrotic cell death in Jurkat cells [30]; this study demonstrated for the first time that the kinase activity of RIP1 is required to activate necrosis in these cells. Moreover, this protein has emerged as a strategic regulator over multiple cellular pathways of inflammation and cell death [47]. In 2005, Degterev and colleagues demonstrated the inhibition of necroptosis by the new small molecules Necrostatin-1 and they next characterized RIP1 as the molecular target of this drug [17, 18]. Recently, the crystal structure of necrostatin-1 and RIP1 has been solved, defining the molecular basis for the action of the anti-necrotic drug [48]. In particular, necrostatin-1 cages the kinase domain of RIP1 stabilizing the protein in an inactive conformation: Ser161 residue has been identified as the target site of drug activity. The identification of necrostatin-1 as a necroptotic inhibitor, was demonstrated by the selective inhibition of cell death in response to TNF-α, of two of the most characterized necrotic models (FADD-deficient Jurkat cells and in L929 murine fibrosarcoma cells). Moreover, Necrostatin-1 delays necrotic morphological appearance and hinders the onset of ischemic brain injury [17]. The allosteric inhibition of RIP1 was demonstrated by three necrostatins analogs which operated with distinct mechanisms [18].

Many cultured cell lines are protected against TNF-induced apoptosis by z-VAD treatment, whereas others undergo TNF-induced necroptosis [45]: RIP1 and RIP3 kinase activity has been implicated in this caspase-independent mode of cell death [40]. Mice lacking RIP3 do not exhibit defects in development, NF-κB activation or apoptosis [49]. FADD-deficient Jurkat cells were used

as necrotic model to identify regulators of necroptosis. A small interfering RNA (siRNA) screening permitted the discovery of RIP3 as a necrotic player that specifically turn on the RIP1 kinase activity [37]. In this study, RIP3 is defined as member of complex II upon necrosis induction. Moreover, RIP3 is shown to control ROS production and results to be important in response to virus-induced cell death. RIP3 has been also described as the essential energy metabolism regulator that switches TNF-induced cell death from apoptosis to necrosis. Zhang and colleagues used NIH-3T3 cells as model to discover the role of RIP3 during necroptosis. Although NIH-3T3 cells (termed A cells) usually undergo apoptosis upon TNF-α stimulation, a caspase-independent cell death is described in a particular NIH-3T3 clone, called N cells. RIP3 expression is detectable only in N cells and its down-regulation abrogates cell death in response to necrotic stimuli [50]. Reintroduction of RIP3, but not its catalytically inactive mutant, in NIH-3T3/A cells sensitizes them to necrotic cell death. Additionally, this work defined RIP1- and RIP3-requirement for TNF-α induced necrosis; indeed, RIP1 expression alone causes a caspase-dependent cell death but the concomitant expression of RIP3 redirects cell death toward necrosis.

The correlation between expression level of RIP3 and propensity to undergo necrosis was demonstrated by He et al in 2009 using a large panel of cell lines [24]. This work demonstrated the perfect match between RIP3 protein expression levels and sensitivity to necrotic cell death.

Cho and colleagues demonstrated that RIP1 and the RIP3 phosphorylation drive the stabilization of *necrosome* complex. They described that upon TNF-α/z-VAD stimulation, RIP3 is recruited at the necrosome, where it controls the binding of RIP1 to the complex and sustains RIP1-dependent pro-necrotic kinase activity. Jurkat cells overexpressing TNFR2 [32] or MEF cells require the phosphorylation of both kinases to enter necrosis. The oligomerization of RIP1 and RIP3, through the RHIM (RIP homotypic interaction motif) domain, seems to be fundamental in this *scenario* [37]. An interesting work published in 2012, reported that the RHIMs of RIP1 and RIP3 mediate the assembly of heterodimeric filamentous structures, which exhibit the classical features of β-amyloid fibrils [51]. Different experimental approaches defined these ultrastable structures and demonstrated that the mutation of RHIM domains compromise their formation with a consequent reduced kinase activity of the complex and reduced necrotic cell death *in vivo*.

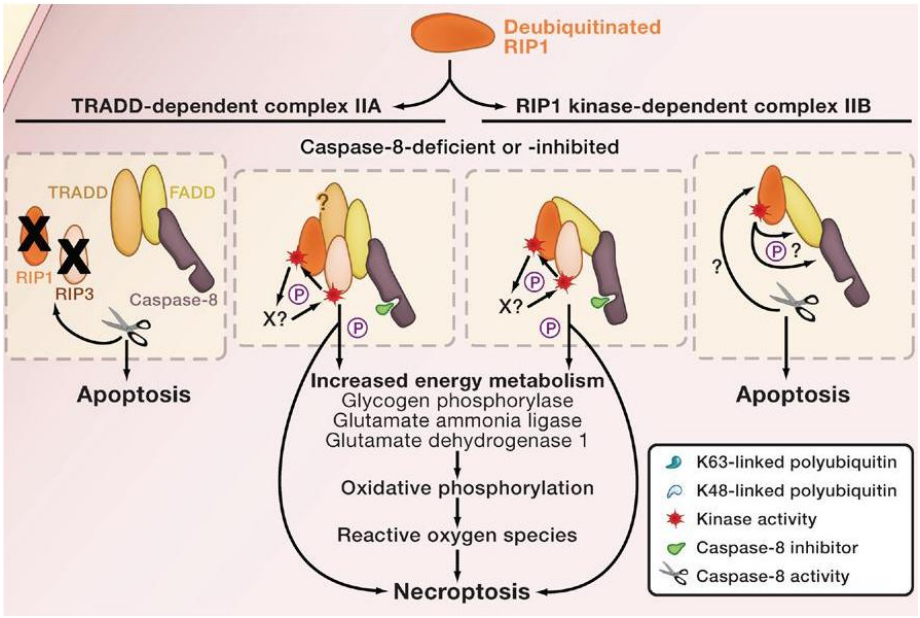

Figure 6. RIP Kinases at the crossroads of cell death. Representation of RIP1 and RIP3 mechanism of action, with their involvement in apoptosis or necrosis. Adapted from [46].

Recently, also the mutual dependency between RIP1/RIP3 in triggering necrotic cell death has been questioned. In specific context, the process could be dictated by only one of the two elements [50, 52]. RIP1-independent but RIP3-dependent necrotic cell death has been described and characterized in response to viral infection [50, 52, 53]. MCMV (Mouse cytomegalovirus) encodes for the structural proteins viral Inhibitor of RIP Activation (vIRA), which has the ability to interact with RIP1 and RIP3 inhibiting necrosome-induced cell death. Mutant forms of vIRA in its RHIM domain show less viral replication and reduced viral pathogenesis. Upton *et al*. demonstrated that vIRA suppresses TNF-α RIP1-RIP3 dependent necroptosis as well as RIP3-dependent but RIP1-independent viral induced necrosis [52]. Furthermore, in condition of RIP1 and caspase-8 or TRADD down-regulation, TNF-α induces a RIP3-dependent necrotic cell death in L929 murine fibrosarcoma cells. Finally, the overexpression of a catalytically active RIP3 has been associated with necrotic ethanol-induced liver injury liver: inhibition of RIP1 does not affect cell death while RIP3 lacking mice are protected [54], underscoring a not absolute requirement of RIP1. Moreover, RIP3 has been identified as the molecular switch between apoptosis and necrosis; cells with high expression of RIP3 reflect the predisposition for necrotic response and apoptosis resistance and *vice versa* [50]. Interestingly, RIP3 is the determinant of embryonic lethality of

caspase-8$^{-/-}$ mice [55]: caspase-8$^{-/-}$ RIP3$^{-/-}$ mice develop normally with a complete formation of the immune compartment. This study defined the mandatory role of RIP3 together with caspase-8 for a correct mammalian development. Oberst attributed the deleterious phenotype of caspase-8 knock-out to RIP3-mediated necrosis; indeed, RIP3 ablation rescues this dramatic effect [56]. In this condition, the intriguing ability of caspase-8/FLIP eterodimer to block RIP3 necrotic cell death without promoting apoptosis has been determined. All these results explain the dependency of regulated necrosis on RIP1 and RIP3, but still little is known about alternative regulated necrotic pathways.

Many evidences highlight the involvement of RIP1 and RIP3 in different pathological conditions with experimental observations using *in vivo* models. For example, recent publications evoke a role of RIP3 in atherosclerosis development [57] and in Gaucher's disease [58]. The generation of atherosclerosis prone mice deficient for RIP3, Ldlr$^{-/-}$ RIP3$^{-/-}$ and Apoe$^{-/-}$ RIP3$^{-/-}$, linked advanced atherosclerotic lesions to RIP3-dependent necrotic cell death of macrophages recruited to the plaques, thus leading to inflammation and atherogenic progression. Furthermore, Vitner and colleagues demonstrated that RIP3 represents a reliable therapeutic target in Gaucher's disease (GD). Caused by mutations in the glucocerebrosidase gene (*GBA*), GD is the most common lysosomal storage disease: loss of neuronal cells is one of the manifestations of the alteration but the mode of death was unknown. Vitner's work defined RIP1 and RIP3 involvement in GD pathological events. They demonstrated an augmented expression of RIP3 in microglia of *Gba*$^{flox/flox}$ nestin-Cre mice, which goes in parallel with the appearance of cell death. Furthermore, RIP3 deficiency reduces the pathological injuries. RIP1 has been recently demonstrated being the critical mediator of Motor Neuron death both in familiar and sporadic models of amyotrophic lateral sclerosis (ALS) [59]. The authors use a coculture of human adult primary sporadic ALS (sALS) astrocytes and human embryonic stem-cell-derived MNs (Motor Neurons) to demonstrate that the loss of MNs was due to necroptotic process. sALS astrocytes specifically kill human ES-MNs and this mechanism of programmed necrosis is governed by RIP1; in fact, its down-regulation or inhibition with Nec-1 reduces neuronal loss. Moreover, the specific inhibition of MLKL, a downstream target of RIP1, reduces by 90% the toxicity of sALS astrocytes for hES-MNs.

Downstream effectors in necroptosis: just the tip of the iceberg

Recently, a growing number of reports have identified multiple effectors of the necroptosis. In 2012, two papers demonstrated the involvement of MLKL (mixed lineage kinase domain like protein) and PGAM5 (phosho glycerate mutase 5) in necrosis. Sun and colleagues identified NSA (called Necrosulfonamide) as a potent inhibitor of necroptosis [60]. Both an affinity probe derived from Necrosulfonamide and co-immunoprecipitation using anti-RIP3 antibodies permitted to identify MLKL as target downstream RIP3 activation in programmed necrosis. These experiments show the involvement of MLKL as an essential target of *necrosome* and characterize threonine 357 and serine 358 human residues as target residues of RIP3 activity. NSA treatment or siRNA-mediated MLKL down-regulation blocks necroptosis at a precise step with the formation of discrete RIP3 punctae. MLKL is a dead kinase closely related to mixed lineage kinases that function as MAPKKs; deficient mice develop normally without any haematological alteration or pathologies but, interestingly, cells derived from them resulted to be necrotic resistant [61]. Phosphorylation-driven structural changes of its pseudoactive site determine a RIP3-independent necrotic pathway in HeLa cells, in particular K219 and Q343A residues of murine polypeptide chain cause a conformational change within MLKL that mimics RIPK3-mediated activation of MLKL to induce spontaneous, RIPK3-independent necroptosis. Upon necrotic stimulation, MLKL is recruited to the necrosome complex. MLKL is essential for the formation and the activity of RIP1/RIP3 complex, towards the downstream substrates.

Necroptotic stimuli promote the trimerization of MLKL [62]. This work elucidates the molecular mechanism of necroptosis, defining the requirement of RIP1 and RIP3 for MLKL trimerization: in particular, the kinase activity of RIP3 is essential in this context. Finally, Cai *et al* demonstrated the plasma membrane translocation of the MLKL trimer, where it governs Ca^{2+} influx through the control of TRPM2 activity.

The study, published by Wang [63], proposed PGAM5 (a peculiar phosphoglycerate mutase functioning as Ser/Thr phosphatase [64]) as possible point of convergence for multiple necrotic stimuli [63]. The authors used Hela cells with an inducible expression of RIP3 (HeLa cells normally do not express RIP3); this system recapitulates other necrotic models, such as HT29 cells, where the high expression of RIP3 is considered the necrotic determinant. PGAM5 activity augments and results to be relevant during necrosis in response to different stimuli. Two PGAM5 isoforms,

PGAM5-L and PGAM5-S, have been identified as downstream players of RIP3 kinase activity [63], both isoforms are also involved during necrosis provoked by ROS generators or calcium ionophore. Activation of this new key player directs insults to mitochondria, leading to Drp1 activation, Drp-1-mediated mitochondrial fragmentation (Fig. 7) and, finally, necrotic cell death. The de-phosphorylation of Drp1 by PGAM5 is proved *in vitro* in response to TNF-α/Smac mimetics/z-VAD; however, this work does not explain how mitochondrial fragmentation represents a crucial step during necrosis.

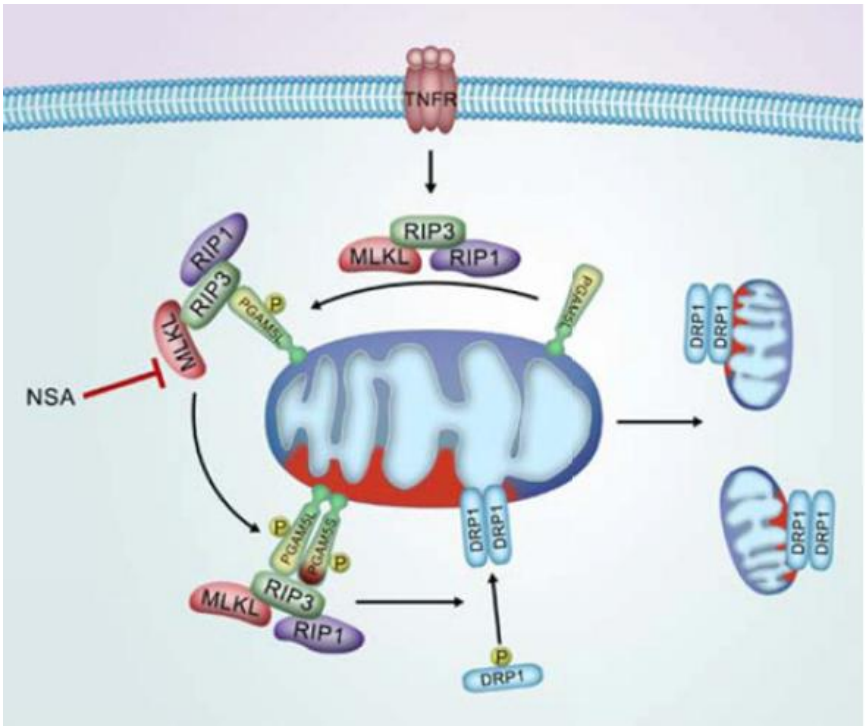

Figure 7. MLKL and PGAM5: two downstream effectors of necroptosis. Receptor mediated necrosis activates the necrosome and a conceivable mechanism of action could be the recruitment of PGAM5 and MLKL and mitochondrial fragmentation and dysfunction. Adapted from [63].

Other downstream effectors of necroptotosis are represented by alteration of metabolic function or energetic production. One of the main features that distinguishes apoptosis and necrosis is the dependence on ATP [65] [66]. In particular, energy depletion during type III cell death is caused by the effect on several biological processes. RIP1 has been associated with the induction of ROS both at mitochondrial and cytosolic level. In U937 cells, TNF-α/z-VAD-induced necrotic death revealed the role of RIP1 on ATP production. RIP1 reduces ANT (adenine nucleotide translocase) activity and interaction with CyPD (cyclophilin-D), resulting in ATP depletion,

energetic deficit and necrosis [67]. This phenomenon correlates with a transient increase in $\Delta\psi_m$ (mitochondrial transmembrane potential) during necrosis, observed in different experimental settings [66, 67]. This hypothesis links the necrotic machinery with the permeability transition pore complex (PTPC) (Fig. 8). The mitochondrial permeability transition is considered a key event both in apoptosis and necrosis, but considerably CyPD (a component of the PTPC) null cells die normally in response to different apoptotic stimuli; in addition, Bid- and Bax-induced cytochrome c release is not blocked by CyPD deficiency and does not affect many forms of apoptotic cell death. On the other side, the $CyPD^{-/-}$ cells result resistant to necrotic insults such as ROS and calcium overload [68]. Moreover, C57BL/6J $CyPD^{-/-}$ mice are more resistant against ischemia-reperfusion injury [68], a classical necrotic insult, with an increased tolerance to calcium increase (without loss of $\Delta\psi$) and resistance to ROS-induced damages. One interesting report by Xu *et al.* also identified the connection between RIP1 and JNK1 kinase, underscoring the importance of PARP-1-RIP1-JNK1 axis during necrosis in MEF cells. The proposed model implied over-activation of PARP1 by MNNG, which causes depletion of NAD^+ and ATP, activation of RIP1/TRAF2 complex and JNK1 phosphorylation and, finally, mitochondrial dysfunction. This cascade indeed alters MPT and triggers AIF release which, finally, provokes necrosis [69]. JNK phosphorylation during necroptosis is demonstrated also downstream MLKL activation, in response to TNF-α/Smac mimetics/z-VAD in HT29 cells, but the role of JNK-mediated ROS accumulation is not considered an absolute determinant of cell death [70]. Moreover, JNK1 activation is responsible for the degradation of ferritin and the increase of labile iron pool, thus causing oxidative stress and cytotoxicity (Fig.8). Another mechanism based on RIP3 activity evokes the alteration of metabolic functions through three possible targets such as PYGL (glycogen phosphorylase), GLUL (glutamate-ammonia ligase) and GLUD1 (glutamate dehydrogenase 1). Indeed, by activating key enzymes of metabolic pathways, RIP3 governs ROS generation in response to TNF-α, which contributes to cell death [50].

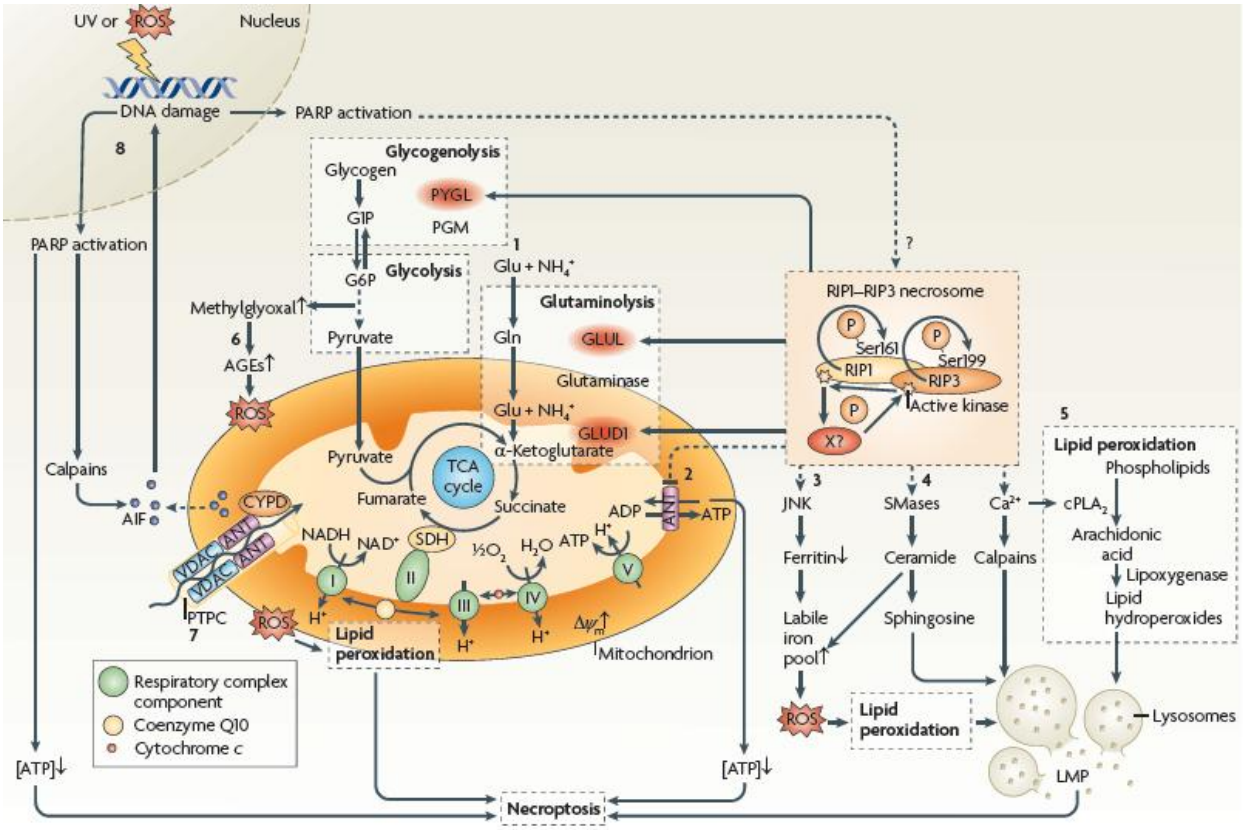

Figure 8: General representation of the pathways and of the key players involved in initiation, amplification and execution of necrosis. ROS, metabolism, necrosome formation and the involvement of mitochondria and lysosomes describe the interconnection and the different insults inducing type III cell death. From [7].

Virus- and pathogens-induced necrosis

Not only cytokines but also multiple viruses, such as HIV-1, HSV-1, WNV and MCMV, are able to induce necrotic cell death. Our knowledge is still in the infancy and different mechanisms have been proposed. Depending on virus type, RIP1 and/or RIP3 kinase activities have been considered fundamental in distinct experimental settings [37] and the polyubiquitylation of RIP1 induced by viral dsRNA is an obligated step during the process. One precise molecular characterization of the necrotic cell death is linked to M45 protein. This viral protein has a RHIM domain and is able to interact with RIP1 and RIP3, interfering with their activity. Indeed, virus mutated in this domain causes a RIP3 dependent necrosis [71]. All these evidences suggest an essential role of necrosome in inflammatory response to activate antiviral host defence [72]. Caspase 1 activation can trigger pyroptosis, a highly inflammatory form of programmed cell death in which dying cells release their

cytoplasmic contents, including inflammatory cytokines, into the extracellular space. Pyroptosis provokes the release of IL-1β, a highly inflammatory cytokine. Recently, pyroptosis has been identified as the main type of cell demise of CD4 T-cell during HIV-1 infection [73].

Pathogens-induced necrotic cell death has been identified but many questions are still opened on this topic. The current debate is about pyroptosis and necrosis as response to microbial infections. Pyronecrosis, the so called necrotic counterpart of pyroptosis, is independent of caspase-1 and caspase-11, but dependent on the inflammasome component ASC (apoptosis-associated speck-like protein containing a CARD) and the lysosomal protein CTSB (cathepsin B), and results in the secretion of the pro-inflammatory mediator HMGB1 (high mobility group box 1) [74, 75]. In some experimental models, ASC/NLRP3-dependent necrotic death is crucial to support the response against pulmonary infection and the release of pro-inflammatory molecules that can reduce mortality against K. Pneumonia [75] (Fig. 9). Other pathogens have been demonstrated to induce a similar form of cell death but the molecular characterization need to be deepened, in order to understand the involvement of inflammatory caspases, *necrosome* complex and cathepsins.

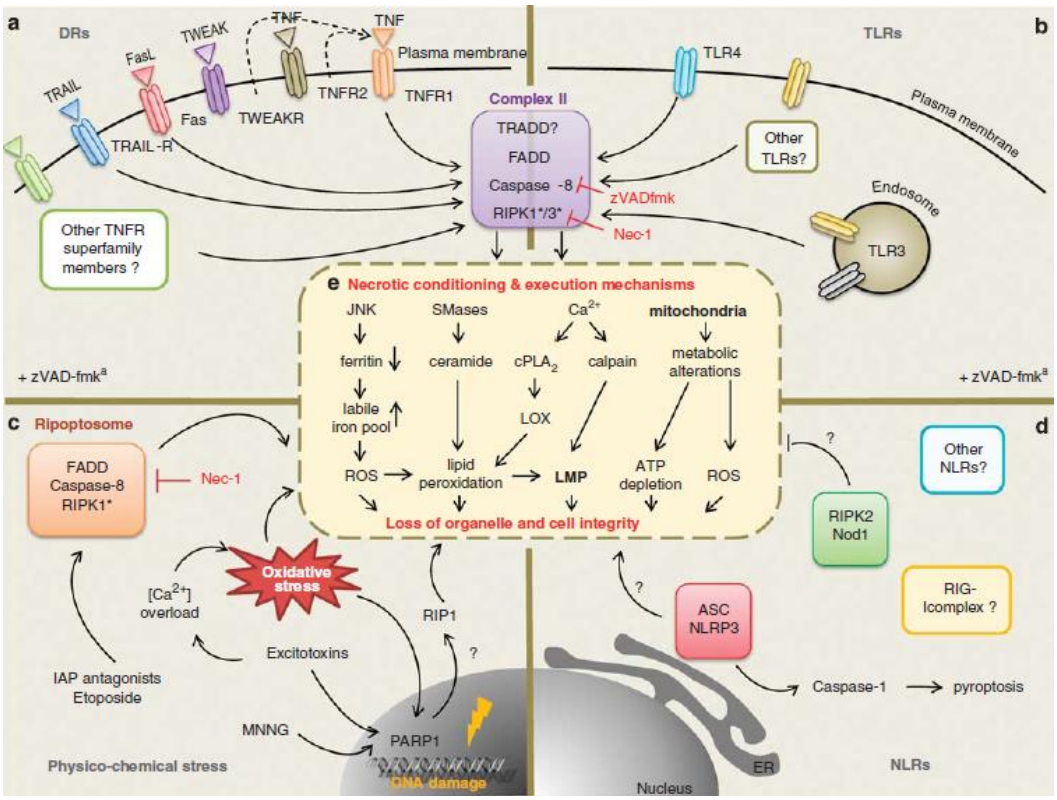

Figure 9: Internal and external stimuli that trigger necrotic cell death. The complex network involved in necrotic cell death. a, b, c and d boxes represent the initiator mechanism of necrosis while the central square depict the execution mechanism of necrosis. Adapted from [72].

Programmed necrosis: not only necroptosis

Other forms of regulated necrosis exist. As common determinant, they have been described to occur independently from RIPK1 or RIPK3, or in the presence of RIPK1 or RIPK3 inhibitors.

Mitochondria: the core of necrosis

Mitochondrial and ROS relevance in necrotic cell death

ROS and radicals can also be viewed as a second messengers. ROS could mediate many different responses in eukaryotic cells depending on the range of ROS production. The generation of radicals species is physiologic throughout cell life during energy supply; moreover, they are essential mediators of different processes from senescence, to proliferation and transcriptional activation of target genes, for example during the immune response [1].

On the other hand, in response to a plethora of stimuli, cell death appears to be mediated and determined by ROS damages and overproduction. The oxidative stress is not an immediate inducer

of cell death but the disequilibrium between production and detoxification at last provokes damage to proteins, DNA, and lipids causing profound alterations of cellular functions. The consequences are linked with inflammation, tumor promotion, ischemia/reperfusion injury (IRI) and neurodegeneration.

MPTP- and CyPD - dependent regulated necrosis

ROS generation is an important effector of necrotic cell death. ROS can induce lipid peroxidation or alter the function of different biological processes leading to necrotic cell injury [76]. TNF-α stimulation of L929 cells provokes *cytolysis* with the involvement of free radicals production but also the participation of arachidonate metabolism [77]. An early mitochondrial degeneration with alteration of mitochondrial electrons transfer chain is demonstrated to be responsible for cytolysis. Electron micrographs show the necrotic phenotype of L929 cells with specific mitochondrial swelling [78].

MPTP has been described as an important step during necroptosis but this phenomenon is tightly regulated also during necrosome-independent programmed necrosis. CyPD gained attention as regulator of this multiproteins complex [79] and for the demonstrated benefits elicited by its inhibition. Cyclosporine A or sanglifehrin A ameliorate necrosis during ischemia-reperfusion injury [80]. CyPD null mice require more calcium to force MPTP opening and MEF cells derived from these mice resulted to be protected against calcium release from endoplasmic reticulum or H_2O_2 treatment. Nakagawa and colleagues showed that CyPD deficiency does not block Bax- and Bak-induced mitochondrial permeability transition and apoptotic cell death, while lack of CyPD protects mice from ischemia-reperfusion necrotic damages in heart and kidney [68, 81]. The role of CyPD/PTP has been demonstrated to be critical during of brain injury in the adult, whereas Bax-dependent mechanisms prevail in the immature brain [82]. Hence, the function of CyPD shifts from pro-survival to a cell death mediator in immature and adult brain of mice respectively. Ca^{2+} and ROS are key mediators of IRI but CyPD-deficient mitochondria accumulate Ca^{2+} without losing $\Delta\psi$; moreover, hepatocytes result resistant to necrotic cell death stimulated by the Ca^{2+} ionophore A23187 or H_2O_2 [68]. On the other hand, overexpression of CyPD provokes cardiac mitochondrial swelling and spontaneous cell death *in vivo*. The mechanism relies again on the regulation MPTP opening [83] and on the decrease in ATP production [81] (Fig. 10). Additional roles of CyPD have been suggested by the identification of amyloid-β protein (Aβ) [84] and p53 [84] as two CyPD binding partners during neuronal and MEF Bak/$Bak^{-/-}$ cell death respectively [85].

The interaction between Aβ and CyPD augments mitochondrial dysfunction and neuronal stress, while CyPD-lacking mitochondria are protected from Aβ-induced cell death and an Alzheimer's disease mouse model deficient for CyPD shows better neurological performances. Implication of MPTP and CyPD in multiple sclerosis (MS) disease has been also demonstrated; indeed, neurons from CyPD-knockout mice are resistant to reactive oxygen and nitrogen species insults and brain mitochondria accumulate high levels of Ca^{2+} [86]. These results define CyPD and MPTP as therapeutical targets for neurodegenerative diseases. During oxidative stress-induced necrosis a rapid stabilization and translocation of p53 to mitochondria, where it interacts with CyPD and regulates MPTP opening, has been proposed [85].

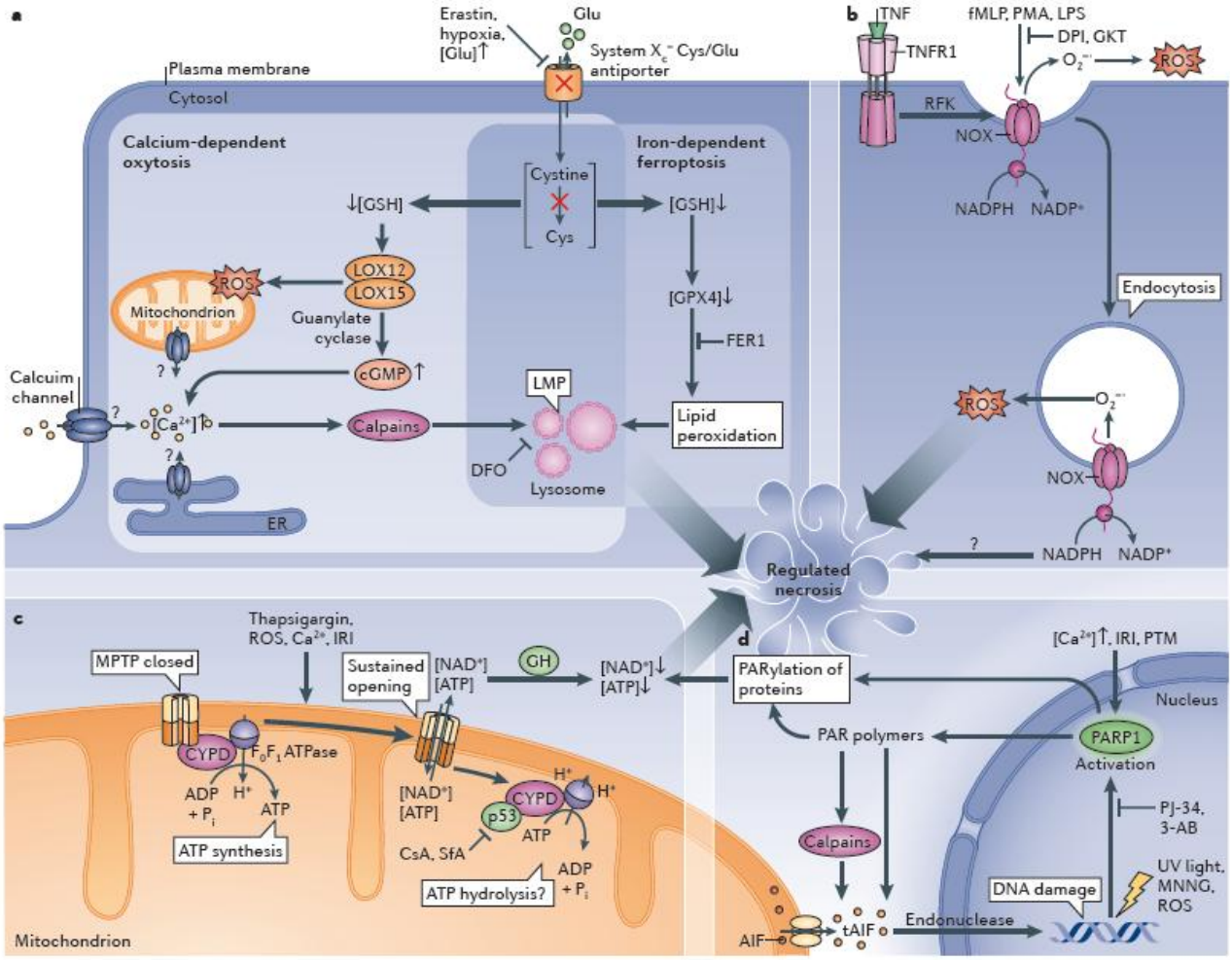

Figure 10. Regulated necrosis: necrosome-independent mechanisms. A) Ferroptosis/excitotoxicity. B) NOX-mediated ROS production and cell death. C) MPTP-regulated necrotic cell death D) Parthanatos: PARP1 programmed necrosis. Adapted from [87]

Parthanatos: PARP1 programmed necrosis

Genomic DNA damage, induced by UV, ROS inducers and alkylating agents (such as MNNG) [88, 89], activates PARPs proteins that transfer ADP-ribose groups from NAD^+ to their targets. In particular, PARP1 (poly (ADP-ribose) polymerase-1) regulates many biological processes through poly(ADP-ribosyl)ation (PARylation) to ensure cellular homeostasis; nevertheless, its overactivation provokes programmed necrosis, called also *parthanatos*. Oxidants provoke PARP-mediated mitochondrial perturbations, with depletion of NAD^+ and subsequently reduction of ATP levels. Necrotic death of thymocytes could be pharmacologically controlled for example with PARP inhibitors [90]; as described in U937, they prevent necrosis and activated apoptosis [91]. One mechanism of action has been proposed through the sequential action of PARP-1, calpain-4 and Bax, which finally provokes AIF translocation and necrotic cell death [89]. Subsequent to AIF release from mitochondria and re-localization to the nucleus, MEF cells undergo necrosis upon MNNG treatment. Calpains involvement has been questioned and they have different relevance in AIF release in different experimental settings [89, 92]. However, PARP-1/AIF response resembles a vicious circle with a continuous DNA damage and ROS production. Oxidative stress generated after IR or due to exposure to ROS inducers (i.e. H_2O_2) is dependent on PARP-1 activity to elicit necrotic cell death and consequently to the depletion of endogenous ATP [72]. Taken together, these observations define PARP-1 as one of the critical enzymes involved in necrosis and a molecular switch between type III and type I cell death. The overactivation of this protein depletes cellular energy resources, inhibiting glycolysis or indirectly destabilizing oxidative phosphorylation process. Consequently, ATP depletion limits ATP-dependent processes, i.e. caspases activation, promoting caspase-independent cell death. Cellular membranes represent important targets of ROS; lipids peroxidation provokes alteration of mitochondrial functionality, causing loss of barrier properties, compromising molecules compartmentalization and failure of Ca^{2+} buffering. In addition to mitochondria, ER and lysosomes are compromised by ROS with the consequent release of protease and ions in the cytosol.

The role of RIP1 is controversial. *In vivo* the pre-treatment with Nec-1 reduces IR tissue damage [17], but this effect was not confirmed *in vitro* in different cell lines [30, 66]. However, RIP1 and RIP3 have been reported to localize to the mitochondria and to target specific metabolic enzymes (PYGL, GLUL, GLUD1 as described above), supporting a direct link with metabolic impairment and

ROS production. Interestingly, ROS-driven necrosis is not fundamental in all cell lines models: scavengers do not protect U937 lymphoma, HT-29 and JURKAT from cell death [24, 67].

Ferroptosis and excitotoxicity

In a particular model of RAS-driven transformation, a new form of non-apoptotic cell death, which depends on intracellular iron metabolism and termed *ferroptosis,* has been revealed [93]. The characteristics of *ferroptosis* are different from a classical necrotic phenotype, with specific phenotypic, genetic and biochemical properties. Fenton reaction, the ferrous ion (Fe^{2+})-dependent decomposition of dihydrogen peroxide generating the highly reactive hydroxyl radical ($Fe^{2+} + H_2O_2 \rightarrow Fe^{3+} + OH^{\bullet} + OH^{-}$), is considered the mechanism, which leads to ROS generation and ferroptotic cell death. Erastin, the first identified small molecule inducer of ferroptosis, has been found to induce lethality in cells overexpressing oncogenic RAS. It provokes metabolic dysfunctions that stimulate the generation of cytosolic ROS, reacting with phospholipids at the PM, independent of mitochondria but dependent on NADPH oxidases (NOX) in some cellular contexts [93]. Erastin-induced ferroptosis is strongly suppressed by NOX inhibitors or inhibition of the NADPH-generating pentose phosphate pathway. This alternative non-apoptotic cell death, specifically inducible in transformed cells, might also be relevant during neurodegeneration. Recently, a wide screening identifies a second generation of ferroptotic inducers (II-FINs) and, at the same time, defines the determinants of this cell death. Certain II-FINs impact on GPX4 (Glutathione (GSH) peroxidase 4) function thus causing a depletion of Glutathione. As a consequence ROS are augmented and lipid peroxidation occurs, thus provoking cell death [94]. Taken together, these evidences describe GPX4 as a central regulator of ferroptosis: its down-modulation either by II-FINs or by RNAi-mediated knockdown induces cell death. A common mechanism of regulation of *ferroptosis,* as well as of H_2O_2 necrotic cell death, is iron chelation (i.e. deferoxamine (DFO)) [66] thus defining a possible mechanism of intervention for clinical purposes.

The use of animal models to study neurodegeneration shows that the large part of neuronal death resembles necrosis [95], [96]. Excitotoxicity, the cell death provoked by excessive stimulation by excitatory amino acids, is often recognized as cell loss mechanism during neurodegenerative disease. The inhibition of Xc-Cys/Glu antiporter system is observed also during this type of cell death. In this condition, ROS generation leads to an increase of the second messenger cGMP, which provokes the opening of Ca^{2+} channels allowing a massive influx of this

ion. Calpains activation and finally lysosomal membrane permeabilization determine the type of death [87].

Other sources of ROS can contribute to necrotic cell death, showing again the NOX involvement, as its localization at the plasma membrane links RIP1 and non-mitochondrial reactive species thus contributing to TNFR-mediated necrosis [97]. Results are still confusing, since NOX1 shuttles between cytoplasm and membrane but many evidences show its role in necrosis and also identify a possible amplification loop for ROS production with mitochondria [7]. A possible connection between ROS and Iron labile pool could be the JNK mediated degradation of ferritin, which reduces the sensibility to Iron reactive species. MEF RIP1$^{-/-}$ do not show any increase in iron labile pool, but the role of RIP1 in this mechanism need to be further characterized [7].

Mitochondria: morphology and necrosis

Mitochondrial morphology is determined by the dynamic equilibrium between fission and fusion, repeated cycles of which redistribute mitochondrial constituents in order to maintain mitochondrial structure and function. Fission is mediated by dynamin-related protein 1 (Drp1), a GTPase that transits from citosol to mitochondria, and Fis1, an outer mitochondrial membrane protein. Fusion is controlled by three dynamin-related GTPases: Mfn1 and Mfn2 in the outer mitochondrial membrane and Opa1 in the inner mitochondrial membrane [98]. The relationships between mitochondrial morphology and cell death are still poorly understood, and alterations of this structure has been observed also during necrosis. Both apoptotic and necrotic stimuli cause mitochondrial fragmentation; however, if this morphological alteration is a mechanism of rescue of induction or rather a consequence of cell death is debated [63, 99]. Moreover, necrotic and apoptotic deaths could be differently linked to mitochondrial fission as demonstrated by Young and colleagues, at least in neurons [100]. Drp1 has been described as modulator of fragmentation and consequently, of cell death. Drp1 has been identified as the downstream effector of the *necrosome* activity. PGAM5 activates Drp1 leading to mitochondrial fragmentation and ROS-mediated cell death [63]. On the contrary, another recent publication identifies the role of Bax in primary necrosis after myocardial infarct *in vivo*. These data indicate that Bax governs mitochondrial fusion state, being critical in cell death; moreover, the authors supposed distinct

role of this protein during apoptotic or necrotic cell death [101]. In conclusion, cell- and context-specific mechanisms determine necrotic death dependence on fusion/fission dynamics.

Pills of metabolic consequences

Physico-chemical stress such as hypoxia, ischemia and dramatic temperature changes are generally considered insults that cause necrotic cell death. Ischemia reperfusion (IR) injury is one of the best example and represents one of the main driving forces to understand the molecular mechanism of necrosis. During IR, low oxygen supply blocks oxidative phosphorylation and ATP synthesis. Cells shift to glycolysis to restore ATP production. However, this process is inefficient during ischemic conditions due to the low levels of oxygen and glucose flow. The direct consequence is the drop of intracellular pH owing to lactate accumulation; hence, cells increase Na^+ influx through Na^+/H^+ antiporter [76]. Ca^{2+} counterbalances Na^+ accumulation, while causing mitochondria overload, thus compromising their functionality with a rise in NADH levels and ROS over-production. Oxidative stress and uncontrolled pH, combined with calcium overload and other factors, such as high phosphate concentrations and low adenine nucleotide levels, trigger the opening of mitochondria permeability transition pore as previously described.

Involvement of LMP in the execution of necroptosis

Beyond to the fundamental role of mitochondria in necrotic cell death, lysosome function is considered a critical point for caspase-independent cell death. Lysosomes are the source of many proteases, which target many cellular structures upon release into the cytoplasm; moreover, lysosomes are the site in which redox-active iron are stored. Hence, the lysosomal membrane permeabilization (LMP) is a critical event for cell lifespan. During necrosis two main stimuli cause LMP: ceramide accumulation and calpains activity [7, 88]. In response to different triggers, such as TNF-α and FAS-L, ceramide accumulates in cells and induces ROS production, thus being converted to sphingosine. The latter possesses lysomotropic properties and destabilizes lysosomal membrane. TNF-α/z-VAD or TNF-α/CHX/z-VAD treatments increase intracellular ceramide in L929, Jurkat and NIH-3T3 cells eliciting caspase-independent death with necrotic morphological features. These results have been confirmed by two independent approaches: i) the overexpression of acid ceramidase, which degrades ceramide, confers resistance to TNF/z-VAD cytotoxic effect; ii) pharmacological inhibitors of A-SMase, an enzyme that generates ceramide,

reduces necrotic cell death [102]. This study also revealed the indispensable role of RIP1 in this programmed cell death, whereas Δψ or cytochrome-C release are not key events. Sphingosine accumulates within the lysosomes, where it can permeabilize the membrane by a detergent-like mechanism, causing LMP in a dose-dependent manner [103] and necrosis at high doses in Jurkat cells.

On the other hand, calpains are a family of cistein-proteases constitutively and ubiquitously expressed in mammalian cells. Their activity is regulated by cytosolic calcium, which converts the inactive precursors to active enzymes that cleave many substrates, thus influencing different signalling pathways. In several animal and cellular models calpains have been described as important mediators of necrotic cell death [95, 104], mainly provoking lysosomal membrane permeabilization. Upon LMP, the necrotic effect is elicited by cathepsins. Yamashima and colleagues postulated their relationship with calpains and calcium overload to induce LMP-mediated necrotic cell death [104]. The characterization of post-ischemic cell death of Cornu Ammonis (CA) 1 neurons of hippocampus revealed that μ-calpain is responsible for lysosomal membrane rupture and subsequently activation of cathepsin-B. Another example of the contribution of cathepsins has been described in response to death receptors stimulation [105].

Necrotic death & Immune response

The early rupture and permeabilization of the plasma membrane during necrosis provoke the release of many immuno-stimulatory factors in the extracellular milieu, which mount a pro-inflammatory response. SAP130, heat shock proteins (HSP90, HSP70), HMGB1 and molecules such as DNA, RNA and monosodium urate crystals bind different pattern recognition receptors on the surface of immune cells, in particular dendritic cells and macrophages, thus modulating their activities. An historically difference between apoptosis and necrosis is explained by HMGB1 release. During late apoptosis (secondary necrosis) HMGB1 is secreted after being oxidized, thus losing its pro-inflammatory properties, whereas the rapid leakage of the protein during necrosis determines an unaltered capacity to engage macrophages [106, 107]. The inflammatory response is also stimulated by an active secretion of cytokines from necrotic cells. IL-6 was found to be actively released just before the membrane rupture [108].

During apoptosis, phosphatidylserine (PS) exposure works as the principal signal to switch on the “eat-me” response of the immune cells. The removal and the disposal of necrotic cells/debris

instead of phagocytosis seem to be carried out by macropinocytosis. PS exposure is not sufficient to remove the necrotic cells, and their clearance is less efficient and delayed. “Eat-me” signals represent the alarm from necrotic cells to be detected and to update the immune system about viral or microbial infection. Alterations of this mechanism result in degenerative disease, sepsis and autoimmune disease. Biological evidences of the immune response exerted by necrosis are well described in RIP3$^{-/-}$ mice models, where necrotic deficiency leads to a less efficient anti-viral response and reduced overall survival of the animals [37].

Pathophysiological aspects

Soon after its discovery, apoptosis has been considered for its pathological implications and the interest was immediately directed to investigate the therapeutic perspectives. In contrast, only the discovery of necrostatins in 2005, introduced necrosis as a relevant mechanism that can be targeted for drug development. In recent years, different studies described necrosis relevance in development and pathological conditions [109].

During development, necrosis could be a main tool to govern both organism shaping and tissues homeostasis. Roach and colleagues defined that chondrocytes cell death also occurs by a non-apoptotic cell death ensuring a physiological development of mammalian organism. A detailed electron microscopy analysis defined the morphological features of chondrocytes death, excluding the typical apoptotic phenotype [21]. Moreover, the use of RIP3 knockout mice and colonscopies from healthy human samples describe the necrosis of intestinal cells as the common and physiological mechanism ensuring tissue maintenance [20, 27]. Necrotic cell death can be engaged as a backup mechanism in a condition of apoptotic deficiency. The apoptotic cell death in the interdigital cells and thymocytes selection is rescued in Apaf$^{-/-}$ mice by necrosis, thus ensuring a correct shaping of the organism [6] and a proper selection of the immune system. The extent and the timing of the cellular demise resemble the correct development of the embryo.

Necrosis is associated with different pathological conditions, such neurodegeneration, ischemia-reperfusion and microbial and virus infection [109]. Excessive stresses including excitotoxicity and mitochondrial dysfunction are implicated in stroke, Alzheimer [84], Huntington’s and Parkinson’s disease [22, 23], as well as Gaucher’s disease and atherosclerosis [57, 58]. Interestingly, necrosis appears to have a prominent role during the control of virus and microbial

infection [37, 71] preventing the mortality through the release of cytokines necessary to stimulate a prompt immune response.

As essential modulator of necrosis, RIP1 should be more studied despite of the non-viable knockout mice. Inhibitors, such as necrostatins and geldamycin, are able to ensure cytoprotective effect in different pathological and experimental settings, showing conceivable clinical perspectives in brain or heart ischemia and in brain trauma *in vivo* [17, 19]. Moreover, loss of CyPD or its inhibition with cyclosporine A attenuates damages in response to well established pathological models of cerebral ischemia and stroke, as well as in response to necrotic stimuli *in vivo* [68, 110, 111]. These and future results will provide candidate targets for a therapeutic intervention. Indeed, many critical nodes in necrotic cell death are promising candidates and, hopefully, specific inhibitors of RIP1/3, PARP-1, CyPD might be clinically relevant.

Necrosis and cancer

The major goal of anticancer therapies is to kill malignant cells. During the last decades, researchers implied a plethora of chemotherapeutic agents to induce cell death of transformed cells. Unfortunately, many tumours show primary or acquired resistance to therapies thus forcing researchers to better understand all the molecular mechanisms governing cell demise. The aim is to design agents able to hit multiple hubs of the network in order to overcome tumour resistance. Generally, all the anti cancer drugs were contemplated for the ability to induce apoptosis and combinatory treatments have been tested to improve the efficacy in the presence of refractory malignancies. Since the discovery of the regulated necrotic death, new innovative targets have emerged and drug development started to be more focused on necrotic cell death response when cancer cells showed apoptotic resistance.

Mounting evidences suggest that necrotic process are disturbed in human malignancies. Chronic lymphocytic leukemia (CLL) exhibits defects in key signalling components: RIP3 and CYLD are frequently down-regulated; this effect could be mediated by the trascriptional repressor LEF-1 [25]. Another example is represented by a single nucleotide polymorphism located in RIP3 gene, which correlates with high risk of non-Hodgkin lymphoma [112]. The compounds capable of triggering necrosis in cancer cells are in an exponential phase of growth, although the comprehension of their mechanisms of action is still at the infancy. One interesting sphingolipid analog, FTY720, targets SET oncoprotein causing the re-activation of PP2A and the induction of cell

death [113]. The induction of necroptosis is mediated by the kinase activity of RIP1. Different reports show that SMAC mimetics (IAPs proteins inhibitors) are responsible for the induction of both apoptotic and necrotic cell death. These molecules sensitise FADD- and caspase 8-lacking cells to TNF-α induced necroptosis in a synergistic fashion. Besides the common anti-cancer drugs, also photodynamic therapy has been shown to provoke necrotic cell death in glioblastoma cells (reviewed in [114]). Finally, a small molecule inhibitor of Bcl-2 proteins, called Obatoclax (GX15-070), induces autophagy-mediated necroptosis in resistant ALL [115]. This interesting result demonstrates the link between Atg5 and RIP1/RIP3 and hence defines the connection between the two programmed cell deaths [116].

Isopeptidases: new targets inside the ubiquitin-proteosome system

Proteins homeostasis is essential to regulate a great number of biological processes. The ubiquitin-proteasome system is the major mechanism responsible for the degradation of the proteins in eukaryotic. Key event in this process is the conjugation of the small protein ubiquitin to target polypeptides. Ubiquitination represents a reversible post-translation modification that, in addition to the essential role in the degradation of target proteins, is involved in many others biological processes. Moreover, several ubiquitin-like proteins (UBLs) have been identified (i.e. ISG15, SUMO, NEDD8, Atg12). Although UBLs share a common structure, they have distinct roles compared with ubiquitin and from each other.

UB or UBL conjugation in general operates an isopeptide bound between the COOH terminus of the glycine on UB/UBL and the ε-amino group of a lysine within the target protein.

Poly-ubiquitin chains are assembled between the carboxy-terminal of glycine on UB and one of the seven internal lysine residues of UB itself (Lys 6,11,27,29,33,48,63). All this forms, together with linear poly-ubiquitylation have been found in eukaryotes, but the most studied are K48 and K63 polyubiquitination. The conjugation of UB or UBLs is governed by a multistep reaction that involves three enzymes called E1, E2 and E3 ligases, which finally creates the isopeptide linkage.

This post-translational modification is reversible. The human genome encodes for approximately 100 isopeptidases: enzymes that reverse the conjugation of UB/UBL to target proteins. Deubiquitinating enzymes (DUBs) are subdivided into six classes based on sequence and structural similarities. Ubiquitin specific proteases (USPs), ubiquitin C-terminal hydrolases (UCHs),

ovarian tumor proteases and Machado-Josef proteases are cistein proteases while JAMM are metalloproteases. Finally, a recently discovered class was referred as monocyte chemotactic protein-induced proteins (MCPIPs). DUBs are responsible for different functions. These enzymes are required for the processing of ubiquitin or UBL precursors: they recycle the poly-ubiquitin chains, just before the degradation of the target protein, to maintain the free ubiquitin pool. DUBs remove this signal or edit it by changing the conformation of the poly-ubiquitin chains. In this manner isopeptidases influence several biological processes (signal transduction, DNA repair, epigenetic, membrane trafficking) not linked to the control of protein-turnover (Fig. 11).

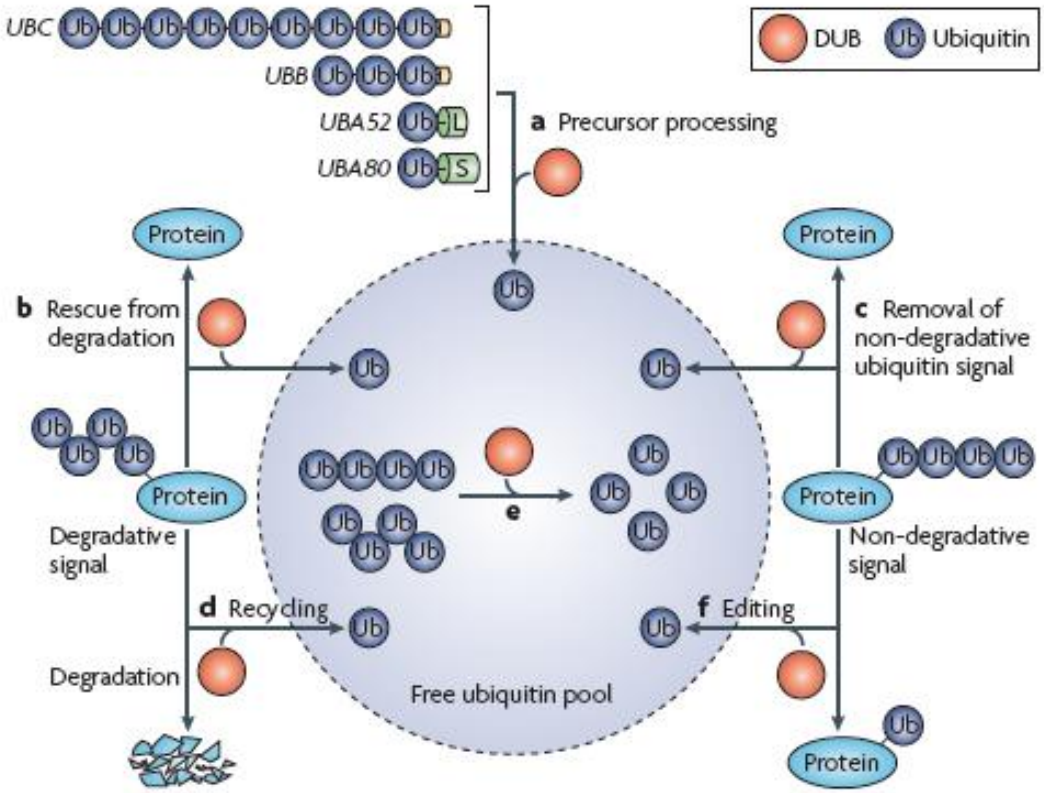

Figure 11: The different functions of DUBs. The de-ubiquitinating enzymes have a role in different steps of UPS. Processing of UB or UBLs precursors, removing of UB/UBL from targets proteins, recycling and editing of poli-Ub chains, not limited to K48 conjugation are all duties of the isopeptidases. From [117].

Biological processes regulated by DUBs

The ubiquitination process regulates different biological responses; consequently, the reversible nature of this modification renders the DUBs critical regulators of many aspects of cell life. Cell cycle regulation is one of the most critical events in cell growth and in tumorigenesis. The

ubiquitin ligases complex, called APC, targets Skp2 to delay the progression of cell cycle and USP44 counteracts this block. For example, USP13 regulates c-Myc degradation, key modulator of cell proliferation. During the DNA damage response USP1 mediates stabilization of Chk1, additionally the rescue of p53 degradation is operated by USP28 and, finally, USP47 participates in BER (base excision repair) by removing ubiquitin chain from Pol-β. As described above, some isopeptidases control the NF-kB pathway. CYLD and A20 remove or edit ubiquitin chains to turn on or shut off the TNF signaling through their influence on complex II (Fig. 12). This activity governs the apoptotic or necrotic outcome of this pathway. Another interesting role of DUBs is the regulation of the localization and recycling of the plasma membrane receptors. USP8 stabilizes RTKs (tyrosine kinase receptors) and affects their trafficking to the plasma membrane. USP18 and AMSH in other ways are involved in the same biological process.

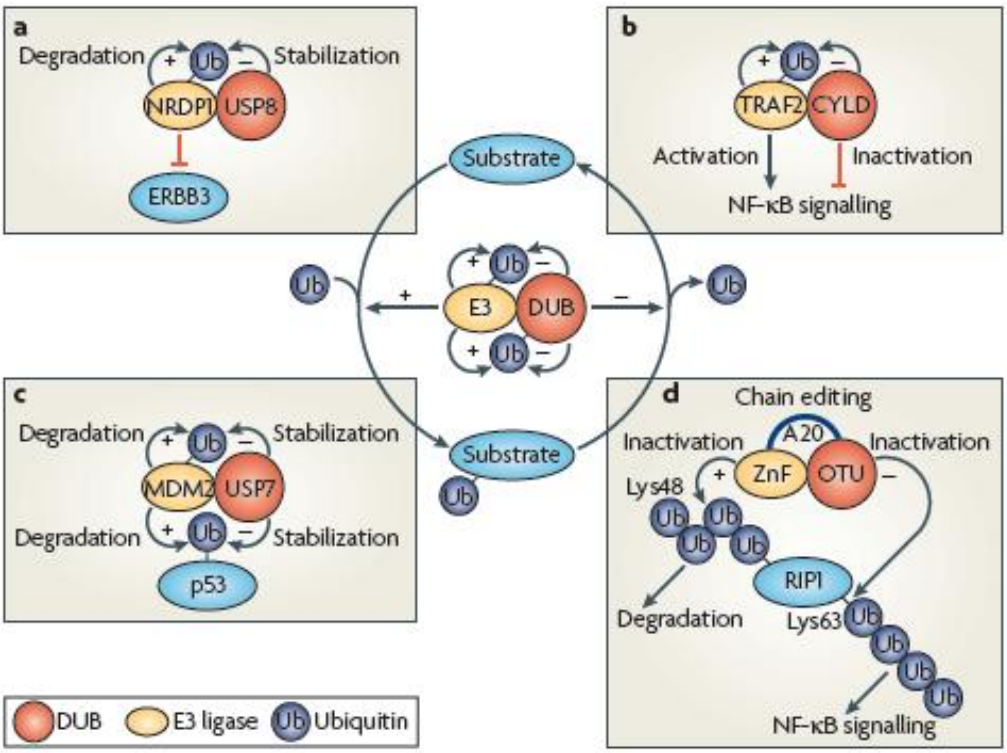

Figure 12: Examples of biological processes in which the de-ubiquitinase activity is an important mechanism of regulation of signalling pathways. a) USP8 is involved in the recycle of RTks by stabilizing the target proteins. b) CYLD is a fundamental regulator of NF-kB signal transduction, removing of poly-Ub chain and thus blocking the downstream pathway. c) USP7 fundamental role in the regulation of MDM2-p53 interaction d) editing of poli-Ub chain by A20/OTU in the NF-kB activation. Adapted from [117].

Cell death pathways activated by UPSI

The multiple biological processes regulated by the ubiquitin-proteasome have open interest to evaluate the UPS as a therapeutic target. The breaking point has been determined by the encouraging anti-cancer effect of bortezomib in multiple myeloma treatment and its approval for clinical use. Nowadays many different inhibitors have been developed and are in preclinical or clinical trials for anticancer therapies [118] [119, 120]. The definition of the cell death mechanisms elicited by the inhibitors of the ubiquitin-proteasome system (UPSIs) and the design of more selective inhibitors to target specific E3 ligase or isopeptidases are the aims of this field of research.

The ability of UPSIs to induce apoptosis in tumor cells is well established. It has been widely confirmed that the induction of apoptosis is the critical response for the antineoplastic efficacy of the UPSIs [119-123]. However, growing evidences suggest that alternative pathways of cell death could be elicited by UPSIs. As described above, many biological processes are regulated by ubiquitin-proteasome system; hence, also several elements of cell death pathways resulted to be modulated. For this reason, they represent broad inducers of apoptosis: they are considered non-specific modulators of the expression/activity of various components of the apoptotic machinery and can simultaneously favor the accumulation of pro- and anti-apoptotic factors. Regarding the extrinsic apoptotic pathway, UPSIs promote death receptors expression and activation [124, 125], stabilization of the cleaved form of BID (tBID) [126]; they engage p53 and thus all the apoptotic players under its direct control; they sustain Smac cytosolic level [127]; they elicit ER-stress and thus promoting Noxa transcription, they can also stabilize Bim and Nbk proteins. On the other hand, UPSIs can also elicit unwanted effects by blocking the proteasome dependent degradation of IAPs, or of Mcl-1.

The detailed definition of molecular mechanisms controlling turnover of key pro- and anti-apoptotic proteins will be instrumental in the design of more specific inhibitors. For instance, these new inhibitors could target the relative E3-ligases or the relative DUBs in order to obtain a more selective modulation of the specific elements and pathways leading to cancer cell death. The promising activity of DUBs inhibitors is the main driving force of this thesis and, behind the discovery of new cellular responses and pathways to control cell survival, the perspective of possible applications in therapy fully justify my interest in this research.

AIM of the Thesis

Necrotic cell death is the highly inflammatory and unregulated form of cell death. This is an ancient concept. Recently necrosis has been included in the programmed forms of cell death, together with autophagy and the well-established apoptotic demise. Thus, the interest on necrosis started to grow and nowadays the implications in several pathological conditions are continuously emerging.

The aim of this thesis fits in this *scenario*; indeed, we have identified a pan isopeptidases inhibitor G5, with the peculiar ability to elicit different modes of cell death. In particular, G5 interesting feature is the ability to kill apoptotic resistant cancer cells through a necrotic mechanism. However, G5-mediated necrotic cell death differs from the emerging pathway of programmed necrosis, such as necroptosis, parthanatos and CypD-regulated necrosis. G5 resulted to be insensitive to RIP1, JNK, PARP inhibitors, unconditioned by Ca^{2+} scavengers and anti-oxidant agents, but characterized by a rapid and dramatic cytoskeletal alteration and counteracted by extracellular matrix elements. Therefore, the aim of this thesis is to address the molecular determinants and the biological mechanisms of this alternative form of necrotic cell death.

Results

Characterization of necrosis as induced by the non-selective isopeptidases inhibitor G5 and the redox cycling quinone, 2,3-dimethoxy-1,4-naphthoquinone (DMNQ)

To explore the existence of different necrotic signaling pathways, we used two different chemical stressors: the isopeptidases inhibitor G5, an inducer of alterations in cell adhesion and actin cytoskeleton and DMNQ a generator of ROS at mitochondrial level.

As cellular model to study necrosis, we selected U87MG glioblastoma cells, because of their intrinsic resistance to apoptosis and the tendency to die by necrosis [128]. In addition, we also overexpressed Bcl-xL to further suppress apoptosis and impinging on the necrotic response. Cells were treated with escalating doses of G5 or DMNQ and cell death was scored by trypan blue assay (Fig. 13 A). The observed cell death was unaffected by caspase inhibition (Fig. 13 B).

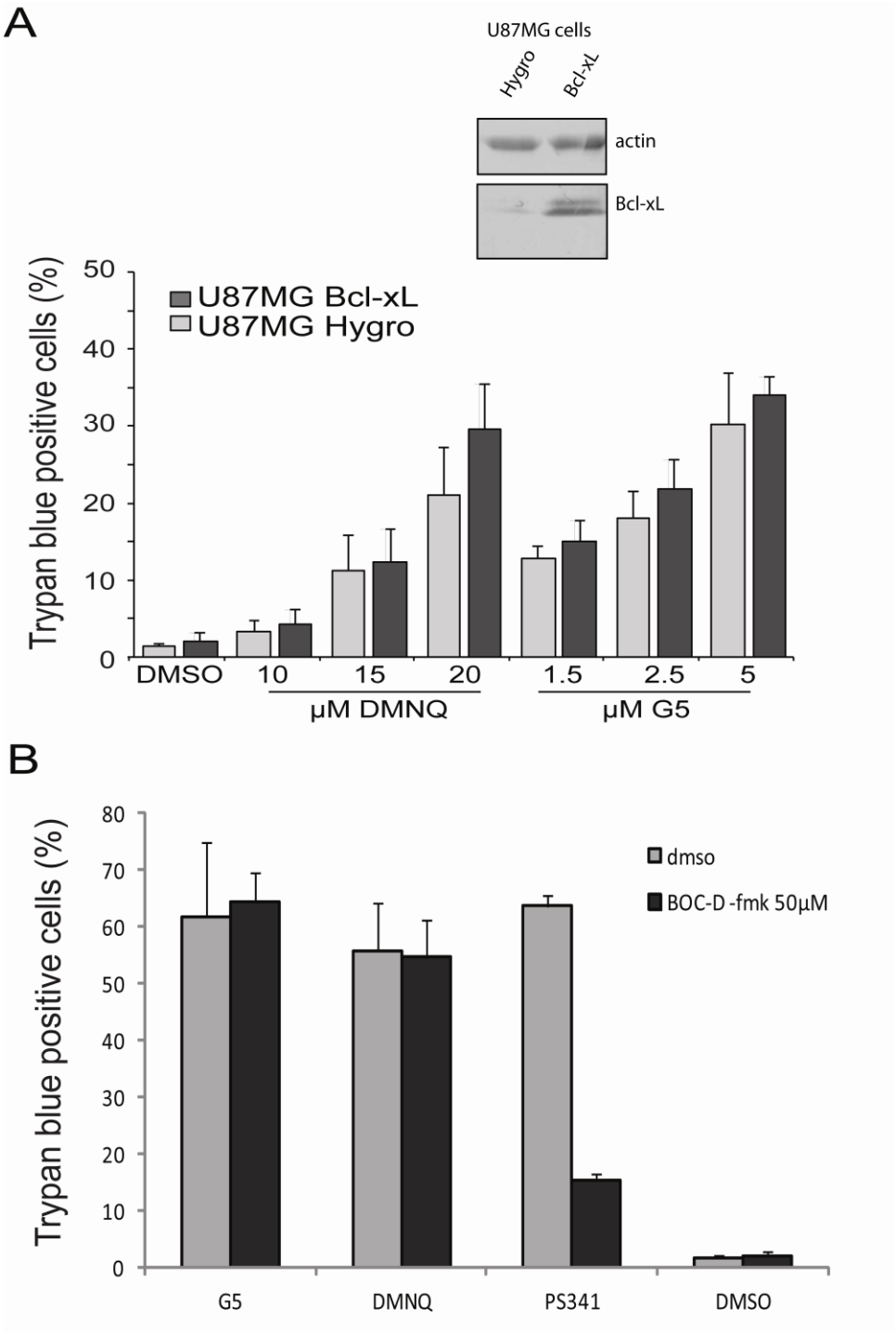

Figure 13. Cell death in U87MG GBM cells in response to G5 or DMNQ treatments. A) U87MG/Hygro and U87MG/Bcl-xL cells were treated with the indicated concentrations for 24 hours (hrs) and the appearance of cell death was scored by trypan blue staining. Columns, mean (n = 3); bars, SD. B) U87MG/Bcl-xL cells were pre-treated with pan caspase inhibitor BOC-D-fmk 50μM for 2hrs and then G5 5μM, DMNQ 20μM and PS341 1μM were added for 36hrs. Appearance of cell death was scored by trypan blue staining. Columns, mean (n = 2); bars, SD.

Next we evaluated the mitochondrial morphology using MitoTracker Red CMXRos, in relation to mitochondrial outer membrane permeabilization (MOMP). As marker of MOMP we explored Smac localization. Both necrotic stimuli induced a dramatic mitochondrial fragmentation (Fig. 14), with the quantitative analysis reported in figure 15 C. Smac was usually localized in the mitochondria (Fig. 14 and 15 A), thus proving the absence of MOMP. Curiously in the case of DMNQ a fraction of cells (10%) presented intact MOM but decreased MitoTracker staining, thus indicating that $\Delta\psi$ collapse occurs before MOMP (Fig. 14 arrow and Fig. 15 B).

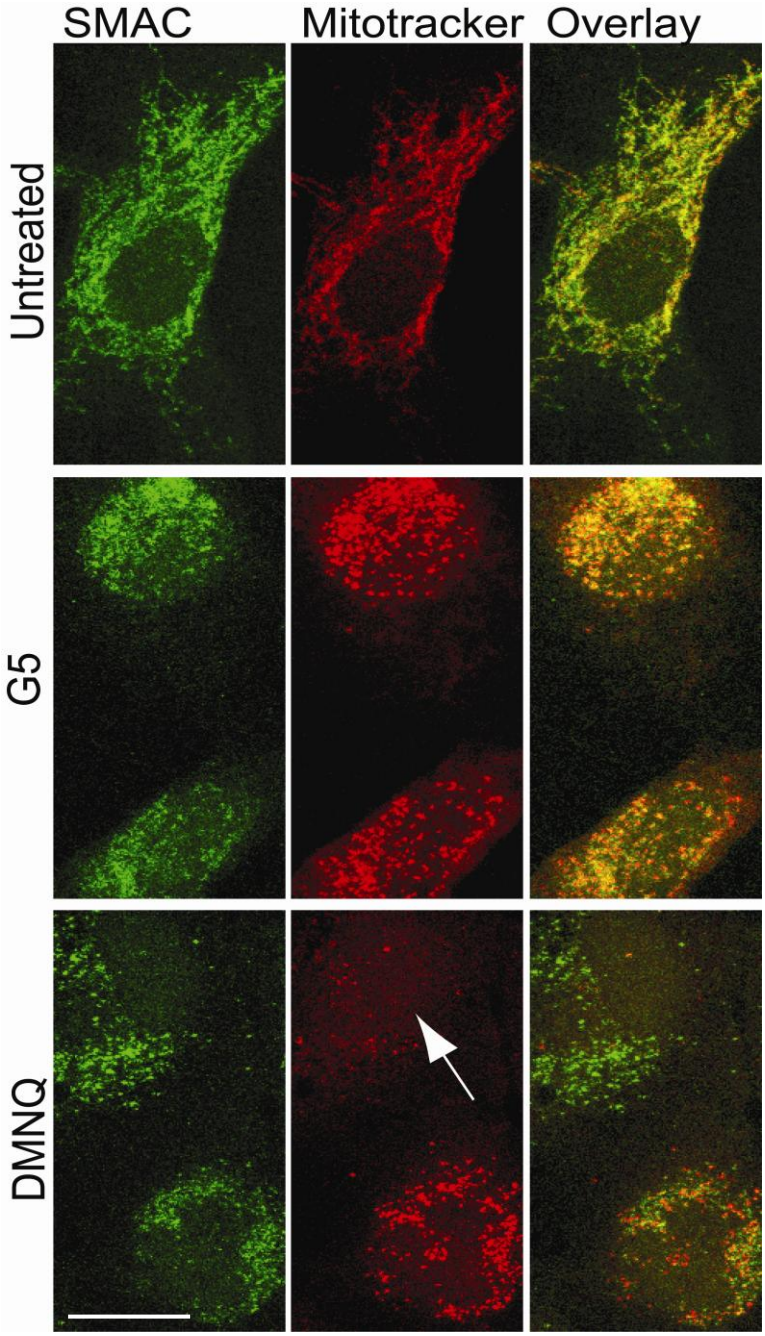

***Figure 14. Mitochondrial fragmentation without MOMP in U87MG/Bcl-xL cells*.** U87MG/Bcl-xL cells were treated with G5 5µM or DMNQ 20µM for 16hrs, MitoTracker Red CMXRos was added to the medium 1hr before fixing. Immunofluorescences were performed to visualize SMAC subcellular localization and mitochondrial morphology. Cells were analyzed at confocal microscopy. Arrows point to cells with evident alterations in Δψ as depicted by reduced MitoTracker Red CMXRos staining. Scale bar, 50µM.

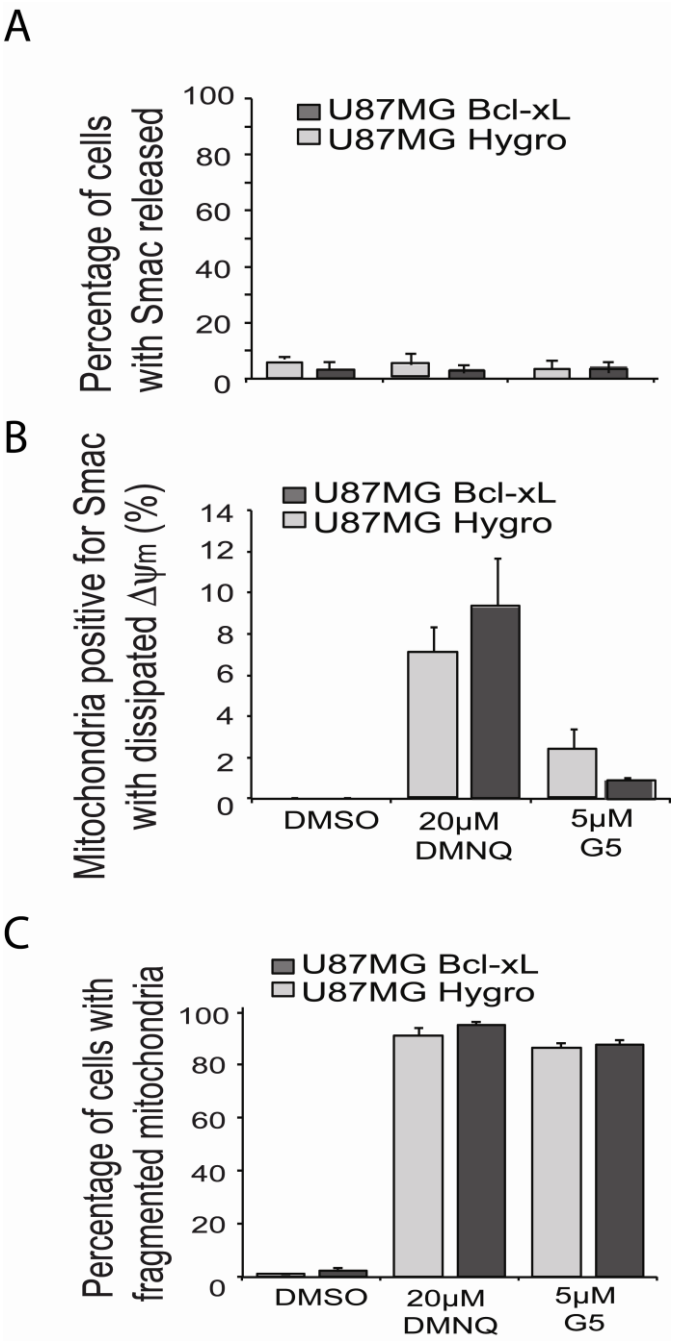

Figure 15. Quantification of mitochondrial fragmentation and Smac release. A) Quantitative analysis of Smac localization in U87MG/Bcl-xL and U87MG/Hygro cells treated as indicated. B) and C) Quantitative analysis of mitochondrial morphology and Smac release in U87MG/Bcl-xL and U87MG/Hygro cells treated as indicated in figure 14. MitoTracker Red CMXRos staining was used to score mitochondrial fragmentation. After immunofluorescence 300 cells have been classified for each treatment in three independent experiments. Columns, mean (n = 3); bars, SD.

Cytoplasmic vacuolization, as consequence of ER stress, occurs in response to the engagement of the unfolded protein response by UPS inhibitors [129]. As shown in figure 16, glioma cells incubated with G5 exhibit cytoplasmic vacuolization (arrows).

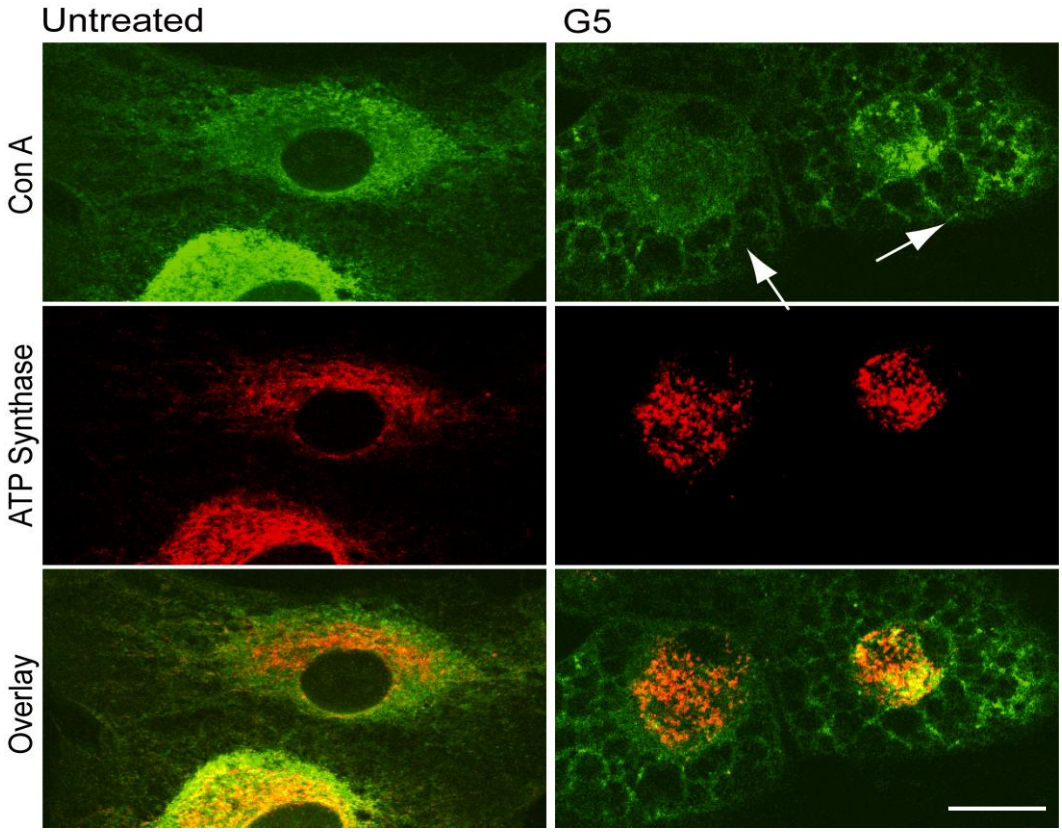

Figure 16. Extensive cytoplasmic vacuolization and mitochondrial fragmentation in U87MG/Bcl-xL. U87MG/Bcl-xL cells were treated with G5 5µM for 12hrs. Immunofluorescence analysis was performed to visualize cytosolic vacuolization, using Concavanalin A (ConA), a lectin that stains the ER, and mitochondria morphology, using anti-ATP synthase antibody. The arrows point to cells with evident cytoplasmic vacuolization. Scale bar, 50µM.

However, when a comparison was performed by time-course analysis, it was clear that mitochondrial fragmentation precedes cytoplasmic vacuolization (Fig. 17). In conclusion, mitochondrial fragmentation represents an early event during cell death induced by G5 treatment.

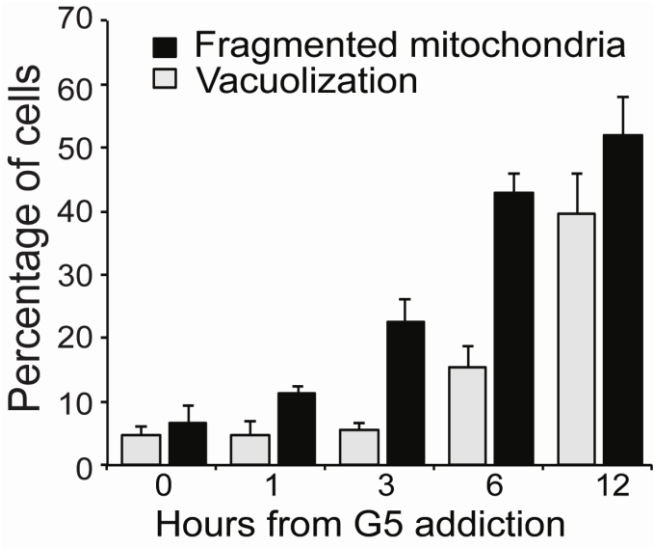

***Figure 17. Mitochondrial fragmentation precedes cytoplasmic vacuolization*.** Time course analysis of changes observed, as exemplified in fig. 16, following treatment of U87MG/Bcl-xL cells with G5 5µM. After immunofluorescence 300 cells have been classified for each treatment in two independent experiments. Columns, mean (n = 2); bars, SD.

G5 and DMNQ activate distinct necrotic pathways

To elucidate the contribution of the mitochondrial fragmentation to the necrotic death induced by G5 and DMNQ, we employed different experimental settings. First U87MG/Bcl-xL cells were treated with the Drp1 inhibitor, mdivi-1 [63]. Interestingly, mdivi-1 attenuated necrosis only in response to DMNQ (Fig. 18).

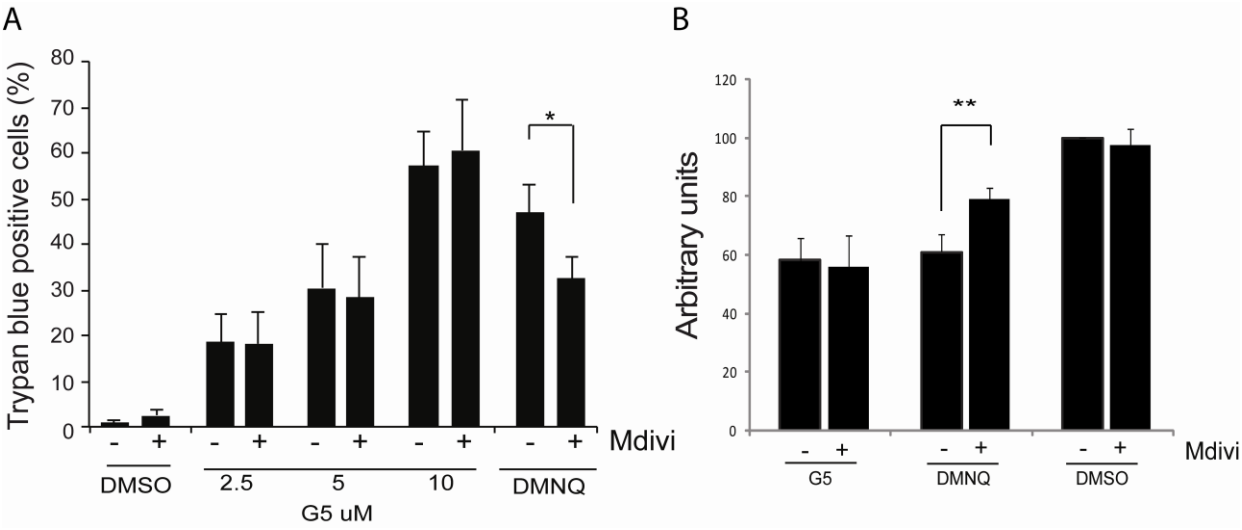

Figure 18. Drp1 inhibition affect only DMNQ-mediated necrotic cell death. U87MG/Bcl-xL cells were pre-treated with the Drp1 inhibitor mdivi-1 (50µM) for 1hr. Next, G5 (indicated concentrations) and DMNQ

30µM were added for 24hrs. A) Appearance of cell death was scored by trypan blue staining. Data are presented as mean ± SD; n = 4. B) Cell survival was scored by resazurin assay. Columns, mean (n = 4); bars, SD.

To confirm this result we generated U87MG/Bcl-xL cells expressing a dominant negative mutant (K38A) of Drp1 (Fig 19 A). Treatment with G5 or with DMNQ of Drp1-K38A overexpressing cells confirmed the result obtained with the Drp1 inhibitor. The dependence from Drp1 activity to fully elicit necrosis was observed only in the case of DMNQ treatment (Fig. 19 B).

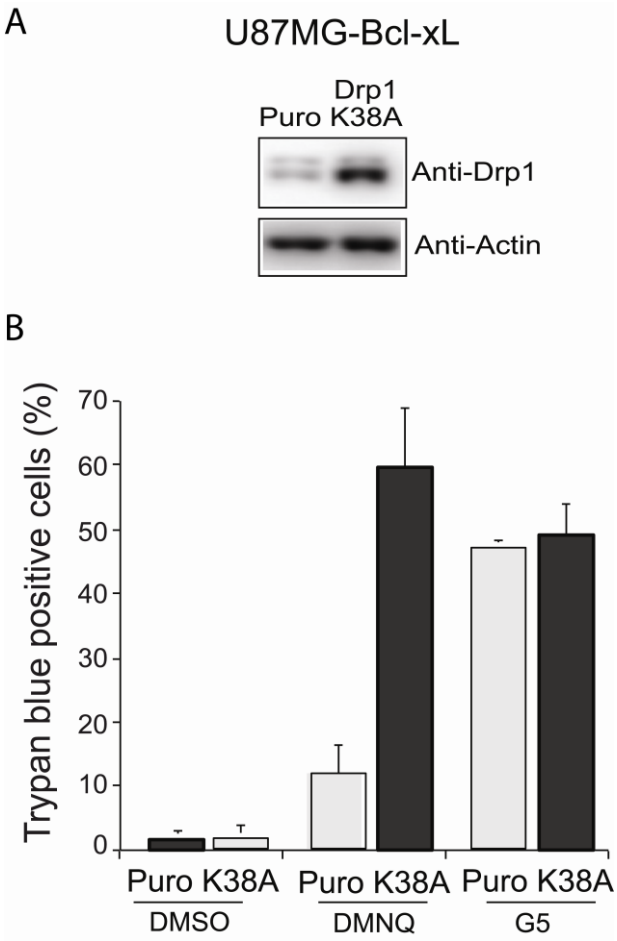

Figure 19. The dominant negative form of Drp1 (K38A) suppresses only DMNQ induced cell death. A) Immunoblot analysis of U87MG/Bcl-xL cells expressing the Drp1 mutant K38A or Puro gene. Cellular lysates were generated and immunoblot analysis performed as indicated. B) U87MG/Bcl-xL/Drp1K38A and U87MG/Bcl-xL/Puro control cells were treated with 5µM G5 and DMNQ 30µM. Appearance of cell death was scored by trypan blue staining. Data are presented as mean ± SD; n = 3

Finally to further prove that two distinct necrotic pathways are involved in DMNQ or G5 induced cell death, we evaluated the contribution of RIP1 by treating cells with the specific inhibitor Nec-1. Cell death was efficiently blocked by Nec-1 only when induced by DMNQ (Fig. 20). Together these results demonstrate that two different necrotic pathways are activated by DMNQ and G5, underscoring the existence of alternative mechanisms beyond necroptosis.

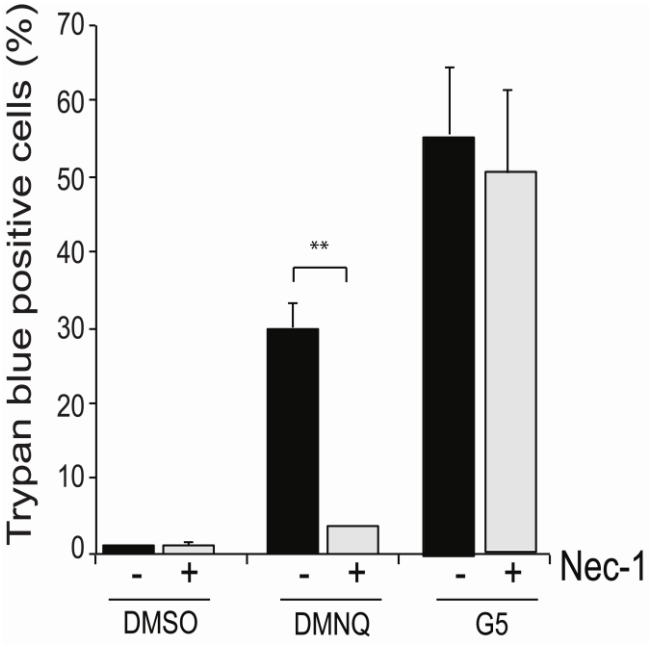

Figure 20. Inhibition of RIP1 confirmed that DMNQ and G5 elicit two alternative necrotic pathways. U87MG/Bcl-xL cells were pre-treated with RIP1 inhibitor Necrostatin-1 (10μM) for 1hr and then G5 5μM and DMNQ 30μM were added for 24hrs. Appearance of cell death was scored by trypan blue staining [columns, mean (n = 3); bars, SD].

Cellular responses to G5 treatment

To gain insight into the necrotic pathway elicited by G5, we decided to monitor the activation of signaling pathway transducing stress and pro-survival signals in G5-treated cells. We evaluated activation or ERKs, p38, JNK and Akt. ERKs and p38, but not JUNK, were transiently activated in response to G5. However, these activations anticipated without mirroring, the appearance of necrosis (Fig. 21).

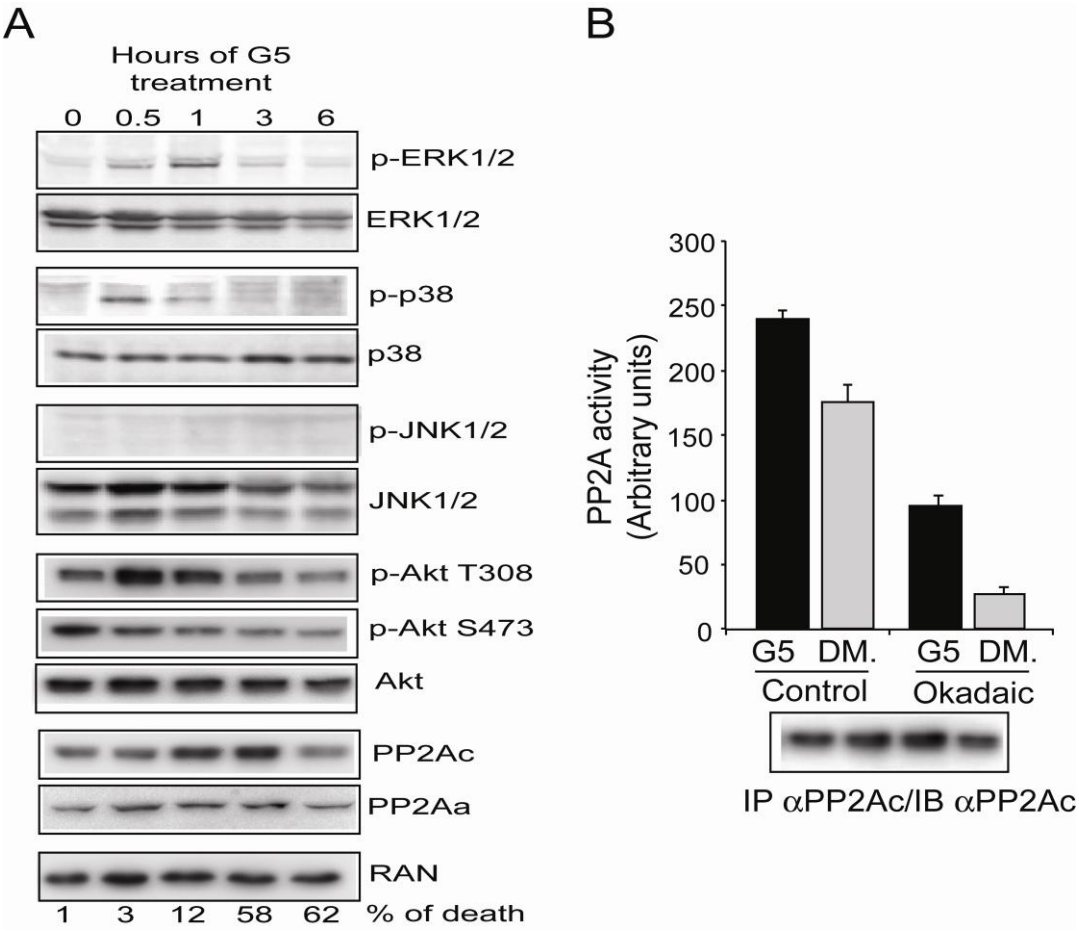

***Figure 21. Multiple signaling pathways are activated in response to G5 treatment*.** A) U87MG/Bcl-xL cells were treated with 10µM of G5 for the indicated times. Cellular lysates were generated and immunoblots performed with the indicated antibodies. In parallel, cell death was scored by trypan blue staining at the same time points; percentage are represented at the bottom. B) Immuno-precipitation of PP2Ac and fluorimetric assay using DiFMUP substrate. U87MG/Bcl-xL cells were treated with 10µM of G5 or DMSO (DM) for 1hr before immuno-precipitation. As control, immuno-complexes were pre-incubated with Okadaic Acid as indicated in M&M. Immunocomplexes were next resolved in SDS/PAGE electrophoresis and immunoblotted to verify the amount of PP2Ac. Data are presented as mean ± SD; n = 3.

When the status of Akt activation was evaluated, it emerged that the kinetic of dephosphorylation of serine 473 and also of threonine 308 (after a transient up-regulation) was paired to the appearance of necrosis (Fig. 21 A). This result suggests that inhibition of Akt could be linked to G5-induced necrosis.

Protein phosphatase 2A (PP2A) can dephosphorylate and inactivate Akt [130]. Hence, we monitored PP2A subunits levels in cells treated with G5. Levels of PP2Ac catalytic subunit were increased until 3 hours from G5 treatment, with a drop at 6 hours, after the advent of necrosis (Fig. 21 A). By contrast, levels of the scaffold subunit A (PR65) were unaffected (Fig. 21 A). Having discovered an increase of the PP2Ac subunit, we next evaluated whether PP2A enzymatic activity was augmented after G5 treatment, thus explaining Akt dephosphorylation and inactivation. Figure 21 B illustrates that PP2A phosphatase activity is augmented in cells treated with G5.

Differential requirements of PP2Ac during necrotic death induced by G5 and DMNQ

To evaluate the contribution of PP2A to G5 induced necrosis we silenced the expression of the catalytic subunit and next incubated U87MG/Bcl-xL cells with G5 or DMNQ. Down-regulation of PP2Ac impacted both necrotic responses, although with opposite effects (Fig. 22 B). PP2Ac is required for necrosis in response to G5, but it can counteract necrosis in response to DMNQ. This evidence further strengthened the hypothesis that cells can engage multiple necrotic pathways.

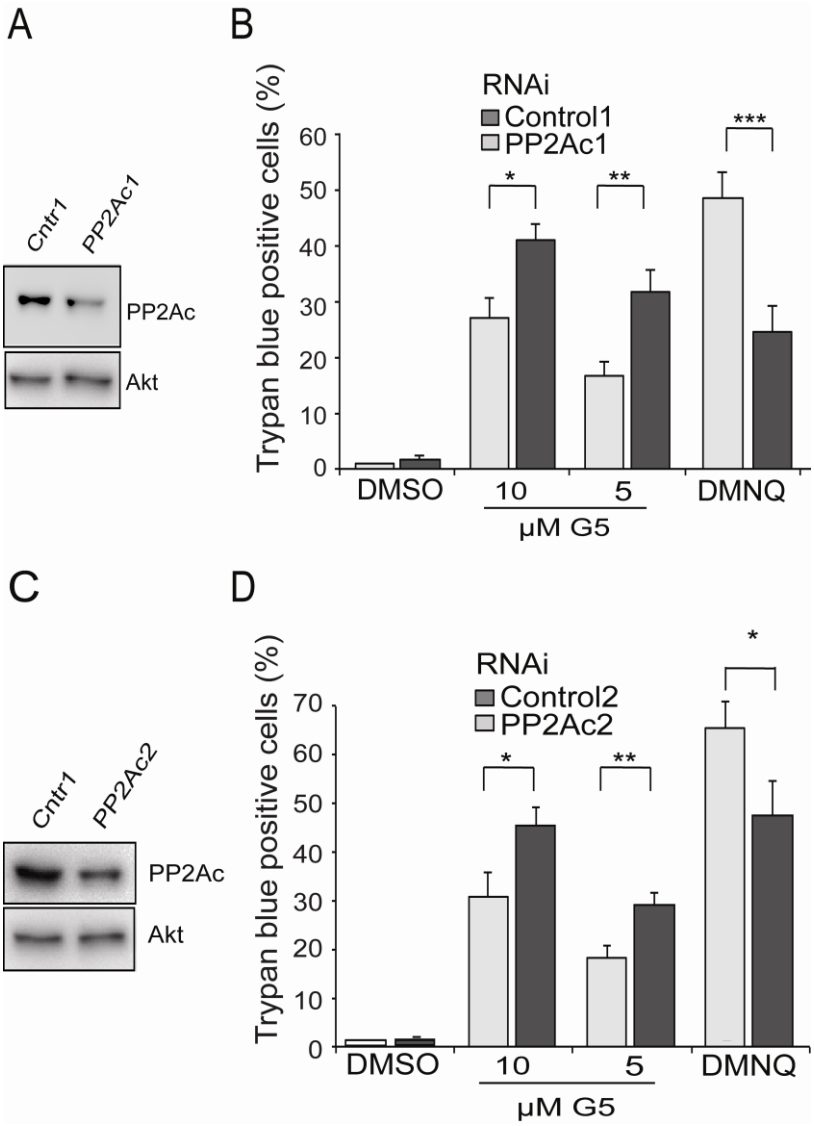

Figure 22. PP2A plays a key role in the necrotic response to G5 and DMNQ treatment. A) and C) Immunoblot analysis to evaluate PP2Ac down-regulation with two different siRNAs. Cells were grown in the presence of the siRNAs for 40hrs, immunoblot analysis was performed to evaluate PP2Ac down-regulation, by using the indicated antibodies. B) and D) U87MG/Bcl-xL cells were grown for 40hrs in the presence of the indicated siRNAs and next treated for 24hrs with G5 5µM or 10µM and 30µM of DMNQ. Appearance of cell death was scored by trypan blue staining. Columns, mean (n = 3); bars, SD.

The impact of PP2A in G5-induced necrosis was also evident at the level of mitochondrial fragmentation (Fig. 23). In cells with reduced PP2Ac expression, mitochondria fragmentation is much less pronounced. To confirm the role of PP2A we used another siRNA, which targets a different region of PP2Ac. Again, down-regulation of PP2Ac limited necrosis in response to G5 and favored necrosis in response to DMNQ (Fig. 22 D).

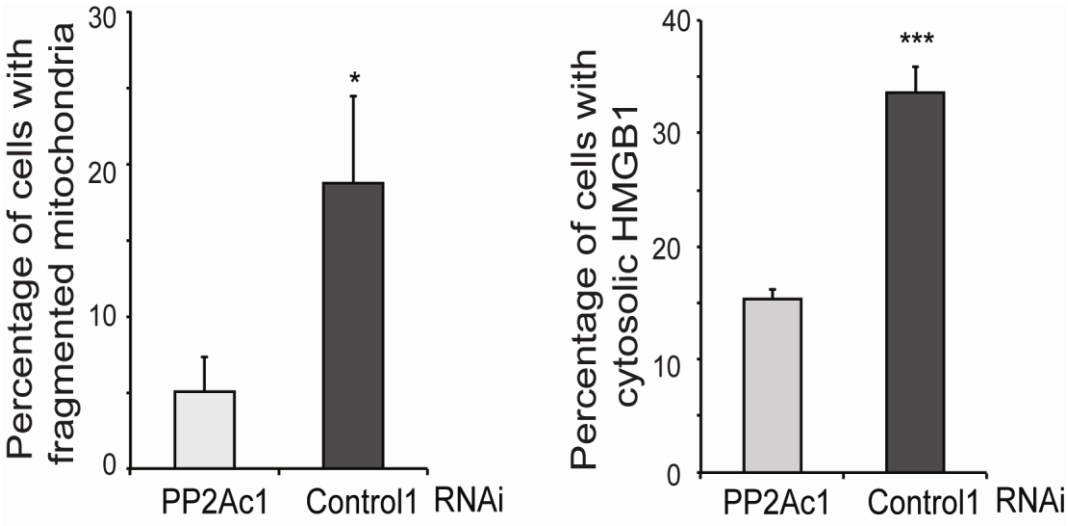

Figure 23. PP2Ac down regulation reduced mitochondrial fragmentation and HMGB1 re-localization in U87MG/Bcl-xL cells treated with G5. U87MG/Bcl-xL cells, transfected with the indicated siRNAs were grown on glass coverslip for 40hrs. Cells were next treated for 18hrs with G5 5μM. After immunofluorescences with anti-ATP synthase antibodies, confocal microscopy was used to score mitochondrial fragmentation. After immunofluorescence 300 cells have been classified for each treatment in three independent experiments. Data are presented as mean ± SD; n = 3.

The impact of PP2A on G5-induced necrosis could be related to the status of Akt activation; hence, we evaluated Akt phosphorylation in cells silenced for PP2Ac and treated with G5 for 1 hour. Western blot and quantitative analysis in figure 24 evidence that phosphorylation at threonine 308 was increased after G5 treatment in PP2Ac silenced cells.

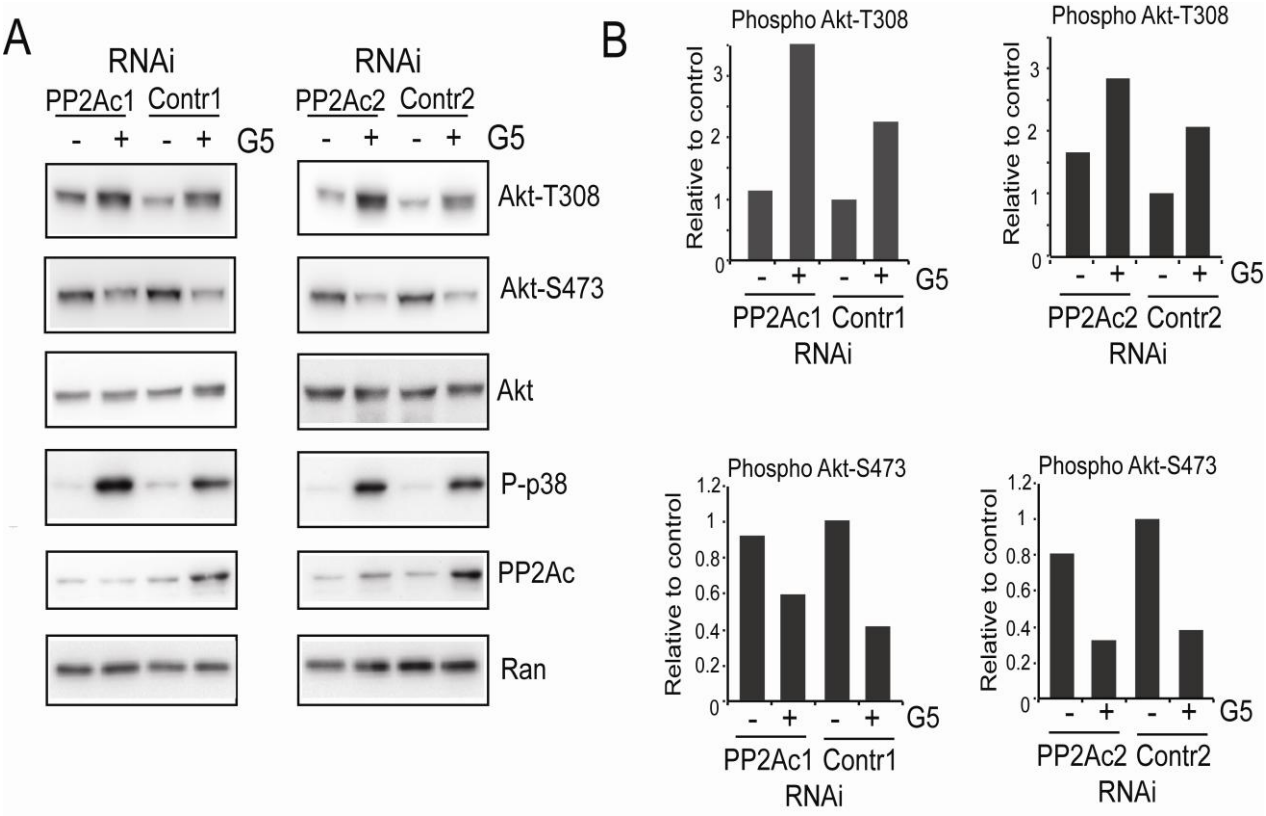

***Figure 24. Akt phosphorylation at threonine 308 was increased after G5 treatment in PP2Ac silenced cells*.** Akt activation in U87MG/Bcl-xL cells treated with G5 and silenced for PP2Ac. Cells were silenced for 48hrs and next treated with 10μM G5 for 1hr. A) Cellular lysates were generated and probed with the indicated antibodies. B) Quantitative densitometric analysis of immunoblots. Data are presented as mean of two experiments.

In addition to its well-established anti-apoptotic role, Akt has been reported to impact on some kinds of necrotic death [131, 132]. Hence, we explored whether the pro-necrotic role of PP2A in G5-treated cells could be explicated through the inhibition of Akt activity. First, by using the PI3K inhibitor LY, we observed that suppression of the PI3K-Akt axis was insufficient for triggering death of U87MG/Bcl-xL cells (Fig. 25).

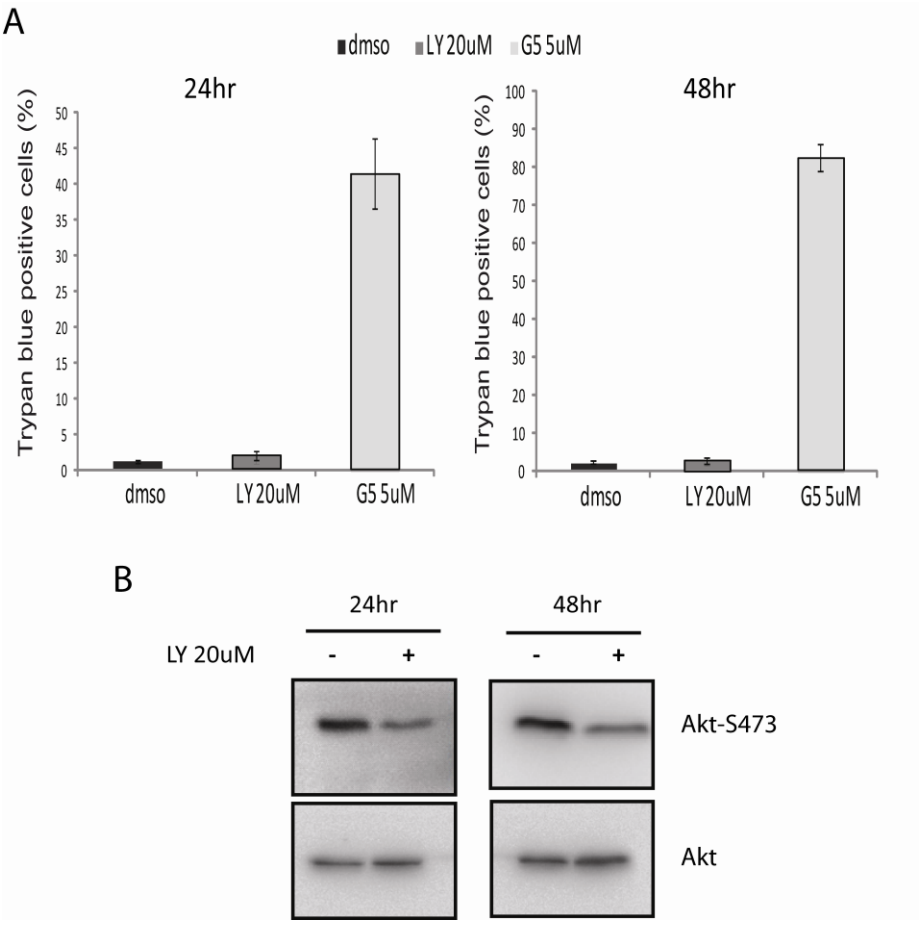

Figure 25. Inhibition of the PI3K-Akt axis is not enough to induce necrotic cell death in U87MG/Bcl-xl cells. A) U87MG/Bcl-xL cells were treated with the indicated concentrations of LY or G5 for 24 and 48hrs. The appearance of cell death was scored by trypan blue staining. Data are presented as mean ± SD; n = 3. B) Immunoblot analysis of Akt phosphorylation status upon LY treatment in U87MG/Bcl-xL cells. Cellular lysates were generated and probed with the indicated antibodies.

Second, G5-induced necrosis was unaffected by the overexpression of a constitutive active form of Akt (Fig. 26 A). In summary, although Akt activity is down-regulated by G5-treatment and PP2A contributes to this modulation, this kinase does not play a major role during G5-induced necrotic death. (Fig. 25 and 26).

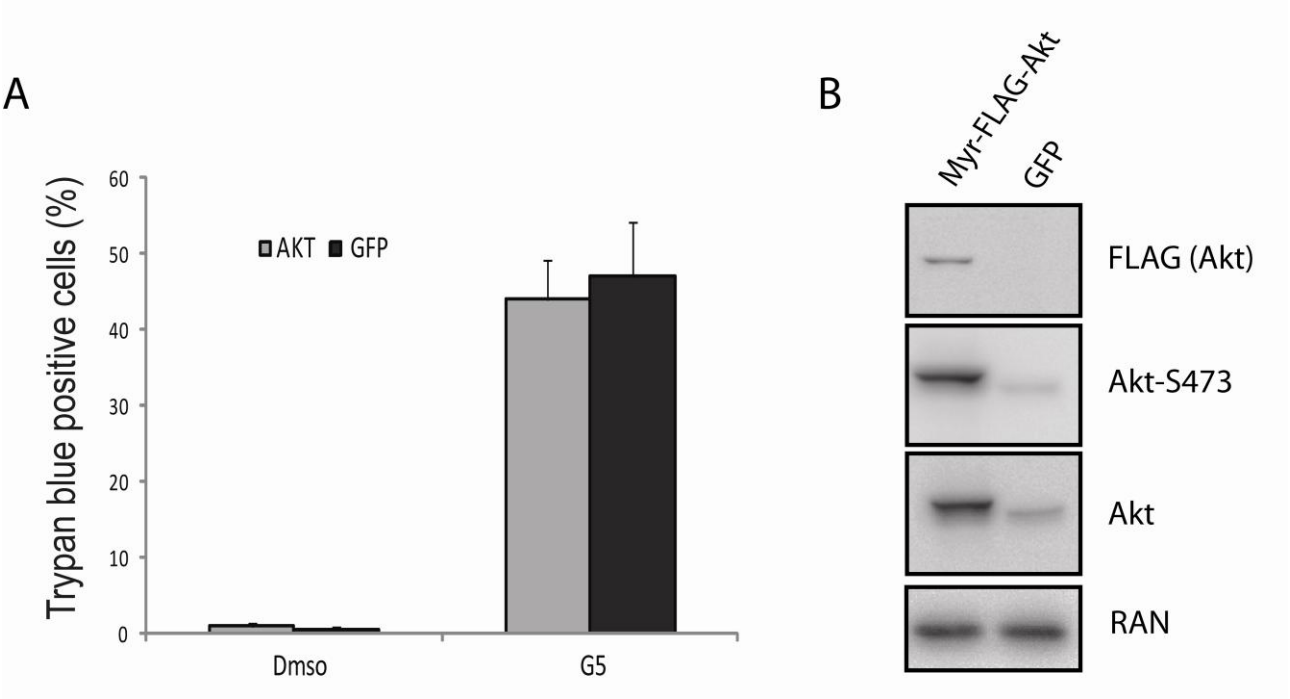

Figure 26. The constitutive form of Akt does not influence G5-mediated death of U87MG cells. A) U87MG cells overexpressing Myr-Akt or GFP were generated and next treated with G5 5μM for 24hrs. The appearance of cell death was scored by Trypan blue staining. Data are presented as mean ± SD; n = 3. B) Characterization of U87MG expressing myristoylated-Akt (Myr-Akt), a constitutively active form of Akt. Cellular lysates were generated and probed with the indicated antibodies.

Necrosis promotes the cytoplasmic accumulation of PP2Ac

To further characterize the role of PP2Ac during G5-induced necrosis, we analyzed its subcellular localization in comparison with HMGB1, a well-known necrotic marker, which translocates from the nucleus into the cytoplasm in response to necrosis [133]. In untreated cells PP2Ac evidences a nuclear or a pan (both nuclear and cytoplasmic) localization (Fig. 27 A) and quantified in figure 27 B. During G5-induced necrosis cells, presenting an exclusively cytoplasmatic localization of PP2Ac, emerge (Fig. 27 A arrow); contemporarily, cells with prominent nuclear PP2Ac disappear (Fig. 27 B). Cells showing accumulation of PP2Ac into the cytosol, similarly translocate HMGB1 from the nucleus into the cytoplasm (Fig. 27 A arrow and 27 C). Interestingly, as shown above, silencing of PP2Ac reduced the percentage of cells exhibiting cytosolic translocation of HMGB1 in response to G5 treatment.

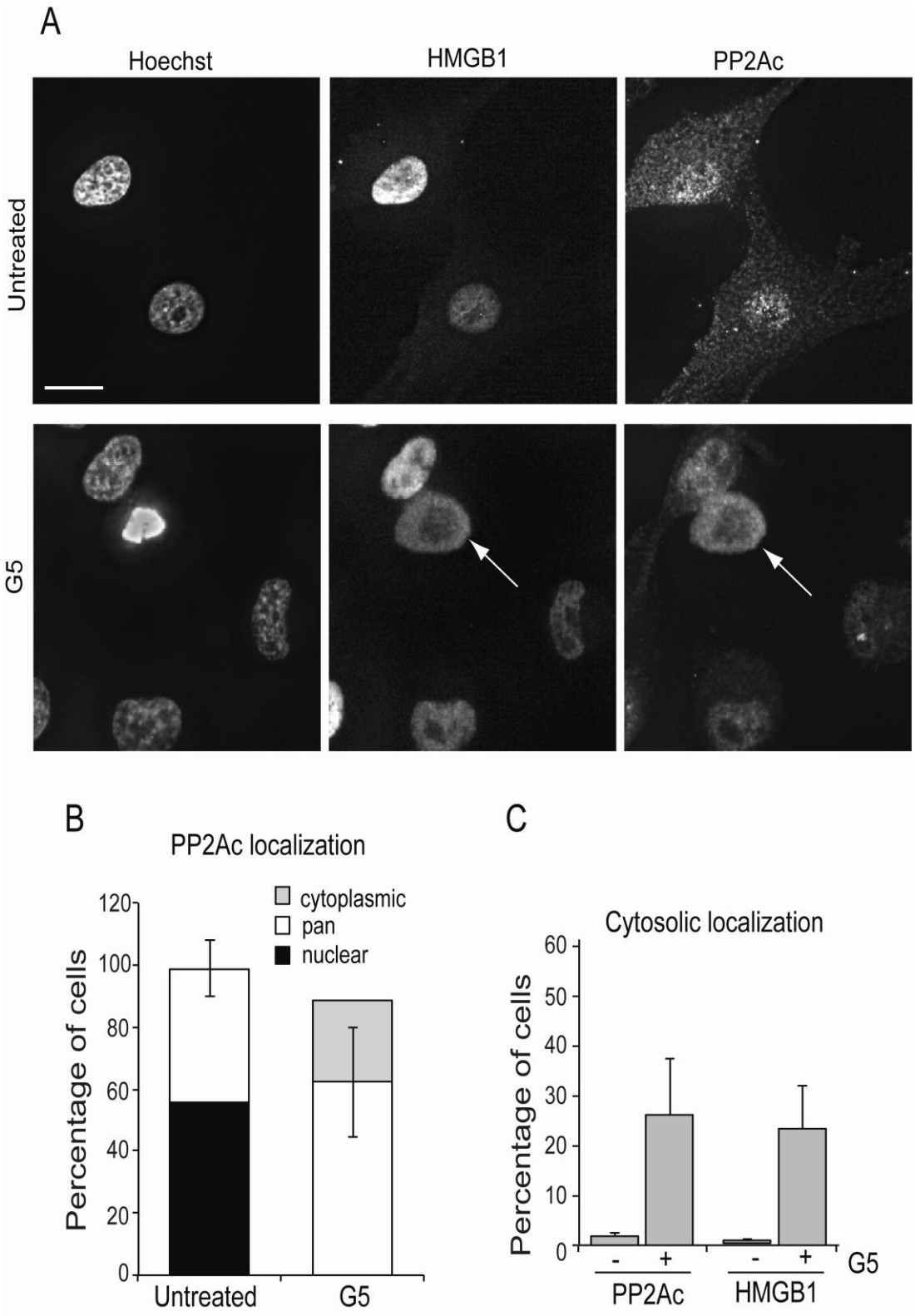

Figure 27. Subcellular re-localization of PP2Ac during G5-induced necrosis. A)U87MG/Bcl-xL cells were treated for 5hrs with G5 5µM. After immunofluorescence, epifluorescence microscopy followed by deconvolution analysis was used to visualize PP2Ac and HMGB1 localization. Hoechst 33258 staining was applied to mark nuclei. The arrow points to a cell with evident PP2Ac cytosolic accumulation. B) Quantitative analysis of PP2Ac re-localization during G5-induced necrosis. Percentage of cells with pan,

cytoplasmic or nuclear PP2Ac localization in untreated or G5 treated cells. C) Comparison between cells with cytosolic accumulation of PP2Ac and HMGB1 in G5 treated and untreated cells. Data are presented as mean ± SD of two experiments, at least 200 cells were counted. Scale bar, 50µM.

The PP2A substrate Cofilin-1 influences in a phosphorylation-dependent manner necrosis induced by G5

PP2A enacts pleiotropic activities in different cellular context, which reflect the considerable number of substrates under its supervision. On the other side G5 treatment induces profound changes in cell spreading and actin cytoskeleton as exemplified in Fig 28 A. Quantitative analysis confirmed the dramatic and rapid alterations in cell morphology upon compound treatment (Fig. 28 B). We also evaluated the contribution of PP2A to the modification of actin cytoskeleton. Cells were silenced for PP2Ac expression and evaluated for changes in adhesion/spreading. As illustrated in figure 28 C and quantified in 28 D, down-regulation of PP2Ac promoted re-organization of actin cytoskeleton and augmented cell spreading. Silencing of PP2Ac was also sufficient to delay the reduction of cell spreading as operated by G5 (Fig 28 D right).

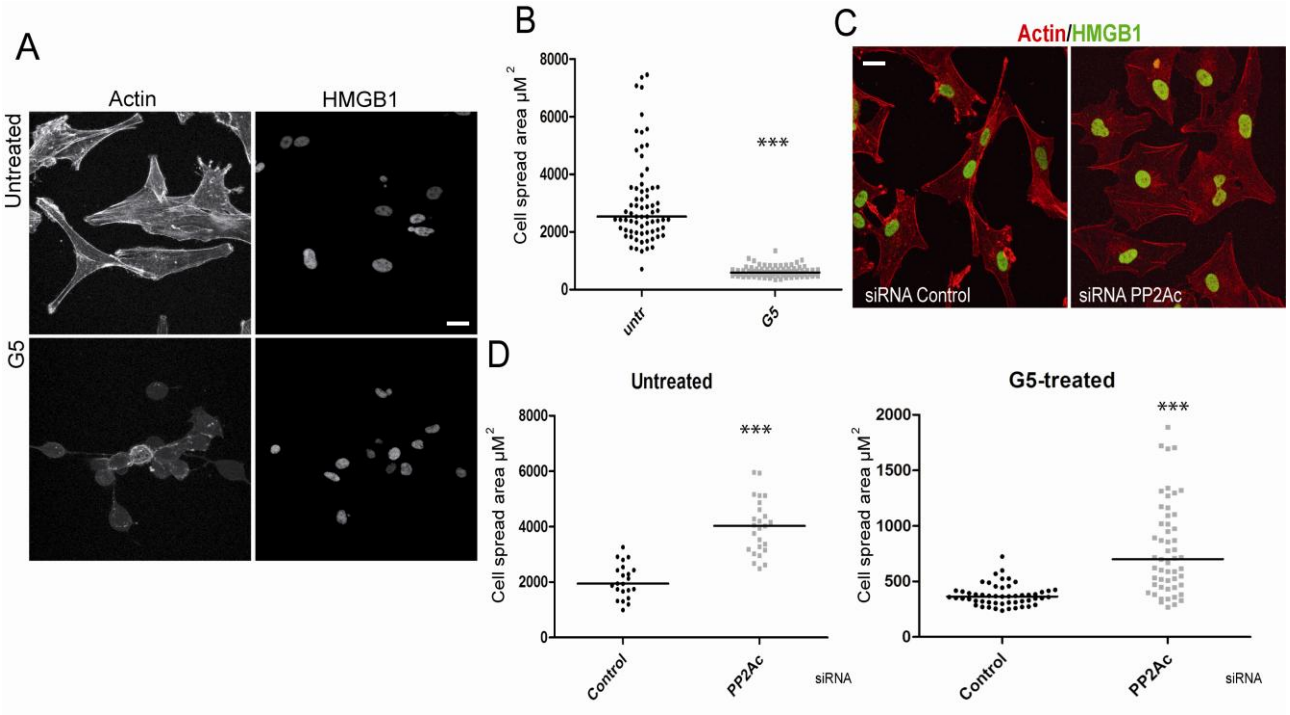

Figure *28. The role of actin cytoskeleton in the necrotic death elicited by G5.* A)U87MG/Bcl-xL cells were treated for 5hrs with G5 5µM. Immunofluorescence analysis were performed to visualize HMGB1 subcellular localization and TRITC-phalloidin was used to decorate actin filaments. B) Cells treated as in A) were analyzed by MetaMorph software to score cell spread area. 70 cells were analyzed for each

treatment, data are presented as median. C) U87MG/Bcl-xL cells, transfected with the indicated siRNAs were grown on glass coverslip for 40hrs. Immunofluorescences were performed to visualize HMGB1 subcellular localization and TRITC-phalloidin was used to decorate actin filaments. D) U87MG/Bcl-xL cells, transfected with the indicated siRNAs were grown on glass coverslip for 40hrs and next treated for 9hrs with DMSO or G5 5μM. Immunofluorescences were analyzed by MetaMorph software to score cell spread area, 100 cells were analyzed for each treatment, data are presented as median. Scale bar, 50μM.

To identify PP2A substrates that could be involved in transducing the necrotic signal we focused our attention to regulators of microfilaments dynamic. Cofilin-1, an actin binding protein with severing activity towards actin filaments was characterized as a PP2A substrate [134]. The activation of cofilin-1 actin depolymerizing function relies on the de-phosphorylation of a serine residue at position 3. Hence, we evaluated the status of cofilin-1 Ser 3 phosphorylation in response to G5. Figure 29 A illustrates that upon G5 treatment cofilin-1 is rapidly de-phosphorylated at serine 3. Next, we evaluated whether in U87MG cells PP2A controls this phosphorylation. In cells silenced for PP2A phosphorylation of Ser 3 is augmented and, following G5 treatment dephosphorylation of this residue is less pronounced (Fig. 29 B). Finally to prove the contribution of cofilin-1 dephosphorylation to the necrotic death elicited by G5 we generated glioblastoma cells stably expressing cofilin-1 wt, phosphomimic S/D substitution and dephosphomimic S/A substitution of serine 3. Immunoblot proved that the different constructs were expressed in U87MG cells, although the levels of the S3D mutant was in general reduced respect to the others (Fig. 29 C). When transgenic cells were treated with G5 necrotic cell death was partially but significantly reduced only in cells expressing the phophomimic S3D mutant that is impaired in the depolymerizing activity (Fig. 29 D).

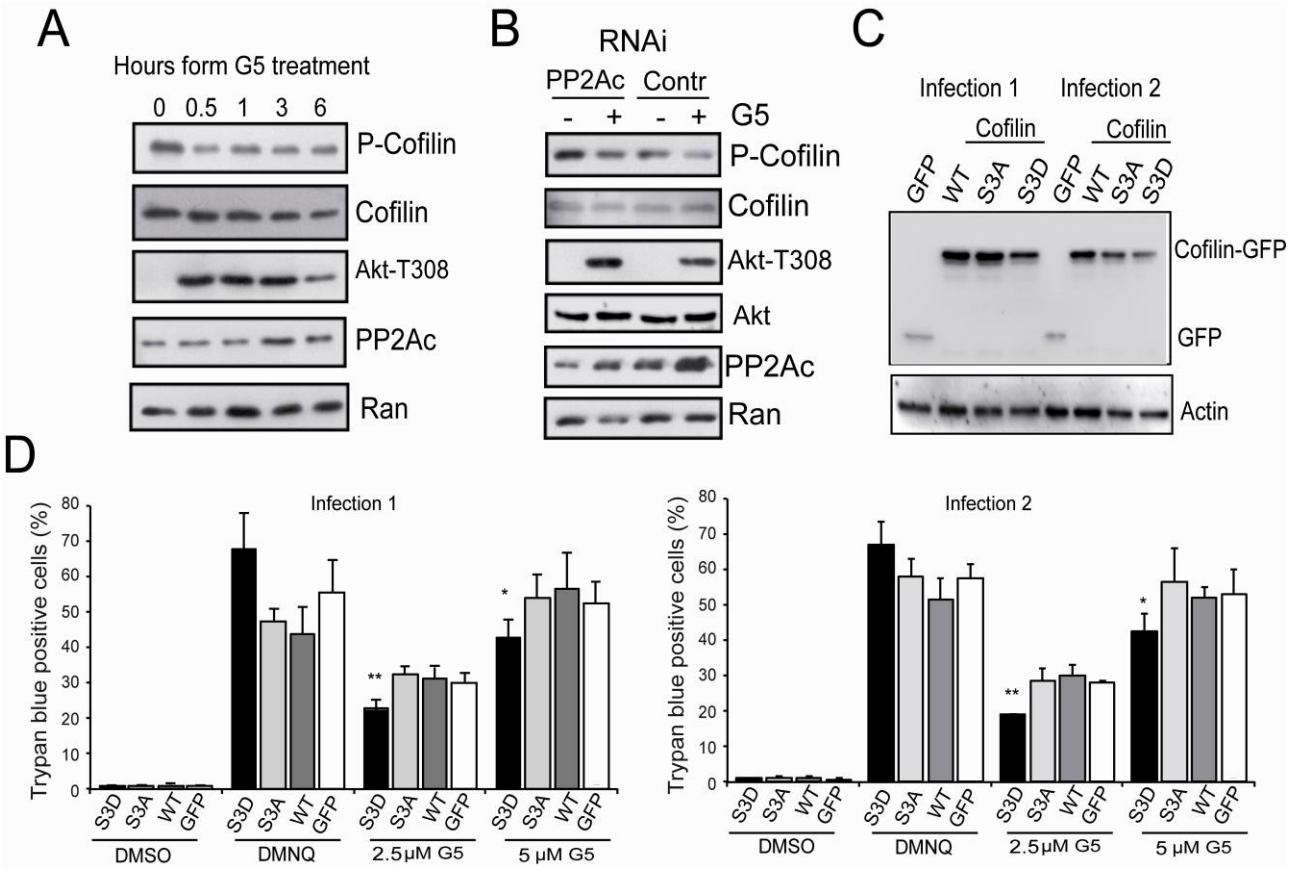

Figure 29. The role of actin cytoskeleton in the necrotic death elicited by G5. A) U87MG/Bcl-xL cells were treated with 10μM of G5 for the indicated times. Cellular lysates were generated and immunoblots performed with the indicated antibodies. B) U87MG/Bcl-xL cells treated with G5 and silenced for PP2Ac Cells were silenced for 48hrs and next treated with 10μM G5 for 1hr. Cellular lysates were generated and probed with the indicated antibodies. C) Characterization U87MG/Bcl-xL cells overexpressing GFP-cofilin WT, S3A or S3D phospho mutants, and GFP alone. Cellular lysates were generated and probed with the indicated antibodies. D) U87MG/Bcl-xL cells overexpressing GFP-cofilin WT, S3A or S3D phospho mutants, and GFP alone were generated and next treated with G5 5μM for 24hrs. The appearance of cell death was scored by Trypan blue staining. Data are presented as mean ± SD; n = 5.

Discussion

Traditionally considered a form of non-regulated cellular demise, necrosis has only recently become a recognized type of programmed cell death. During the past decade the traditional point of view radically changed, defining necrosis as a regulated mechanism with relevance during development and tissue homeostasis. A growing body of evidences describe alternative pathways of necrosis identifying different mediators and regulators for this form of cell death [87]. In this *scenario,* it is important to understand the signaling pathways and the molecular mechanisms that govern the regulated forms of necrosis in order to impact when their dysregulation is causative of diseases.

One of the cancer hallmarks is represented by the resistance to death, partly due to accumulation of mutations in the apoptotic machinery [135, 136]. It is mandatory for anti-cancer research to develop new drugs with the ability to kill cancer cells through alternative mechanisms, in particular through regulated forms of necrosis. Inhibition of the ubiquitin-proteasome system (UPS) represents a promising therapeutic opportunity. Inhibitors of the UPS usually exert anti-tumor activities by promoting apoptosis through multiple mechanisms. Induction of ER stress, activation of the death receptors and of the JNK pathway, suppression of NF-kB, induction of p53 and of the BH3-only proteins Noxa, Bim, and NBK/Bik [137]; they are all part of the complex stress response elicited by the block of protein-turnover.

We identified G5, as a non-selective isopeptidases inhibitor (NS-II) capable of eliciting different types of cell death [122, 128, 138]. Interestingly, G5 kills apoptosis-resistant cells with a peculiar necrotic cell death, regardless of common anti-necrotic agents, anti-oxidants or Ca^{2+} scavengers, overcoming JNK and PARP inhibition. Main feature of G5-induced necrosis is an early and dramatic actin/cytoskeleton alteration coupled to impairment in cell adhesion [128, 138].

The present work describes an alternative mechanism of programmed necrosis in U87MG glioblastoma cells. I have characterized the main cellular effects and identified in the Ser/Thr phosphatase PP2A a necrotic regulator, which possesses distinct functions in response to different insults. I have described two alternative pathways of regulated necrosis in response to isopeptidases inhibition and ROS induction, highlighting the existence of a distinct mechanism beyond necroptosis. G5 was previously characterized for its ability to elicit necrotic cell death in apoptotic resistant U87MG glioblastoma cells, but the underlying mechanisms of this effect

remained elusive [128]. Over-expression of Bcl-xL in U87MG cells, to enforce the anti-apoptotic character of U87MG cells, has no influence on the appearance of necrosis in response to both G5 and DMNQ. Moreover, caspases inhibition does not block G5-induced cell death. Thus, neither enhancement of anti-apoptotic machinery nor caspase inhibition block G5 and DMNQ necrotic triggers. Glioblastoma is widely described as an apoptotic resistant cancer, with limited response to conventional chemotherapy and the marked ability to escape from apoptotic stimuli. However concomitantly, high index of necrotic death represents a peculiar characteristic of glioblastoma multiforme. Here I have demonstrated that the pan isopeptidases inhibitor G5 and the ROS inducer DMNQ have the ability to by-pass the apoptotic resistance forcing glioma cells to undergo necrotic cell death.

To gain insight into the necrotic response, we initially evaluated the mitochondrial alteration previously associated to necroptosis and other necrotic deaths [139]. Mitochondria represent a key compartment for cell survival and are considered the main guardians of cell survival, representing the central node for the decision between life or death: energetic supply, compartmentalization of pro-apoptotic factors, source of ROS, ions buffering are fundamental processes governed by this organelle [98]. Mitochondria relevance during necrosis is well established. Alterations in metabolic processes [50], loss $\Delta\psi$ and MPT [100], depletion of ATP production [65] and finally modification of the mitochondrial tubular network [63, 122] are well known necrotic markers. Mitochondrial morphology lies on the balance between fission and fusion, maintained by Dynamin-like proteins. Alterations in the continuous and repetitive cycle of fusion and fission processes contribute to mitochondrial dysfunction and cell death [63] [101]. Fragmentation has been described during necrotic process provoking ROS over-production [63]. Confocal microscopy analysis of U87MG/Bcl-xL cells revealed that both stimuli trigger a dramatic mitochondrial fragmentation: 80% of the cells is characterized by mitochondrial fragmentation with peri-nuclear clusterization. However, this alteration is not paired with Smac release into the cytoplasm, indicating absence of MOMP and thus no release of apoptogens for the downstream activation of apoptosis.

A particular response to DMNQ treatment, recognized in a little percentage of cells was the overt alteration in mitochondria functionality, without MOMP (as scored by Smac release). This observation highlights that DMNQ can induce mitochondrial dysfunction and necrotic death, without MOMP. The investigation of mitochondrial fragmentation in response to G5, revealed that

its appearance precedes another peculiar response to UPSIs treatment: cytoplasmic vacuolization. Indeed treatments with ubiquitin-proteasome inhibitors induce endoplasmic reticulum (ER) stress, with engulfment and enlargement of the ER, which results in extensive cytoplasmic vacuolization [140].

Mitochondrial fragmentation has been defined as an obligate step during necroptotic process [63], thus we determined its requirement in response G5 and DMNQ. Interestingly programmed necrosis evoked by G5 does not rely on mitochondrial fragmentation for the completion of the process. On the opposite, DMNQ is tightly linked to mitochondrial fragmentation for the execution of regulated necrosis. Indeed the inhibition of Drp-1 fission protein, using its specific allosteric inhibitor Mdivi-1 or the over-expression of the dominant negative form of Drp-1 (K38A), significantly reduced cell death in response to DMNQ, while G5-mediated cell death was unaffected. In summary, mitochondrial fragmentation seems to be only a secondary effect during G5 induced necrosis.

The necroptotic pathway relies on the formation of the necrosome complex and on the activity of RIP1 to activate the downstream executioners. Using Necrostatin-1, a specific RIP1 inhibitor, we demonstrate once more the hypothesis that distinct pathways govern DMNQ and G5 regulated necrosis. DMNQ relies on necroptotic players with the involvement of the RIP1-Drp-1 axis and mitochondrial fragmentation, while G5 works independently from this pathway. These observations demonstrate the existence of alternative necrotic pathways beyond necroptosis, in which both RIP1 and Drp-1 resulted to be dispensable.

A plethora of biological processes is regulated by isopeptidases [117], thus not surprisingly several immediate responses are stimulated by NS-II. Upon G5 different pro-survival signalling pathway and stress response are engaged. Here we observed the rapid and transient activation of p38, ERK and Akt pathways while JNK phosphorylation was not observed during G5 treatment. JNK kinase is a mediator of certain necrotic responses [69] but the lack of its activation in glioblastoma cells confirms also previous results, where although JNK was activated its inhibition did not influenced G5 necrotic death [138].

Interestingly, after an initial increase dephosphorylation of Akt at Thr308 is coupled to necrosis appearance and it parallels the increase of PP2A catalytic subunit. PP2A is a pleiotropic enzyme controlling a huge number of activities including cell cycle progression, survival and apoptosis [141]. The heterotrimeric PP2A holoenzyme exhibits substrate specificity, on the basis of the

several alternative regulatory subunits found in the complex [142]. This heterogeneous molecular architecture could explain the apparent paradox of the antagonistic responses.

Via negative control of PI3K/Akt pathway and regulating anti-apoptotic Bcl-2 proteins and activating pro-apoptotic factors, such as BAD and BIM, PP2A can influence survival [143]. A pro-death role of PP2A has been reported in response for death receptor stimulation, impinging on different signalling cascades, such MAPKs or NF-kB. PP2A activating drugs has been recently demonstrated to markedly reduce survival and self-renewal of CML quiescent HSCs, while sparing normal HSCs [144]. The re-activation of PP2A in CML cells provoked apoptosis.

The down-regulation of PP2Ac highlighted its "double edge sword" role during necrosis. PP2A is required during G5-mediated cell death, while it counteracts necrotic death provoked by DMNQ. As I observed in the case of ROS inducer DMNQ, the protective role of PP2A was similarly demonstrated upon H_2O_2 treatment [145]. The role of PP2A was confirmed by the reduction of mitochondrial fragmentation and the diminished release of nuclear HMGB1, markers of G5-mediated necrotic cell death.

Here I determined the accumulation/activation of the catalytic subunit upon G5 treatment, moreover interestingly we determined a re-localization of the protein into the cytoplasm early during necrosis. The accumulation of PP2A into the cytosol is timely coupled with HMGB1 release. This phenomenon needs to be further characterized to discern between a stress response with an indiscriminate release of several molecules or a specific spatial and temporal regulation of PP2Ac localization during the necrotic response. Certainly, in addition to the increased activity linked to G5 treatment also enzyme redistribution could contribute to generate a necrotic specific phosphoproteome.

The outstanding effect of PP2A during G5-mediated necrosis was observed at the level of actin cytoskeleton organization of U87MG cells. PP2A down-regulation increases the spreading area and consequently reduces the early and dramatic detachment of the cells in response to isopeptidases inhibition. My observation on PP2A sustains previous studies on G5-induced necrosis where actin de-polymerazion was reported [138]. Furthermore, G5-induced necrosis is highly dependent from adhesion signals [128, 138]. Interestingly G5 is not a unique signal capable of eliciting a cytoskeletal-dependent apoptosis (i.e. Citochalasins, Lantruculin, Nocodazole, Paclitaxel).

Curiously, although relationships between PP2A and actin/cytoskeleton or microtubules structures have been studied in the past, very few substrates influencing the cytoskeleton have

been identified. Cofilin-1, an actin binding protein with severing activity towards actin filaments, is a PP2A substrate [134]. The activation of actin depolymerizing function of cofilin-1 relies on the de-phosphorylation of serine residue at position 3. In this thesis, I observed a partial but reproducible anti-necrotic effect of the phospho-mimic mutant of Cofilin-1. Interestingly, G5 treatment elicited a rapid decrease of Cofilin-1 Ser3 phosphorylation. The down-regulation of PP2Ac increased Ser 3 phosphorylation and the concomitant treatment with G5 attenuated the de-phosphorylation/activation of Cofilin respect to control. However, the modest protective effect observed with the phosphor-mimic mutant of Cofilin-1 during G5-induced cell death leads to consider that other biological targets of PP2Ac and actin/cytoskeleton elements are involved in the PP2A dependent modulation of adhesion in glioblastoma cells.

A specific investigation should be addressed to clarify how adhesion to the extracellular matrix, elements of the actin/cytoskeleton and PP2A create a cellular state resistant or susceptible to G5 mediated cell death. PP2Ac was previously proposed as a regulator of adhesion properties and actin/cytoskeleton organization [146, 147], possibly through its influence on integrins signaling or DAPK and RhoA/ROCK/MLC signaling pathways.

Akt was previously recognized as a modulator of necrotic death [131, 132], with different roles, either pro- or anti-necrotic. G5 treatment, provokes a concomitant increased of Thr308 and reduced Ser473 phosphorylation in U87MG cells which represent a PTEN mutated context, thus highlighting a possible peculiar regulation of its kinase activity. However, although the down-regulation of PP2A sustains the phosphorylation of Thr308 of Akt, this kinase does not play a critical role during necrosis in response to G5 and DMNQ.

Conclusions

The definition of necroptosis represented the starting point for introducing the new concept of regulated necrosis. However, regulated necrosis is not limited merely to necroptosis. The results obtained in this thesis describe and sustain the existence of alternative necrotic programs. DMNQ necrotic cell death is dependent on the canonical necroptotic elements while G5 relies on different players. In glioblastoma cells, we identify PP2Ac, which could be considered a new mediator of the necrotic cell death. However, in our experimental models, not surprisingly, PP2Ac acts with opposite consequences depending from the specific context. Moreover, I finally proved for the first time a connection between PP2A, actin/cytoskeleton remodeling and necrotic death, thus defining a signaling pathway that could be pharmaceutically targeted. It will be important to investigate whether this necrotic signaling is linked to specific pathological status.

Our focus on the necrotic cell death induced by the non-selective isopeptidases inhibitor G5 is motivated by the therapeutic implications. The stimulation of necrosis as a strategy to overcome apoptotic resistance of cancer cells represents an interesting opportunity that needs to be fully verified in vivo.

Materials & Methods

Cell Culture Conditions, Cell Death, and Retroviral Infection

Human GBM cell lines U87MG were grown in DMEM supplemented with 10% fetal bovine serum, penicillin (100 U/mL), glutamine (2 mmol/L), and streptomycin (100 µg/mL) at 37°C in 5% CO2 atmosphere. U87MG cells expressing Bcl-xL, Drp1 K38A, GFP, Cofilin constructs, myristoylated-Akt, were generated by retroviral infection (12). pBABE-puro-hDrp1(K38A), were bought from Addgene (plasmid #37243). pMXS PURO vectors encoding GFP, cofilin-1-GFP, cofilin-1 S3A-GFP, cofilin-1 S3D-GFP were received from prof. Anne Blangy [148], Montpellier, France. Briefly, retroviral vectors were transfected in the amphotropic packaging cell line LinXa with the calcium phosphate method. After 60 h post-transfection, viral supernatants were collected, filtered, supplemented with 8 µg/ml Polybrene, and combined with fresh medium in order to infect U87MG cells.

In all trypan blue exclusion assays, at least 400 cells from three independent samples were counted for each data point. Data were represented as arithmetic mean±SD for at least three independent experiments. Resazurin assay was performed adding resazurin sodium salt (Sigma Aldrich) to the medium for 1hr (final concentration 10µM) and analyzed by EnSpire Multimode Plate Reader.

RNA interference

Stealth RNA interference (RNAi) were purchased from Invitrogen (Carlsbad, CA) and from Dharmacon. Stealth RNAi were purchased from Invitrogen: PP2A/C RNAi (base pairs PP2A, FW 5′-GCAAGAGGUUCGAUGUCCAGUUACU-3′; RV 5′-AGUAACUGGACAUCGAACCUCUUGC-3′); scramble control siRNA CCAGTATTTGCTTAGGAAGCACTAT. Dharmacon RNAi: ON-target plus PP2Ac (target sequence CCGGAAUGUAGUAACGAUU) or ON-target plus non-targeting control #1 (Dharmacon, Thermo Fisher Scientific). Cells were transfected 24 hours after plating by adding the Opti-MEM medium containing LipofectAMINE (Invitrogen) plus RNAi oligos at final concentrations 50-100nM.

Western Blotting

Proteins obtained after an SDS denaturating lysis and sonication were transferred to a 0.2-µm-pore-sized nitrocellulose membrane and incubated with the specific primary antibodies. After several washes, blots were incubated with peroxidase-conjugated goat anti-rabbit or goat anti-mouse (Sigma) for 1 h at room temperature. Finally, blots were developed with Super Signal West Dura, as recommended by the vendor (Pierce). For primary antibody stripping, blots were incubated for 30 min at 60°C in stripping solution (62.5mM Tris-HCl pH 6.8, 2% SDS) containing 100 mM β-mercaptoethanol. Quantitative densitometric analysis of immunoblots were performed by ChemiDoc software (BioRad).

PPase assay

Cells were lysed directly in Petri dishes with lysis buffer (50 mM Tris-HCl, pH 8.0, 100 mM NaCl, 2 mM EDTA, and 1% (v/v) Igepal CA-630, PMSF and proteases inhibitor cocktail (Sigma)), collected with cell scraper and subjected to immunoprecipitation. Whole cell lysates were incubated over night with total of 1.5 µg of anti-PP2Ac or anti-FLAG as a control IgG of immunoprecipitation. After 1 h of incubation with protein A-beads (GE healtcare), several washes were performed with Lysis buffer. Beads immuno-complexes were resuspended in phosphatase assay buffer (50 m*M* Tris-HCl pH 7.0, and 0.1 m*M* $CaCl_2$), incubated for 30 min at 37°C with or without Okadaic acid–sodium salt 100nM (Alexis USA, San Diego, CA), in presence of 1mM $NiCl_2$ and 0.125 mg/mL BSA and then analyzed by fluorimetric assay using 6,8-difluoro-4-methylumbelliferyl phosphate (DiFMUP; Molecular Probes, Eugene, OR) substrate as described in [149], with EnSpire Multimode Plate Reader using 96 multiwells black plates (excitation: 358nm emission: 455nm wavelengths). Immunocomplexes were recollected after the fluorimetric assay and next resolved in SDS/PAGE electrophoresis and immunoblotted to verify the amount of PP2Ac.

Reagents and Antibodies

The following chemicals were used (the final concentrations are indicated): LY (LY294002; LC laboratories), BOC-D-fluoromethylketone (Imgenex), Velcade/Bortezomib (LC laboratories) 2,3-Dimethoxy-1,4-naphthoquinone (DMNQ), Necrostatin-1; resazurin sodium salt, Mdivi-1 and dimethyl sulfoxide (DMSO) (all from Sigma-Aldrich), Mitotraker Red CMXRos (Molecular Probes Probes, Inc. Eugene, OR). Primary antibodies: anti hemagglutinin (anti-HA), anti-FLAG and anti-Actin (Sigma-Aldrich), anti-nucleoporin p62, anti-RAN, anti-Bcl-xL, anti-Drp1 (DLP1) (BD,

Bioscences), anti-JNK pThr183/Tyr185, anti-JNK, anti-p38, anti-phospho p38, anti-Erk, ant-pErk, anti-Akt, anti-Akt p473, anti-Akt p308 (Cell Signaling), anti-F1-ATP synthase, anti-cofilin-1 and anti-Ser3 phospho cofilin-1 (Santa Cruz Biotechnologies), anti-Smac/DIABLO [150], anti-PP2A/C subunit, anti-PP2A/A subunit (Upstate, Lake Placid, NY); anti-HMGB1 (AbCam, Cambridge, UK).

Immunofluorescence microscopy.

Mitochondria were labeled in vivo for 1 hour with 25 nmol/L MitoTracker Red CMXRos (Molecular Probes, Eugene, OR). Concavanalin-A biotin conjugated from Sigma was used to stain cytoplasmic structures, Alexa Fluor 488 streptavidin (Molecular Probes, Eugene, OR). Phalloidin-TRITC (Sigma) was used to visualize actin filaments (Molecular Probes, Eugene, OR). After 16 hours of treatment with the different compounds, cells were fixed with 3% paraformaldehyde in PBS for 20 minutes at room temperature. Fixed cells were washed with PBS/ 0.1 mol/L glycine (pH 7.5) and then permeabilized with 0.1%-0.5% Triton X-100 in PBS for 5 minutes. The coverslips were treated with specific antibodies diluted in PBS for 45 minutes in a moist chamber at 37°C. They were then washed twice with PBS and incubated with Alexa Fluor 488–conjugated secondary antibodies (Molecular Probes) for 30 minutes at 37°C. Cells were examined by epifluorescence and images were collected with a cooled CCD camera mounted on a time-lapse imaging system (Leica AF6000 LX), and they were analyzed using MetaMorph software or with a Zeiss (Oberkochen, Germany) Axiovert 35 microscope or with a Leica (Wetzlar, Germany) SP laser scan microscope equipped with a 488-nm argon laser and a 543-nm helium neon laser. Cell images for deconvolution were

taken using the Leica AF6000 LX microscope at X63 magnification and z-stacks were captured for each cell. The LAS AF Deconvolution software was used for image deconvolution and three-dimensional view reconstruction. Quantification analysis were performed by counting at least 200 cells in three different experiments, or by MetaMorph software.

Statistical analysis

Results are expressed as the means ± SD, Student's *t* test was performed with Excel software. p-values are represented as: * $p < 0.05$, ** $p < 0.01$, *** $p < 0.005$. Data of spreading area in Fig. 28 were analyzed using Non-parametric Mann-Whitney test (Prism GraphPad Software); *** $p < 0.0001$.

Acknowledgments

Firstly, I would like to thank my supervisor, Pr. Claudio Brancolini for accepting me as his PhD student. I consider myself extremely lucky to have had the chance to work with him and to face the research field with critical thinking every day. A very special thanks to Prof. Tatiana Cosima Baldari; her expertise, critical thinking and kindness added considerably to my experience. I thank Anne Blangy for providing me cofilin-1 constructs.

I would like to thank AIRC to fund my current research activity (Annual Fellowship 2014 "Centro Studi Ricerche Ligabue" Rif. 15048).

I am heartily grateful to Dr. Andrea Clocchiatti; his scientific knowledge, kindness and scholarship were fundamental to my academic and personal growth. Thank you so much Clocchete.

I would like to extend my deepest gratitude to Eros, Paolo, Andrea S., Rosario, Enrico and Giulia, whose collaboration, help and friendship have been essential in my PhD experience. Thanks for making my working days very pleasant.

Last but not least, I would like to thank my families and friends for their constant and precious support, encouragement and patience during these years. Thanks for your smile, thank you for making me smile: I love you all.

Pubblications

Characterization of caspase-dependent and caspase-independent deaths in glioblastoma cells treated with inhibitors of the ubiquitin-proteasome system.

Foti C., Florean C., Pezzutto A., Roncaglia P., **Tomasella A.**, Gustincich S., Brancolini C. Mol Cancer Ther. 2009 Nov;8(11):3140-50. Impact Factor 5.56.

Type I IFNs signaling and apoptosis resistance in glioblastoma cells.

Sgorbissa A., **Tomasella A.**, Potu H., Manini I, and Brancolini C. Apoptosis 2011, Vol 16; 1229-44. Impact factor 3.95.

The DeISGylase USP18 limits TRAIL-induced apoptosis through the regulation of TRAIL levels: Cellular levels of TRAIL influences responsiveness to TRAIL-induced apoptosis.

Manini I., Sgorbissa A., Potu H., **Tomasella A.**, Brancolini C. Cancer Biol Ther. 2013 Sep 19;14(12).Impact Factor 3.29.

Bibliography

1. **Giorgio, M., et al., *Hydrogen peroxide: a metabolic by-product or a common mediator of ageing signals?* Nat Rev Mol Cell Biol, 2007. 8(9): p. 722-8.**
2. **Taylor, R.C., S.P. Cullen, and S.J. Martin, *Apoptosis: controlled demolition at the cellular level.* Nat Rev Mol Cell Biol, 2008. 9(3): p. 231-41.**
3. **Cotter, T.G., *Apoptosis and cancer: the genesis of a research field.* Nat Rev Cancer, 2009. 9(7): p. 501-7.**
4. **Vaux, D.L., S. Cory, and J.M. Adams, *Bcl-2 gene promotes haemopoietic cell survival and cooperates with c-myc to immortalize pre-B cells.* Nature, 1988. 335(6189): p. 440-2.**
5. **Tsujimoto, Y., *Stress-resistance conferred by high level of bcl-2 alpha protein in human B lymphoblastoid cell.* Oncogene, 1989. 4(11): p. 1331-6.**
6. **Chautan, M., et al., *Interdigital cell death can occur through a necrotic and caspase-independent pathway.* Curr Biol, 1999. 9(17): p. 967-70.**
7. **Vandenabeele, P., et al., *Molecular mechanisms of necroptosis: an ordered cellular explosion.* Nat Rev Mol Cell Biol, 2010. 11(10): p. 700-14.**
8. **Golstein, P. and G. Kroemer, *Cell death by necrosis: towards a molecular definition.* Trends Biochem Sci, 2007. 32(1): p. 37-43.**
9. **Kerr, J.F., A.H. Wyllie, and A.R. Currie, *Apoptosis: a basic biological phenomenon with wide-ranging implications in tissue kinetics.* Br J Cancer, 1972. 26(4): p. 239-57.**
10. **Thornberry, N.A. and Y. Lazebnik, *Caspases: enemies within.* Science, 1998. 281(5381): p. 1312-6.**
11. **Ashkenazi, A., *Directing cancer cells to self-destruct with pro-apoptotic receptor agonists.* Nat Rev Drug Discov, 2008. 7(12): p. 1001-12.**
12. **Ea, C.K., et al., *Activation of IKK by TNFalpha requires site-specific ubiquitination of RIP1 and polyubiquitin binding by NEMO.* Mol Cell, 2006. 22(2): p. 245-57.**
13. **Laster, S.M., J.G. Wood, and L.R. Gooding, *Tumor necrosis factor can induce both apoptic and necrotic forms of cell lysis.* J Immunol, 1988. 141(8): p. 2629-34.**
14. **Letai, A.G., *Diagnosing and exploiting cancer's addiction to blocks in apoptosis.* Nat Rev Cancer, 2008. 8(2): p. 121-32.**
15. **Chipuk, J.E., et al., *The BCL-2 family reunion.* Mol Cell, 2010. 37(3): p. 299-310.**
16. **Sheridan, C., et al., *Bax- or Bak-induced mitochondrial fission can be uncoupled from cytochrome C release.* Mol Cell, 2008. 31(4): p. 570-85.**
17. **Degterev, A., et al., *Chemical inhibitor of nonapoptotic cell death with therapeutic potential for ischemic brain injury.* Nat Chem Biol, 2005. 1(2): p. 112-9.**
18. **Degterev, A., et al., *Identification of RIP1 kinase as a specific cellular target of necrostatins.* Nat Chem Biol, 2008. 4(5): p. 313-21.**
19. **Lim, S.Y., et al., *The cardioprotective effect of necrostatin requires the cyclophilin-D component of the mitochondrial permeability transition pore.* Cardiovasc Drugs Ther, 2007. 21(6): p. 467-9.**
20. **Barkla, D.H. and P.R. Gibson, *The fate of epithelial cells in the human large intestine.* Pathology, 1999. 31(3): p. 230-8.**
21. **Roach, H.I. and N.M. Clarke, *Physiological cell death of chondrocytes in vivo is not confined to apoptosis. New observations on the mammalian growth plate.* J Bone Joint Surg Br, 2000. 82(4): p. 601-13.**
22. **Artal-Sanz, M. and N. Tavernarakis, *Proteolytic mechanisms in necrotic cell death and neurodegeneration.* FEBS Lett, 2005. 579(15): p. 3287-96.**

23. **Millay, D.P., et al., *Genetic and pharmacologic inhibition of mitochondrial-dependent necrosis attenuates muscular dystrophy.* Nat Med, 2008. 14(4): p. 442-7.**
24. **He, S., et al., *Receptor interacting protein kinase-3 determines cellular necrotic response to TNF-alpha.* Cell, 2009. 137(6): p. 1100-11.**
25. **Liu, P., et al., *Dysregulation of TNFalpha-induced necroptotic signaling in chronic lymphocytic leukemia: suppression of CYLD gene by LEF1.* Leukemia, 2012. 26(6): p. 1293-300.**
26. **Majno, G. and I. Joris, *Apoptosis, oncosis, and necrosis. An overview of cell death.* Am J Pathol, 1995. 146(1): p. 3-15.**
27. **Welz, P.S., et al., *FADD prevents RIP3-mediated epithelial cell necrosis and chronic intestinal inflammation.* Nature, 2011. 477(7364): p. 330-4.**
28. **Zhang, H., et al., *Functional complementation between FADD and RIP1 in embryos and lymphocytes.* Nature, 2011. 471(7338): p. 373-6.**
29. **Bonnet, M.C., et al., *The adaptor protein FADD protects epidermal keratinocytes from necroptosis in vivo and prevents skin inflammation.* Immunity, 2011. 35(4): p. 572-82.**
30. **Holler, N., et al., *Fas triggers an alternative, caspase-8-independent cell death pathway using the kinase RIP as effector molecule.* Nat Immunol, 2000. 1(6): p. 489-95.**
31. **Vercammen, D., et al., *Inhibition of caspases increases the sensitivity of L929 cells to necrosis mediated by tumor necrosis factor.* J Exp Med, 1998. 187(9): p. 1477-85.**
32. **Chan, F.K., et al., *A role for tumor necrosis factor receptor-2 and receptor-interacting protein in programmed necrosis and antiviral responses.* J Biol Chem, 2003. 278(51): p. 51613-21.**
33. **Micheau, O. and J. Tschopp, *Induction of TNF receptor I-mediated apoptosis via two sequential signaling complexes.* Cell, 2003. 114(2): p. 181-90.**
34. **Bertrand, M.J., et al., *cIAP1 and cIAP2 facilitate cancer cell survival by functioning as E3 ligases that promote RIP1 ubiquitination.* Mol Cell, 2008. 30(6): p. 689-700.**
35. **Xu, G., et al., *Ubiquitin-specific peptidase 21 inhibits tumor necrosis factor alpha-induced nuclear factor kappaB activation via binding to and deubiquitinating receptor-interacting protein 1.* J Biol Chem, 2010. 285(2): p. 969-78.**
36. **Christofferson, D.E. and J. Yuan, *Necroptosis as an alternative form of programmed cell death.* Curr Opin Cell Biol, 2010. 22(2): p. 263-8.**
37. **Cho, Y.S., et al., *Phosphorylation-driven assembly of the RIP1-RIP3 complex regulates programmed necrosis and virus-induced inflammation.* Cell, 2009. 137(6): p. 1112-23.**
38. **Chen, M.C., et al., *The role of apoptosis signal-regulating kinase 1 in lymphotoxin-beta receptor-mediated cell death.* J Biol Chem, 2003. 278(18): p. 16073-81.**
39. **Lin, Y., et al., *Cleavage of the death domain kinase RIP by caspase-8 prompts TNF-induced apoptosis.* Genes Dev, 1999. 13(19): p. 2514-26.**
40. **Feng, S., et al., *Cleavage of RIP3 inactivates its caspase-independent apoptosis pathway by removal of kinase domain.* Cell Signal, 2007. 19(10): p. 2056-67.**
41. **Feoktistova, M., et al., *cIAPs block Ripoptosome formation, a RIP1/caspase-8 containing intracellular cell death complex differentially regulated by cFLIP isoforms.* Mol Cell, 2011. 43(3): p. 449-63.**
42. **Wang, L., F. Du, and X. Wang, *TNF-alpha induces two distinct caspase-8 activation pathways.* Cell, 2008. 133(4): p. 693-703.**
43. **Hitomi, J., et al., *Identification of a molecular signaling network that regulates a cellular necrotic cell death pathway.* Cell, 2008. 135(7): p. 1311-23.**
44. **Tenev, T., et al., *The Ripoptosome, a signaling platform that assembles in response to genotoxic stress and loss of IAPs.* Mol Cell, 2011. 43(3): p. 432-48.**
45. **Festjens, N., et al., *RIP1, a kinase on the crossroads of a cell's decision to live or die.* Cell Death Differ, 2007. 14(3): p. 400-10.**
46. **Declercq, W., T. Vanden Berghe, and P. Vandenabeele, *RIP kinases at the crossroads of cell death and survival.* Cell, 2009. 138(2): p. 229-32.**

47. **Ofengeim, D. and J. Yuan, *Regulation of RIP1 kinase signalling at the crossroads of inflammation and cell death.* Nat Rev Mol Cell Biol, 2013. 14(11): p. 727-36.**
48. **Xie, T., et al., *Structural basis of RIP1 inhibition by necrostatins.* Structure, 2013. 21(3): p. 493-9.**
49. **Newton, K., X. Sun, and V.M. Dixit, *Kinase RIP3 is dispensable for normal NF-kappa Bs, signaling by the B-cell and T-cell receptors, tumor necrosis factor receptor 1, and Toll-like receptors 2 and 4.* Mol Cell Biol, 2004. 24(4): p. 1464-9.**
50. **Zhang, D.W., et al., *RIP3, an energy metabolism regulator that switches TNF-induced cell death from apoptosis to necrosis.* Science, 2009. 325(5938): p. 332-6.**
51. **Li, J., et al., *The RIP1/RIP3 necrosome forms a functional amyloid signaling complex required for programmed necrosis.* Cell, 2012. 150(2): p. 339-50.**
52. **Upton, J.W., W.J. Kaiser, and E.S. Mocarski, *Virus inhibition of RIP3-dependent necrosis.* Cell Host Microbe, 2010. 7(4): p. 302-13.**
53. **Vanlangenakker, N., et al., *TNF-induced necroptosis in L929 cells is tightly regulated by multiple TNFR1 complex I and II members.* Cell Death Dis, 2011. 2: p. e230.**
54. **Roychowdhury, S., et al., *Absence of receptor interacting protein kinase 3 prevents ethanol-induced liver injury.* Hepatology, 2013. 57(5): p. 1773-83.**
55. **Kaiser, W.J., et al., *RIP3 mediates the embryonic lethality of caspase-8-deficient mice.* Nature, 2011. 471(7338): p. 368-72.**
56. **Oberst, A., et al., *Catalytic activity of the caspase-8-FLIP(L) complex inhibits RIPK3-dependent necrosis.* Nature, 2011. 471(7338): p. 363-7.**
57. **Lin, J., et al., *A role of RIP3-mediated macrophage necrosis in atherosclerosis development.* Cell Rep, 2013. 3(1): p. 200-10.**
58. **Vitner, E.B., et al., *RIPK3 as a potential therapeutic target for Gaucher's disease.* Nat Med, 2014.**
59. **Re, D.B., et al., *Necroptosis Drives Motor Neuron Death in Models of Both Sporadic and Familial ALS.* Neuron, 2014.**
60. **Sun, L., et al., *Mixed lineage kinase domain-like protein mediates necrosis signaling downstream of RIP3 kinase.* Cell, 2012. 148(1-2): p. 213-27.**
61. **Murphy, J.M., et al., *The pseudokinase MLKL mediates necroptosis via a molecular switch mechanism.* Immunity, 2013. 39(3): p. 443-53.**
62. **Cai, Z., et al., *Plasma membrane translocation of trimerized MLKL protein is required for TNF-induced necroptosis.* Nat Cell Biol, 2014. 16(1): p. 55-65.**
63. **Wang, Z., et al., *The mitochondrial phosphatase PGAM5 functions at the convergence point of multiple necrotic death pathways.* Cell, 2012. 148(1-2): p. 228-43.**
64. **Takeda, K., et al., *Mitochondrial phosphoglycerate mutase 5 uses alternate catalytic activity as a protein serine/threonine phosphatase to activate ASK1.* Proc Natl Acad Sci U S A, 2009. 106(30): p. 12301-5.**
65. **Leist, M., et al., *Intracellular adenosine triphosphate (ATP) concentration: a switch in the decision between apoptosis and necrosis.* J Exp Med, 1997. 185(8): p. 1481-6.**
66. **Vanden Berghe, T., et al., *Necroptosis, necrosis and secondary necrosis converge on similar cellular disintegration features.* Cell Death Differ, 2010. 17(6): p. 922-30.**
67. **Temkin, V., et al., *Inhibition of ADP/ATP exchange in receptor-interacting protein-mediated necrosis.* Mol Cell Biol, 2006. 26(6): p. 2215-25.**
68. **Nakagawa, T., et al., *Cyclophilin D-dependent mitochondrial permeability transition regulates some necrotic but not apoptotic cell death.* Nature, 2005. 434(7033): p. 652-8.**
69. **Xu, Y., et al., *Poly(ADP-ribose) polymerase-1 signaling to mitochondria in necrotic cell death requires RIP1/TRAF2-mediated JNK1 activation.* J Biol Chem, 2006. 281(13): p. 8788-95.**
70. **Zhao, J., et al., *Mixed lineage kinase domain-like is a key receptor interacting protein 3 downstream component of TNF-induced necrosis.* Proc Natl Acad Sci U S A, 2012. 109(14): p. 5322-7.**

71. **Upton, J.W., W.J. Kaiser, and E.S. Mocarski, *Cytomegalovirus M45 cell death suppression requires receptor-interacting protein (RIP) homotypic interaction motif (RHIM)-dependent interaction with RIP1.* J Biol Chem, 2008. 283(25): p. 16966-70.**
72. **Vanlangenakker, N., T. Vanden Berghe, and P. Vandenabeele, *Many stimuli pull the necrotic trigger, an overview.* Cell Death Differ, 2012. 19(1): p. 75-86.**
73. **Doitsh, G., et al., *Cell death by pyroptosis drives CD4 T-cell depletion in HIV-1 infection.* Nature, 2014. 505(7484): p. 509-14.**
74. **Willingham, S.B., et al., *Microbial pathogen-induced necrotic cell death mediated by the inflammasome components CIAS1/cryopyrin/NLRP3 and ASC.* Cell Host Microbe, 2007. 2(3): p. 147-59.**
75. **Willingham, S.B., et al., *NLRP3 (NALP3, Cryopyrin) facilitates in vivo caspase-1 activation, necrosis, and HMGB1 release via inflammasome-dependent and -independent pathways.* J Immunol, 2009. 183(3): p. 2008-15.**
76. **Moquin, D. and F.K. Chan, *The molecular regulation of programmed necrotic cell injury.* Trends Biochem Sci, 2010. 35(8): p. 434-41.**
77. **Matthews, N., et al., *Tumour cell killing by tumour necrosis factor: inhibition by anaerobic conditions, free-radical scavengers and inhibitors of arachidonate metabolism.* Immunology, 1987. 62(1): p. 153-5.**
78. **Schulze-Osthoff, K., et al., *Cytotoxic activity of tumor necrosis factor is mediated by early damage of mitochondrial functions. Evidence for the involvement of mitochondrial radical generation.* J Biol Chem, 1992. 267(8): p. 5317-23.**
79. **Giorgio, V., et al., *Dimers of mitochondrial ATP synthase form the permeability transition pore.* Proc Natl Acad Sci U S A, 2013. 110(15): p. 5887-92.**
80. **Clarke, S.J., G.P. McStay, and A.P. Halestrap, *Sanglifehrin A acts as a potent inhibitor of the mitochondrial permeability transition and reperfusion injury of the heart by binding to cyclophilin-D at a different site from cyclosporin A.* J Biol Chem, 2002. 277(38): p. 34793-9.**
81. **Devalaraja-Narashimha, K., A.M. Diener, and B.J. Padanilam, *Cyclophilin D gene ablation protects mice from ischemic renal injury.* Am J Physiol Renal Physiol, 2009. 297(3): p. F749-59.**
82. **Wang, X., et al., *Developmental shift of cyclophilin D contribution to hypoxic-ischemic brain injury.* J Neurosci, 2009. 29(8): p. 2588-96.**
83. **Baines, C.P., et al., *Loss of cyclophilin D reveals a critical role for mitochondrial permeability transition in cell death.* Nature, 2005. 434(7033): p. 658-62.**
84. **Du, H., et al., *Cyclophilin D deficiency attenuates mitochondrial and neuronal perturbation and ameliorates learning and memory in Alzheimer's disease.* Nat Med, 2008. 14(10): p. 1097-105.**
85. **Vaseva, A.V., et al., *p53 opens the mitochondrial permeability transition pore to trigger necrosis.* Cell, 2012. 149(7): p. 1536-48.**
86. **Forte, M., et al., *Cyclophilin D inactivation protects axons in experimental autoimmune encephalomyelitis, an animal model of multiple sclerosis.* Proc Natl Acad Sci U S A, 2007. 104(18): p. 7558-63.**
87. **Vanden Berghe, T., et al., *Regulated necrosis: the expanding network of non-apoptotic cell death pathways.* Nat Rev Mol Cell Biol, 2014. 15(2): p. 135-47.**
88. **Vanlangenakker, N., et al., *Molecular mechanisms and pathophysiology of necrotic cell death.* Curr Mol Med, 2008. 8(3): p. 207-20.**
89. **Moubarak, R.S., et al., *Sequential activation of poly(ADP-ribose) polymerase 1, calpains, and Bax is essential in apoptosis-inducing factor-mediated programmed necrosis.* Mol Cell Biol, 2007. 27(13): p. 4844-62.**
90. **Virag, L., A.L. Salzman, and C. Szabo, *Poly(ADP-ribose) synthetase activation mediates mitochondrial injury during oxidant-induced cell death.* J Immunol, 1998. 161(7): p. 3753-9.**
91. **Palomba, L., et al., *Prevention of necrosis and activation of apoptosis in oxidatively injured human myeloid leukemia U937 cells.* FEBS Lett, 1996. 390(1): p. 91-4.**

92. **Wang, Y., et al.,** ***Calpain activation is not required for AIF translocation in PARP-1-dependent cell death (parthanatos).*** **J Neurochem, 2009. 110(2): p. 687-96.**
93. **Dixon, S.J., et al.,** ***Ferroptosis: an iron-dependent form of nonapoptotic cell death.*** **Cell, 2012. 149(5): p. 1060-72.**
94. **Yang, W.S., et al.,** ***Regulation of Ferroptotic Cancer Cell Death by GPX4.*** **Cell, 2014. 156(1-2): p. 317-31.**
95. **Yamashima, T., et al.,** ***Sustained calpain activation associated with lysosomal rupture executes necrosis of the postischemic CA1 neurons in primates.*** **Hippocampus, 2003. 13(7): p. 791-800.**
96. **Tsukada, T., M. Watanabe, and T. Yamashima,** ***Implications of CAD and DNase II in ischemic neuronal necrosis specific for the primate hippocampus.*** **J Neurochem, 2001. 79(6): p. 1196-206.**
97. **Kim, Y.S., et al.,** ***TNF-induced activation of the Nox1 NADPH oxidase and its role in the induction of necrotic cell death.*** **Mol Cell, 2007. 26(5): p. 675-87.**
98. **Detmer, S.A. and D.C. Chan,** ***Functions and dysfunctions of mitochondrial dynamics.*** **Nat Rev Mol Cell Biol, 2007. 8(11): p. 870-9.**
99. **Szabadkai, G., et al.,** ***Drp-1-dependent division of the mitochondrial network blocks intraorganellar Ca2+ waves and protects against Ca2+-mediated apoptosis.*** **Mol Cell, 2004. 16(1): p. 59-68.**
100. **Young, K.W., et al.,** ***Different pathways lead to mitochondrial fragmentation during apoptotic and excitotoxic cell death in primary neurons.*** **J Biochem Mol Toxicol, 2010. 24(5): p. 335-41.**
101. **Whelan, R.S., et al.,** ***Bax regulates primary necrosis through mitochondrial dynamics.*** **Proc Natl Acad Sci U S A, 2012. 109(17): p. 6566-71.**
102. **Thon, L., et al.,** ***Ceramide mediates caspase-independent programmed cell death.*** **FASEB J, 2005. 19(14): p. 1945-56.**
103. **Kagedal, K., et al.,** ***Sphingosine-induced apoptosis is dependent on lysosomal proteases.*** **Biochem J, 2001. 359(Pt 2): p. 335-43.**
104. **Yamashima, T., et al.,** ***Inhibition of ischaemic hippocampal neuronal death in primates with cathepsin B inhibitor CA-074: a novel strategy for neuroprotection based on 'calpain-cathepsin hypothesis'.*** **Eur J Neurosci, 1998. 10(5): p. 1723-33.**
105. **Nakayama, M., et al.,** ***Multiple pathways of TWEAK-induced cell death.*** **J Immunol, 2002. 168(2): p. 734-43.**
106. **Kazama, H., et al.,** ***Induction of immunological tolerance by apoptotic cells requires caspase-dependent oxidation of high-mobility group box-1 protein.*** **Immunity, 2008. 29(1): p. 21-32.**
107. **Zitvogel, L., O. Kepp, and G. Kroemer,** ***Decoding cell death signals in inflammation and immunity.*** **Cell, 2010. 140(6): p. 798-804.**
108. **Vanden Berghe, T., et al.,** ***Necrosis is associated with IL-6 production but apoptosis is not.*** **Cell Signal, 2006. 18(3): p. 328-35.**
109. **Zong, W.X. and C.B. Thompson,** ***Necrotic death as a cell fate.*** **Genes Dev, 2006. 20(1): p. 1-15.**
110. **Lin, M.T. and M.F. Beal,** ***Mitochondrial dysfunction and oxidative stress in neurodegenerative diseases.*** **Nature, 2006. 443(7113): p. 787-95.**
111. **Schinzel, A.C., et al.,** ***Cyclophilin D is a component of mitochondrial permeability transition and mediates neuronal cell death after focal cerebral ischemia.*** **Proc Natl Acad Sci U S A, 2005. 102(34): p. 12005-10.**
112. **Cerhan, J.R., et al.,** ***Genetic variation in 1253 immune and inflammation genes and risk of non-Hodgkin lymphoma.*** **Blood, 2007. 110(13): p. 4455-63.**
113. **Saddoughi, S.A., et al.,** ***Sphingosine analogue drug FTY720 targets I2PP2A/SET and mediates lung tumour suppression via activation of PP2A-RIPK1-dependent necroptosis.*** **EMBO Mol Med, 2013. 5(1): p. 105-21.**
114. **Fulda, S.,** ***The mechanism of necroptosis in normal and cancer cells.*** **Cancer Biol Ther, 2013. 14(11): p. 999-1004.**

115. **Bonapace, L., et al., *Induction of autophagy-dependent necroptosis is required for childhood acute lymphoblastic leukemia cells to overcome glucocorticoid resistance.* J Clin Invest, 2010. 120(4): p. 1310-23.**
116. **Basit, F., S. Cristofanon, and S. Fulda, *Obatoclax (GX15-070) triggers necroptosis by promoting the assembly of the necrosome on autophagosomal membranes.* Cell Death Differ, 2013. 20(9): p. 1161-73.**
117. **Komander, D., M.J. Clague, and S. Urbe, *Breaking the chains: structure and function of the deubiquitinases.* Nat Rev Mol Cell Biol, 2009. 10(8): p. 550-63.**
118. **Mattern, M.R., J. Wu, and B. Nicholson, *Ubiquitin-based anticancer therapy: carpet bombing with proteasome inhibitors vs surgical strikes with E1, E2, E3, or DUB inhibitors.* Biochim Biophys Acta, 2012. 1823(11): p. 2014-21.**
119. **D'Arcy, P., et al., *Inhibition of proteasome deubiquitinating activity as a new cancer therapy.* Nat Med, 2011. 17(12): p. 1636-40.**
120. **Anchoori, R.K., et al., *A bis-Benzylidine Piperidone Targeting Proteasome Ubiquitin Receptor RPN13/ADRM1 as a Therapy for Cancer.* Cancer Cell, 2013. 24(6): p. 791-805.**
121. **Chauhan, D., et al., *A novel orally active proteasome inhibitor induces apoptosis in multiple myeloma cells with mechanisms distinct from Bortezomib.* Cancer Cell, 2005. 8(5): p. 407-19.**
122. **Aleo, E., et al., *Identification of new compounds that trigger apoptosome-independent caspase activation and apoptosis.* Cancer Res, 2006. 66(18): p. 9235-44.**
123. **Fribley, A., Q. Zeng, and C.Y. Wang, *Proteasome inhibitor PS-341 induces apoptosis through induction of endoplasmic reticulum stress-reactive oxygen species in head and neck squamous cell carcinoma cells.* Mol Cell Biol, 2004. 24(22): p. 9695-704.**
124. **Liu, X., et al., *The proteasome inhibitor PS-341 (bortezomib) up-regulates DR5 expression leading to induction of apoptosis and enhancement of TRAIL-induced apoptosis despite up-regulation of c-FLIP and survivin expression in human NSCLC cells.* Cancer Res, 2007. 67(10): p. 4981-8.**
125. **He, Q., Y. Huang, and M.S. Sheikh, *Proteasome inhibitor MG132 upregulates death receptor 5 and cooperates with Apo2L/TRAIL to induce apoptosis in Bax-proficient and -deficient cells.* Oncogene, 2004. 23(14): p. 2554-8.**
126. **Breitschopf, K., A.M. Zeiher, and S. Dimmeler, *Ubiquitin-mediated degradation of the proapoptotic active form of bid. A functional consequence on apoptosis induction.* J Biol Chem, 2000. 275(28): p. 21648-52.**
127. **MacFarlane, M., et al., *Proteasome-mediated degradation of Smac during apoptosis: XIAP promotes Smac ubiquitination in vitro.* J Biol Chem, 2002. 277(39): p. 36611-6.**
128. **Foti, C., et al., *Characterization of caspase-dependent and caspase-independent deaths in glioblastoma cells treated with inhibitors of the ubiquitin-proteasome system.* Mol Cancer Ther, 2009. 8(11): p. 3140-50.**
129. **Mimnaugh, E.G., et al., *Simultaneous inhibition of hsp 90 and the proteasome promotes protein ubiquitination, causes endoplasmic reticulum-derived cytosolic vacuolization, and enhances antitumor activity.* Mol Cancer Ther, 2004. 3(5): p. 551-66.**
130. **Kuo, Y.C., et al., *Regulation of phosphorylation of Thr-308 of Akt, cell proliferation, and survival by the B55alpha regulatory subunit targeting of the protein phosphatase 2A holoenzyme to Akt.* J Biol Chem, 2008. 283(4): p. 1882-92.**
131. **McNamara, C.R., et al., *Akt Regulates TNFalpha synthesis downstream of RIP1 kinase activation during necroptosis.* PLoS One, 2013. 8(3): p. e56576.**
132. **Mochizuki, T., et al., *Akt protein kinase inhibits non-apoptotic programmed cell death induced by ceramide.* J Biol Chem, 2002. 277(4): p. 2790-7.**
133. **Scaffidi, P., T. Misteli, and M.E. Bianchi, *Release of chromatin protein HMGB1 by necrotic cells triggers inflammation.* Nature, 2002. 418(6894): p. 191-5.**
134. **Ambach, A., et al., *The serine phosphatases PP1 and PP2A associate with and activate the actin-binding protein cofilin in human T lymphocytes.* Eur J Immunol, 2000. 30(12): p. 3422-31.**

135. **Hanahan, D. and R.A. Weinberg, *Hallmarks of cancer: the next generation.* Cell, 2011. 144(5): p. 646-74.**
136. **Rodriguez-Nieto, S. and B. Zhivotovsky, *Role of alterations in the apoptotic machinery in sensitivity of cancer cells to treatment.* Curr Pharm Des, 2006. 12(34): p. 4411-25.**
137. **Brancolini, C., *Inhibitors of the Ubiquitin-Proteasome System and the cell death machinery: How many pathways are activated?* Curr Mol Pharmacol, 2008. 1(1): p. 24-37.**
138. **Fontanini, A., et al., *The Isopeptidase Inhibitor G5 Triggers a Caspase-independent Necrotic Death in Cells Resistant to Apoptosis: A COMPARATIVE STUDY WITH THE PROTEASOME INHIBITOR BORTEZOMIB.* J Biol Chem, 2009. 284(13): p. 8369-81.**
139. **Baines, C.P., *Role of the mitochondrion in programmed necrosis.* Front Physiol, 2010. 1: p. 156.**
140. **Ding, W.X., H.M. Ni, and X.M. Yin, *Absence of Bax switched MG132-induced apoptosis to non-apoptotic cell death that could be suppressed by transcriptional or translational inhibition.* Apoptosis, 2007. 12(12): p. 2233-44.**
141. **Perrotti, D. and P. Neviani, *Protein phosphatase 2A: a target for anticancer therapy.* Lancet Oncol, 2013. 14(6): p. e229-38.**
142. **Shi, Y., *Serine/threonine phosphatases: mechanism through structure.* Cell, 2009. 139(3): p. 468-84.**
143. **Janssens, V. and A. Rebollo, *The role and therapeutic potential of Ser/Thr phosphatase PP2A in apoptotic signalling networks in human cancer cells.* Curr Mol Med, 2012. 12(3): p. 268-87.**
144. **Neviani, P., et al., *PP2A-activating drugs selectively eradicate TKI-resistant chronic myeloid leukemic stem cells.* J Clin Invest, 2013. 123(10): p. 4144-57.**
145. **Chen, L., et al., *Hydrogen peroxide-induced neuronal apoptosis is associated with inhibition of protein phosphatase 2A and 5, leading to activation of MAPK pathway.* Int J Biochem Cell Biol, 2009. 41(6): p. 1284-95.**
146. **Martin, M., et al., *PP2A regulatory subunit Balpha controls endothelial contractility and vessel lumen integrity via regulation of HDAC7.* EMBO J, 2013. 32(18): p. 2491-503.**
147. **Widau, R.C., et al., *Protein phosphatase 2A (PP2A) holoenzymes regulate death-associated protein kinase (DAPK) in ceramide-induced anoikis.* J Biol Chem, 2010. 285(18): p. 13827-38.**
148. **Blangy, A., et al., *Cofilin activation during podosome belt formation in osteoclasts.* PLoS One, 2012. 7(9): p. e45909.**
149. **Wegner, A.M., et al., *An automated fluorescence-based method for continuous assay of PP2A activity.* Methods Mol Biol, 2007. 365: p. 61-9.**
150. **Henderson, C.J., et al., *Caspase activation and apoptosis in response to proteasome inhibitors.* Cell Death Differ, 2005. 12(9): p. 1240-54.**

Characterization of caspase-dependent and caspase-independent deaths in glioblastoma cells treated with inhibitors of the ubiquitin-proteasome system

Carmela Foti,[1] Cristina Florean,[1] Antonio Pezzutto,[1] Paola Roncaglia,[2] Andrea Tomasella,[1] Stefano Gustincich,[2] and Claudio Brancolini[1]

[1]Dipartimento di Scienze e Tecnologie Biomediche, Sezione di Biologia and MATI Center of Excellence Università degli Studi di Udine, Udine, Italy and [2]Neurobiology Sector, International School for Advanced Studies, AREA Science Park, Trieste, Italy

Abstract

The regulation of the necrotic death and its relevance in anticancer therapy are largely unknown. Here, we have investigated the proapoptotic and pronecrotic activities of two ubiquitin-proteasome system inhibitors: bortezomib and G5. The present study points out that the glioblastoma cell lines U87MG and T98G are useful models to study the susceptibility to apoptosis and necrosis in response to ubiquitin-proteasome system inhibitors. U87MG cells show resistance to apoptosis induced by bortezomib and G5, but they are more susceptible to necrosis induced by G5. Conversely, T98G cells are more susceptible to apoptosis induced by both inhibitors but show some resistance to G5-induced necrosis. No overt differences in the induction of Noxa and Mcl-1 or in the expression levels of other components of the apoptotic machinery were observed between U87MG and T98G cells. Instead, by comparing the transcriptional profiles of the two cell lines, we have found that the resistance to G5-induced necrosis could arise from differences in glutathione synthesis/utilization and in the microenvironment. In particular, collagen IV, which is highly expressed in T98G cells, and fibronectin, whose adhesive function is counteracted by tenascin-C in U87MG cells, can restrain the necrotic response to G5. Collectively, our results provide an initial characterization of the molecular signals governing cell death by necrosis in glioblastoma cell lines. [Mol Cancer Ther 2009;8(11):3140–50]

Received 5/14/09; revised 9/9/09; accepted 9/21/09; published OnlineFirst 11/3/09.

Grant support: AIRC, MIUR, and Regione Friuli-Venezia Giulia grant AITT-LR25/07 (C. Brancolini).

The costs of publication of this article were defrayed in part by the payment of page charges. This article must therefore be hereby marked *advertisement* in accordance with 18 U.S.C. Section 1734 solely to indicate this fact.

Note: Supplementary material for this article is available at Molecular Cancer Therapeutics Online (http://mct.aacrjournals.org/).

C. Foti and C. Florean contributed equally to this work.

Requests for reprints: Claudio Brancolini, Dipartimento di Scienze e Tecnologie Biomediche, Sezione di Biologia Universita' di Udine. P.le Kolbe 4-33100 Udine, Italy. Phone: 0432-494382; Fax: 0432-494301. E-mail: claudio.brancolini@uniud.it

doi:10.1158/1535-7163.MCT-09-0431

Introduction

Glioblastomas (GBM) are among the most lethal tumors. In particular, grade IV GBMs (WHO grade 4) are highly recalcitrant to radiotherapies and chemotherapies, exhibiting robust angiogenesis, resistance to apoptosis, and propensity to necrosis. Median survival is about 1 year from the time of diagnosis, and despite great efforts during the last decade, improvement in survival of patients has been modest (1, 2).

A large body of evidences has established that inhibition of the ubiquitin-proteasome system (UPS) promotes cancer cell death by apoptosis (3). Food and Drug Administration and European Medicine Agency approval of the UPS inhibitor (UPSI) bortezomib for the treatment of multiple myeloma has validated the UPS as a novel target in anticancer therapy (4). Isopeptidases are attractive alternative targets of the UPS for developing new antitumor therapies (5). Isopeptidases can be generally subdivided into deubiquitinating enzymes and ubiquitin-like (Ubl) specific proteases, which, respectively, deconjugate ubiquitin or Ubl molecules, such as SUMO, NEDD8, or ISG15, from target proteins. These enzymes modulate several biological processes through the control of the lifetime, localization, and activity of ubiquitin or Ubl-modified proteins (6, 7).

We have recently identified two new isopeptidase inhibitors, F6 and G5 (8). F6 and G5 inhibit isopeptidases by reacting with the sulfhydryl group of the catalytic cysteine (9). Because the vast majority of ubiquitin and Ubl proteases are cystein proteases (6), G5 and F6 are rather broad (nonselective) isopeptidase inhibitors (10).

G5, differently from bortezomib, can induce a necrotic death in cells resistant to apoptosis (11). Apoptosis resistance and susceptibility to necrosis are distinctive features of GBM (1). Hence, GBM cell lines represent the ideal model to investigate the pronecrotic activity of G5. In the present study, we have characterized the prodeath activities of bortezomib and G5 in two GBM cell lines and discovered the transcriptome differences that govern the necrotic susceptibility to G5.

Materials and Methods

Reagents

Information on antibodies and reagents is provided in Supplementary Data.

Cell Culture Conditions, Time-Lapse Analysis, Cell Death, and Retroviral Infection

Human GBM cell lines U87MG and T98G, tested by microarray analysis, were grown in DMEM supplemented with 10% fetal bovine serum, penicillin (100 U/mL), glutamine (2 mmol/L), and streptomycin (100 μg/mL) at 37°C in 5% CO_2 atmosphere. U87MG cells expressing mutant p53 and Bcl-xL were generated by retroviral infection (12), after cloning mutant *p53R175H* and *bcl-xL*, respectively, into pWZL-hygro and pWZL-Neo retroviral vectors.

For studying the role of extracellular matrix (ECM) on G5-induced necrosis plates were coated with fibronectin, collagen IV, or bovine serum albumin (10 μg/mL). Cells were seeded at 15×10^4/mL and were then allowed to adhere for 6 h at 37°C before treatments. In all trypan blue exclusion assays, 400 cells, from three independent samples, were counted for each data point.

Western Blotting

Proteins obtained after an SDS denaturating lysis and sonication were transferred to a 0.2-μm-pore-sized nitrocellulose membrane and incubated with the specific primary antibodies. After several washes, blots were incubated with peroxidase-conjugated goat anti-rabbit or goat anti-mouse (Euroclone Milano I) for 1 h at room temperature. Finally, blots were developed with Super Signal West Pico, as recommended by the vendor (Pierce).

RNA Expression Array and Data Analysis

Total RNA was isolated using TRIzol (Invitrogen) according to manufacturer's instructions, and purified with the RNeasy Mini kit (Qiagen). A 6-μg-amount of each total RNA sample was labeled according to the standard one-cycle amplification and labeling protocol (Affymetrix). Hybridization and analysis methods are detailed in the Supplementary Data.

Results

Death of GBM Cells in Response to G5 and Bortezomib

To study the prodeath activities of bortezomib and G5, we selected two GBM cell lines: T98G cells, mutated for p53, and U87MG cells, wild-type for p53 (13). Cells were treated with different concentrations of the drugs, and cell death was analyzed 20 hours later. Both compounds similarly induced the accumulation of polyubiquitinated proteins (data not shown).

Dose-dependent studies showed that U87MG cells are more prone to die in response to G5 compared with T98G cells (Fig. 1A). Incubation with 10 μmol/L of G5 elicited death in >90% of U87MG cells, whereas death was around 40% in T98G cells. In particular, in T98G cells, death was only marginally increased, despite dose escalation from 2.5 up to 10 μmol/L of G5. Surprisingly, bortezomib achieved an opposite effect. U87MG cells were more resistant to cell death (~30% of dead cells after incubation with 10 μmol/L of bortezomib), whereas T98G cells were more sensitive (>80% of death under the same conditions).

Next, we evaluated caspase-3 and caspase-7 activities (DEVDase). In cells treated with bortezomib, there is a perfect correlation between the DEVDase activity and the appearance of cell death (Fig. 1B). During the time of the analysis in the responsive T98G cells, bortezomib activates caspases and induces cell death, whereas in U87MG cells caspase activity is negligible.

In response to low doses of G5 (0.6 and 1.25 μmol/L), caspase activity parallels the induction of death in both cell lines (Fig. 1B). On the contrary, at higher doses of G5 (5 and 10μmol/L) that promptly kills U87MG cells, caspase activity declines.

To confirm the pattern of caspase activity, we investigated caspase-2 and HDAC4 proteolytic processing by immunoblots. As shown Fig. 1C and D, cleavages of HDAC4 and caspase-2 in response to different doses of G5 or bortezomib can be superimposed to the DEVDase activities shown in Fig. 1B. In particular, higher doses of G5 suppressed caspase-2 and HDAC4 processing in U87MG cells. Analogous results were acquired when caspase-3 processing was investigated by immunoblot (data not shown).

G5 Induces a Caspase-Independent Necrotic Death in Apoptosis-Resistant U87MG Cells

The progressive decline of caspase activities observed in U87MG cells treated with escalating doses of G5 is reminiscent of a caspase-independent necrotic death. To prove this hypothesis, we evaluated the ability of a pan-caspase inhibitor to influence death of U87MG and T98G cells in response to G5 or bortezomib.

The caspase inhibitor did not influence death of U87MG cells in response to G5, whereas cell death in response to bortezomib was partially impaired (Fig. 2A, *top*). In T98G cells, bortezomib-induced death was strongly affected by the caspase inhibitor, whereas death in response to G5 was inhibited to some extent (Fig. 2A, *bottom*). These results suggest that death in U87MG cells is prevalently caspase independent (necrotic), whereas in T98G cells it is prevalently caspase dependent (apoptotic).

Apoptosis in response to proteasome inhibition requires the synthesis of new proteins such as the BH3-only Noxa (3). Figure 2B shows that G5-induced death in T98G cells was inhibited by the protein synthesis inhibitor CHX, whereas the same treatment was ineffective in preventing death of U87MG cells. This result further suggests that G5 induces different types of death in U87MG and T98G cells.

High concentrations of the redox cycling quinone DMNQ can induce necrosis and kill cells mutated for Bax and Bak (11). G5 diverges from DMNQ because it can induce necrosis without eliciting oxidative stress. To understand whether U87MG cells are in general more prone to die by necrosis, we assessed cell death in response to DMNQ and G5 treatments. Figure 2C illustrates that U87MG cells are more prone to die in response to G5 compared with DMNQ, whereas T98G cells, on the opposite, are more prone to die in response to DMNQ. These data indicate that U87MG cells are highly susceptible to G5-induced necrosis but resistant to a redox-dependent necrotic insult.

Finally, the induction of necrosis in U87MG cells was unambiguously proved by time-lapse epifluorescence microscopy in living cells, which discriminates the appearance of necrosis, apoptosis, and secondary necrosis as a consequence of apoptosis (Supplementary Fig. S1).

Expression of Bcl-2 Family Members in Response to G5 or Bortezomib Treatments

The delicate balance among Bax and Bak proteins and their antagonists, Bcl-2, Bcl-xL, and Mcl-1, dictates the apoptotic susceptibility to UPSIs (3). Hence, we investigated Bcl-2, Bcl-xL, Mcl-1, Bax, and Bak levels in U87MG and T98G cells treated with bortezomib or G5. We also analyzed expression levels of direct (p53) and indirect (the BH3-only protein Noxa) targets of bortezomib and G5. Since certain Bcl-2 family members are cleaved and downregulated by caspases, as an effect of the amplificatory mechanisms (14), to avoid massive caspase activation, incubations were done for limited times and with low concentrations of G5 or bortezomib.

Overall Bcl-2, Bcl-xL, Bax, and Bak were similarly expressed in the two GBM cell lines (Fig. 3A). Only minor differences can be observed. Bak and Bcl-xL levels were increased in T98G cells, whereas Bcl-2 and Bax were augmented in U87MG cells. Mcl-1 and Noxa were similarly induced by G5 and bortezomib treatments in both cell lines, and as expected, p53 was stabilized only in U87MG cells, but here again at comparable levels by the two inhibitors.

The only exception concerned the downregulation of Bcl-xL levels in U87MG cells treated with G5. To prove whether the downregulation of Bcl-xL in response to G5 could be important for the manifestation of necrosis, cells overexpressing Bcl-xL were generated by retroviral infection (Fig. 3B). Moreover, because T98G and U87MG cells differ for the p53 status, we investigated the role of p53 in G5-induced death by producing U87MG cells expressing the hotspot mutation of p53 R175H (Fig. 3B).

Initially, we verified the ability of mutated p53 and Bcl-xL to modulate apoptosis in response to DNA damage. As recently observed (15), we confirmed that downregulation of wild-type p53 promotes death of U87MG cells in response to DNA-damaging agents. However, the introduced p53 mutant did not influence the necrotic response activated by G5 (Fig. 3C and D). Similarly, overexpressed Bcl-xL was able to reduce cell death in response to DNA damage, but it failed in counteracting G5-induced necrosis (Fig. 3C and D).

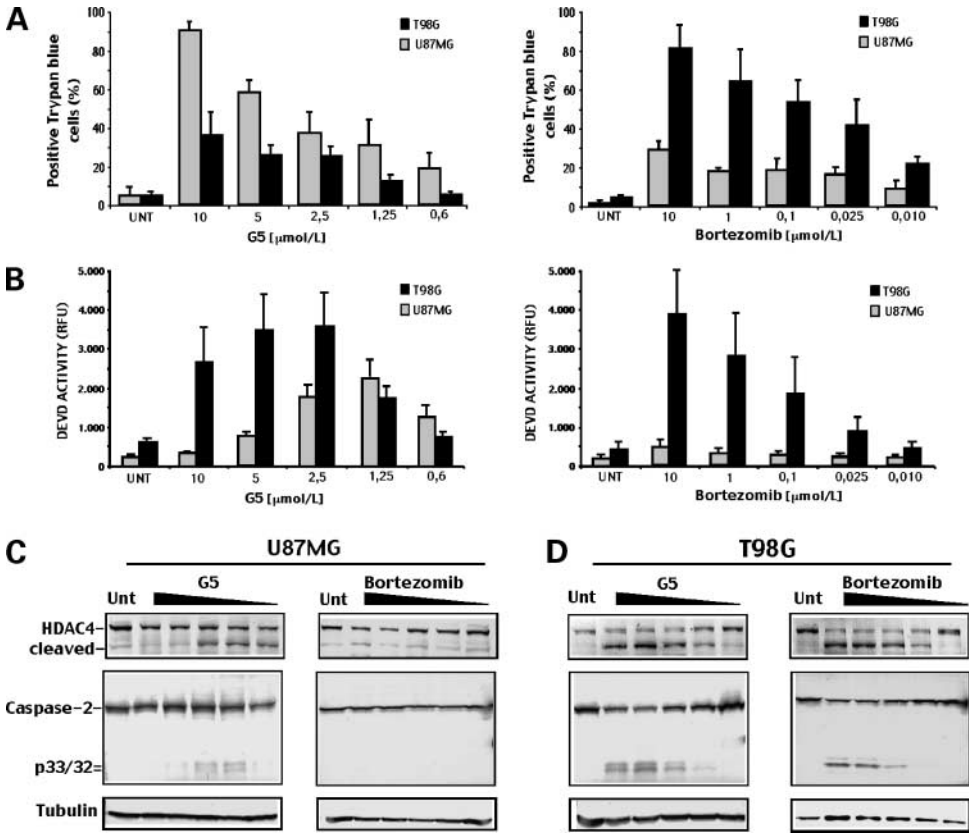

Figure 1. Cell death in GBM cells in response to G5 or bortezomib treatments. **A,** U87MG and T98G cells were treated with the indicated concentrations of G5 or bortezomib for 20 h, and the appearance of cell death was scored by trypan blue staining [*columns,* mean (n = 3); *bars,* SD]. **B,** caspase-3/7 (DEVDase) activity in U87MG and T98G cells treated with the indicated concentrations of G5 or bortezomib for 20 h [*columns,* mean (n = 3); *bars,* SD]. Processing of caspase-2 and HDAC4 in U87MG (**C**) or T98G (**D**) cells treated for 20 h with escalating concentrations of G5 or bortezomib as in **A** and **B**, respectively. Equal amounts of cell lysates were subjected to SDS-PAGE electrophoresis. Immunoblots were done using the indicated antibodies. Tubulin was used as loading control.

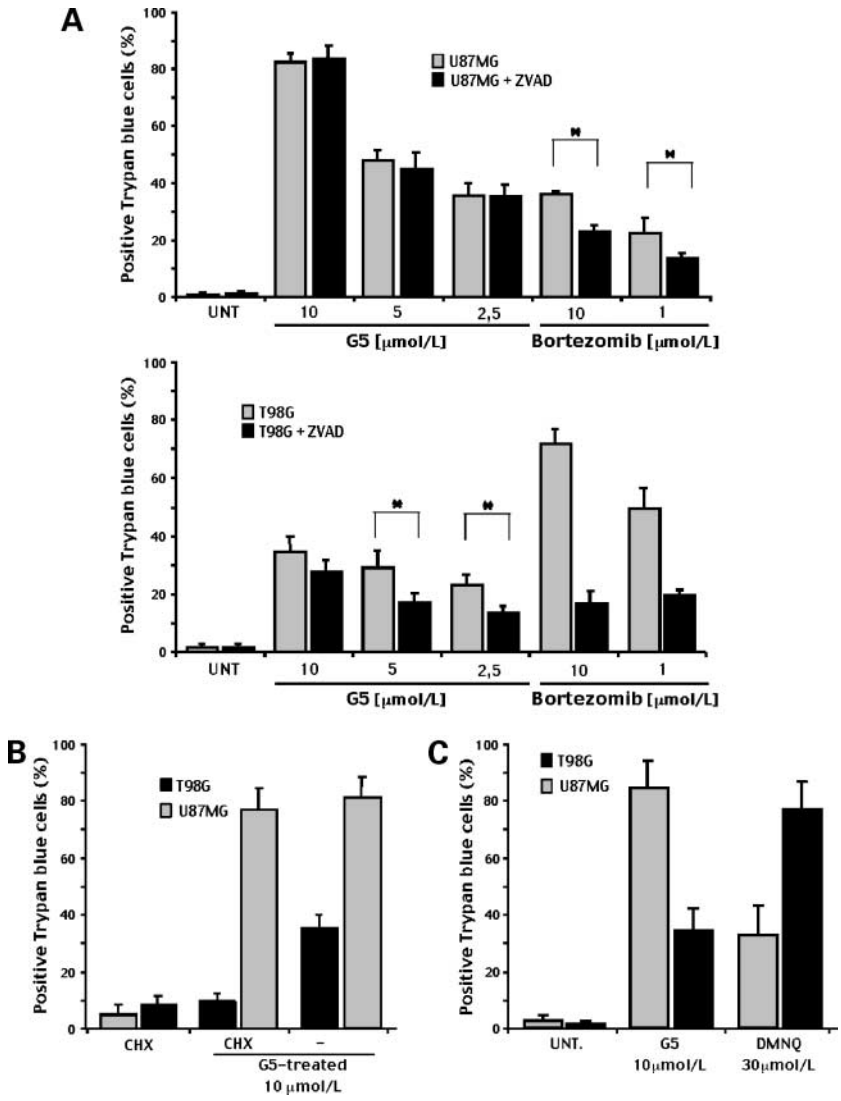

Figure 2. G5 but not bortezomib can activate a caspase independent necrotic death in U87MG cells. **A,** U87MG and T98G cells were treated for 20 h with the indicated concentrations of G5 or bortezomib in the presence or not of the caspase inhibitor zVAD.fmk. Cell death was scored by trypan blue staining [*columns,* mean; (n = 4); *bars,* SD]. *, $P < 0.05$. **B,** U87MG and T98G cells were pretreated for 1 h with CHX (1 μg/mL) and then incubated with the indicated concentration of G5. Cell death was scored 20 h later. *Columns,* mean (n = 5); *bars,* SD. *, $P < 0.05$. **C,** U87MG and T98G cells were treated with the indicated concentrations of G5 and DMNQ. Cell death was scored 20 h later.

Transcriptome Analysis of U87MG and T98G Cells

To understand the gene expression basis of the divergent death responses elicited by UPSIs in U87MG and T98G cells, we compared the gene expression profiles of the two cell lines using Affymetrix GeneChip Human Genome U133A 2.0 Arrays. After statistical test, probe sets with signal intensities displaying over 2-fold difference between the two cell lines were selected. Overall, 2,522 genes appear differentially expressed between U87MG and T98G cells, thus confirming a certain degree of genetic heterogeneity in GBM cell lines, as observed in other gene expression profile studies (16). The top 20 upregulated and downregulated genes are shown in Table 1. Many of these genes point to relevant differences in the microenvironment as generated by soluble and insoluble factors secreted by the two cell lines and in the detoxification systems (see also Supplementary Tables S2–4). Although T98G and U87MG cells differ profoundly for the susceptibility to apoptosis in response to UPSIs, expression profile analysis of apoptosis regulators, including inhibitor of apoptosis caspases and Bcl-2 family members, has not revealed overt differences between the two cell lines (Supplementary Table S1).

U87MG cells harbor a homozygous deletion of the entire *IFNA/IFNW* gene cluster and of the *IFNB1* gene (17). The microarray analysis confirmed that the expression of many IFN-induced genes is higher in T98G cells; however, treatment of U87MG cells with IFN-α does not influence cell death induced by G5 or bortezomib (data not shown).

Glutathione Depletion Sensitizes Gliobastoma Cells to G5-Induced Death

Genes regulating oxidative stress (*GSTM3, PXDN*, and *GPX3*) are among the 20 highest differentially expressed genes in T98G compared with U87MG cells (Table 1). We also analyzed in detail the expression levels of genes involved in glutathione (GSH) synthesis and use (Supplementary Table S2). In particular, T98G cells express higher levels of GSH transferase M3 (*GSTM3*) and of glutamate-cysteine ligase (*GCLC*) transcripts, whereas U87MG express other GSH *S*-transferase (GST) isoforms. Differences in the expression

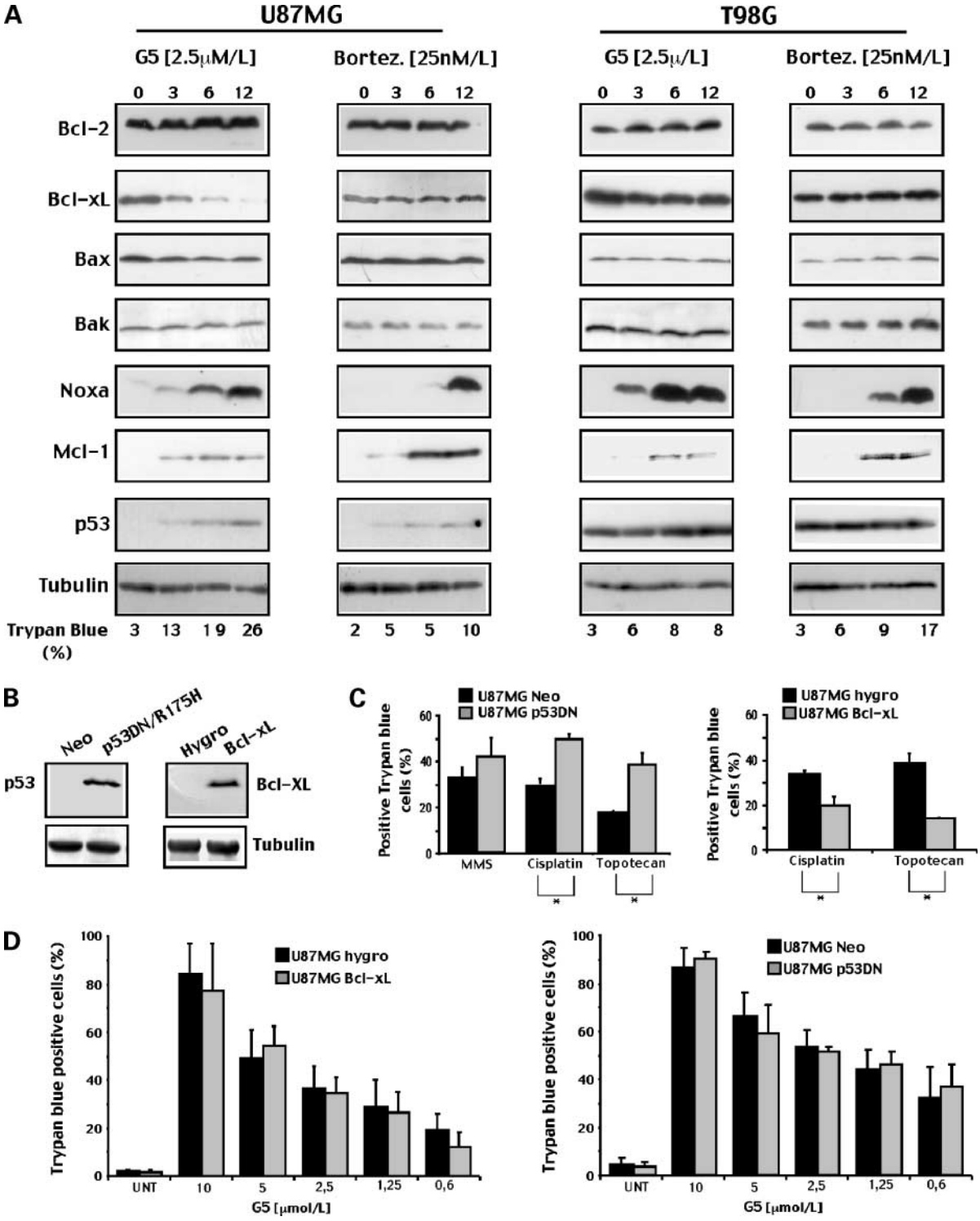

Figure 3. Regulation of Bcl-2 family member expression in GBM cells in response to G5 or bortezomib. **A,** time course analysis of the expression levels of Bcl-2 family members and p53. Lysates from U87MG and T98G cells treated with G5 or bortezomib for the indicated times were prepared and subjected to immunoblot analysis using the specific antibodies. **B,** generation of U87MG cells expressing dominant-negative p53 or Bcl-xL. Equal amounts of cellular lysates from U87MG cells expressing *bcl-xL, p53R175H*, or the relative resistance genes were subjected to SDS-PAGE electrophoresis. Immunoblots were done using the indicated antibodies. **C,** U87MG cells expressing p53R175H mutant, Bcl-xL, or the relative control genes were treated for 24 h with MMS (100 μg/mL), or for 48 h with cisplatin (250 μmol/L) or topotecan (1 μmol/L). Cell death was scored by trypan blue staining [*columns,* mean ($n = 3$); *bars,* SD]. *, $P < 0.05$. **D,** U87MG cells expressing p53R175H mutant, Bcl-xL, or the relative control genes were treated with the indicated concentrations of G5 for 20 h, and the appearance of cell death was scored by trypan blue staining [*columns,* mean ($n = 3$); *bars,* SD].

Table 1. Top 20 upregulated and top 20 downregulated genes in T98G cells relative to U87MG cells

Gene symbol	Fold difference*	Gene name	Function	Localization	ProbeSet ID	*P*
IGFBP5	8,64	Insulin-like growth factor binding protein 5	Signaling	Secreted	211959_at	6,20E-09
CDH6	7,89	Cadherin 6, type 2, K-cadherin (fetal kidney)	Adhesion	Plasma membrane	205532_s_at	1,53E.-08
THBS1	7,88	Thrombospondin 1	Adhesion/signaling	Secreted/ECM	201109_s_at	2.30E-08
CDH11	7,38	Cadherin 11, type 2, OR-cadherin (osteoblast)	Adhesion	Plasma membrane	207173_x_at	7,51E-08
TNFRSF11B	6,83	Tumor necrosis factor receptor superfamily, member 11b	Signaling	Secreted	204933_s_at	2,3OE-08
GSTM3	6,81	GST M3 (brain)	Redox	Intracellular	202554_s_at	2,30E-08
CXCL12	6,70	Chemokine(C-X-Cmotif) ligand 12 (stromal cell–derived factor 1)	Signaling	Secreted	209687_at	5,85E-08
GPX3	6,64	Glutathione peroxidase 3 (plasma)	Redox	Secreted	201348_at	9.93E-09
MYH10	6,51	Myosin, heavy chain 10, nonmuscle	Cytoskelelon	cytoplasmic	212372_at	3,52E-06
PDGFD	6,44	Platelet-derived growth factor D	Signaling	Secreted	219304_s_at	7,71E-08
COLEC12	6,31	Collectin subfamily member 12	Host defense	Plasma membrane	221019_s_at	7,51E-08
PXDN	6,26	Peroxidasin homologue (Drosophila)	Redox	Secreted/ECM	212013_at	2.13E-08
HSPA1A	6,25	Heat shock 70 kDa protein 1A	Chaperon	Intracellular	200799_at	2,30E-08
SLC2A10	6,23	Solute currier family 2 (facilitated glucose transporter), member 10	Transport	Plasma membrane	221024_s_at	3,98E-07
NIDI	6,18	Nidogen 1	Adhesion	Secreted/ECM	202007_at	7,51E-08
TUSC3	6,10	Tumor suppressor candidate 3	N-Glycosylation	ER	213423_x_at	2,30E-08
RHBDL2	6,07	Rhomboid, veinlet-like 2 (Drosophila)	Signaling	Plasma membrane	219489_s_at	7,67E-08
GABRA2	5,92	γ-Aminobutyric acid (GABA) A receptor, α 2	Ion transport	Plasma membrane	207014_at	2,77E-06
CYTL1	5,84	Cytokine-like 1	Signaling	Secreted	219837_s_at	1,53E-08
NPTX1	5,78	Neuronal pentraxin I	Synaptic transmission	Intracellular	204684_at	5,82E-08
EREG	–8,27	Epiregulin	Signaling	Secreted	205767_at	3,14E-08
GREM1	–7,90	Gremlin 1, cysteine knot superfamily, homologue (*Xenopus* laevis)	Signaling	Secreted	218468_s_at	7,68E-08
PRSS7	–7,38	Protease, serine, 7 (enterokinase)	Proteolysis	Plasma Membrane	207638_at	5,39E-08
FABP5	–7,22	Fatty acid binding protein 5 (psoriasis associated)	Transport	Cytoplasmic	202345_s_at	1,57E-08
NETO2	–6,91	Neuropilin (NRP) and tolloid (TLL)-like 2	Signaling?	Plasma Membrane	218888_s_at	5,32E-08
NRIP3	–6,73	Nuclear receptor interacting protein 3	Unknown	Unknown	219557_s_at	5.82E-08
ETVl	–6,62	Ets variant gene 1	Trancription	Nuclear	221911_at	7,68E-08
C3orf14	–6,42	Chromosome 3 open reading frame 14	Unknown	Unknown	219288_at	8,02E-08
SVIL	–6,41	Supervillin	Cytoskeleton	Plasma Membrane	202565_s_at	373E-08
PLAGL1	–5,86	Pleiomorphic adenoma gene-like 1	Trancription	Nuclear/Cytoplasm.	209318_x_at	1.11E-06
PKIA	–5,67	Protein kinase (CAMP-dependent, catalytic) inhibitor α	Signaling	Nuclear/Cytoplasm.	204612_at	2,55E-08
MCTP1	–5,65	Multiple C2 domains, transmembrane 1	Unknown	Plasma Membrane	220122_at	8.54E-07

(Continued on the following page)

Table 1. Top 20 upregulated and top 20 downregulated genes in T98G cells relative to U87MG cells (Cont'd)

Gene symbol	Fold difference*	Gene name	Function	Localization	ProbeSet ID	*P*
MYO1B	−5,64	Myosin IB	Cytoskeleton	Cytoplasmic	212364_at	167E-07
HGF	−5,55	Hepatneyte growth factor (hepapoietin A; scatter factor)	Signaling	Secreted	210997_at	2,55E-08
ABCA1	−5,50	ATP-binding cassette, subfamily A (ABC1), member 1	Transport	Plasma Membrane	203504_s_at	5.94E-08
AHNAK2	−5,47	AHNAK nucleoprotein 2	Transport	Secreted	212992_at	8,35E-08
PLTP	−5,45	Phospholipid transfer protein	Scaffolding	Nuclear/Cytoplasm.	202075_s_at	8,29E-08
PRRX1	−5,38	Paired related homeobox 1	Trancription	Nuclear	205991_s_at	1,13E-07
HS3ST3A1	−5,35	Heparan sulfate (glucosamine) 3-O-sulfotransferase 3A1	ECM modifier	Plasma Membrane	219985_at	6,19E-08
UGT8	−5,34	UDP glycosyltransferase 8	Sphingolipids biosynth.	ER	208358_s_at	3,43E-07

*(log2) – mean fold differences.

levels of the GST enzymes were also confirmed by affinity purification and by measuring enzymatic activities (Supplementary Fig. S2).

GSTs are crucial enzymes in the detoxification process, catalyzing the nucleophilic attack of GSH on toxic electrophilic substrates (18). *De novo* GSH synthesis is governed by γ-glutamylcysteine synthetase, a heterodimer constituted by a catalytic subunit (GCLC) and a modulatory subunit (GCLM; ref. 19).

The GSH system can modulate chemoresistance (20, 21); hence, differential detoxification abilities between the two cell lines could explain the resistance to G5-dependent necrosis observed in T98G cells. To answer this question, cells were depleted of GSH, by pretreatment with buthionine sulfoximine (BSO), a selective inhibitor of γ-glutamylcysteine synthetase (22). The appearance of death was then analyzed in response to G5 or bortezomib.

As shown in Fig. 4A, in agreement with previous studies (23), GSH depletion does not induce cell death. However, when GSH-depleted cells were treated with G5, cell death was similarly augmented in T98G and U87MG cells. On the contrary, cell death induced by bortezomib was unaffected by BSO treatment.

Next, we evaluated whether the death of T98G cells in the presence of BSO was still caspase dependent. As shown in Fig. 4B, in response to 2.5 μmol/L of G5, death of T98G cells was caspase dependent, whereas at 10 μmol/L, it was largely caspase independent. Caspase inhibitors failed to block apoptosis induced by 2.5 μmol/L of G5 when BSO was present. As observed in other models (24), caspase inhibitors augmented necrosis in response to 10 μmol/L of G5, possibly by suppressing autophagy (25). Finally, as described before (Fig. 2), death of U87MG was largely caspase independent.

The Extracellular Environment Modulates the Susceptibility to Necrosis

The most prominent group of highly differential expressed genes between U87MG and T98G cells comprises components of the microenvironment, including elements of the ECM (Supplementary Tables S3 and S4; Table 1). Transcripts for thrombospondin (*THBS1*), collagen type III, IV, and XVIII (*CL3A1, COL18A1*, and *COL4A1*) are the top highest expressed ECM components in T98G cells (Supplementary Table S4). Transcripts for osteopontin (*SPP1*), mesotypsin (*PRRS3*), tenascin C (*TNC*), and collagen I (*COL1A*) are the top highest expressed ECM components in U87MG cells (Supplementary Table S3). Differential expression of TNC and collagen IV in U87MG and T98G cells was validated at protein levels (Fig. 5A and B).

We have recently shown that ECM components collagen and fibronectin can counteract G5-dependent necrosis (11). Therefore, different types of ECM, as produced by the GBM cell lines, could influence the susceptibility to G5-induced necrosis. To answer this question, U87MG and T98G cells were plated on fibronectin, collagen IV, or on bovine serum albumin–coated Petri dishes and next treated with G5.

Figure 5C illustrates that collagen IV and fibronectin can counteract the necrotic response to G5 in U87MG cells. An ~40% reduction in necrosis is manifested by both ECM components in U87MG cells treated for 24 hours with 10 μmol/L of G5. Death of T98G cells was less influenced by fibronectin and collagen IV (Fig. 5D), presumably because it is also apoptotic. An ~30% reduction with collagen IV and a 22% reduction with fibronectin were observed in the presence of high concentrations of G5.

Discussion

Apoptosis and necrosis represent the most common forms of cell death. Traditionally, apoptosis is considered a form of regulated cellular mechanism in contrast to necrosis, which is described as a form of passive death. Necrosis appears when cells suffer excessive stresses that finally cause the rupture of the plasma membrane and the spillage of cellular macromolecules, which act as proinflammatory signals (26, 27). More recent data have challenged this view and the existence of regulated forms of necrosis is becoming evident (27, 28).

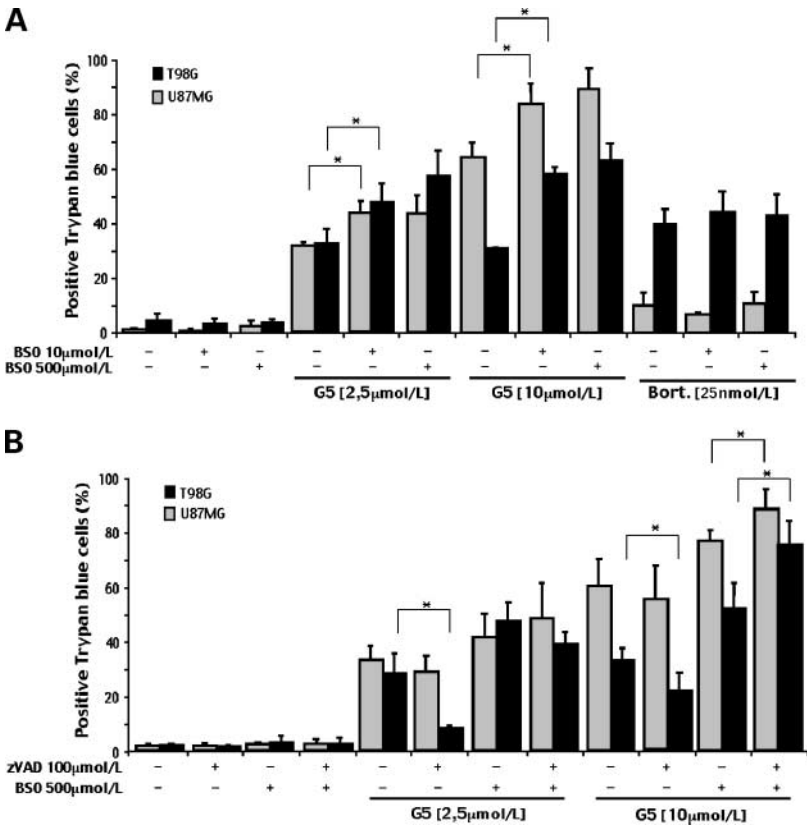

Figure 4. GSH depletion modulates cell death in response to G5 and the apoptotic/necrotic switch. **A,** U87MG or T98G cells were pretreated with BSO for 24 h. Next, G5 or bortezomib were added for further 24 h. Cell death was scored by trypan blue staining [*columns,* mean (n = 3); *bars,* SD]. *, $P < 0.05$. **B,** U87MG or T98G cells were pretreated with BSO for 24 h followed by 1 h of pretreatment with zVAD.fmk (100 μmol/L). Next, G5 or bortezomib was added for further 24 h as indicated. Cell death was scored by trypan blue staining [*columns,* mean (n = 3); *bars,* SD]. *, $P < 0.05$.

Apoptosis

U87MG cells show resistance to apoptosis but they are susceptible to die by G5-induced necrosis. In contrast, T98G cells are susceptible to die by apoptosis in response to both inhibitors but show some resistance to G5-induced necrosis. Interestingly, a difference in the apoptotic response to bortezomib, between these cell lines, can also be appreciated from previous studies (29, 30).

Our data do not disclose robust alterations in the expression or modulation of components of the apoptotic machinery between T98G and U87MG cells. Bax and Bak, which are necessary for apoptosis in response to UPSIs (11), are similarly expressed in the two cell lines. Noxa and Mcl-1, two Bcl-2 family members under the regulation of UPSIs, are alike induced by the two insults. Moreover, expression profile studies did not evidence overt differences in the expression levels of Bcl-2 family members, caspases, and inhibitors of apoptosis. Moreover, we noted that bortezomib failed to induce mitochondrial outer membrane permeabilization in U87MG cells.[3] Hence, it is possible that other mechanisms, acting upstream of mitochondria, are responsible for the divergences in the apoptotic responsiveness.

Necrosis

U87MG cells are susceptible to G5-induced necrosis, whereas T98G cells show some resistance. This necrotic susceptibility was specific for G5. In fact, in response to oxidative stress, T98G cells were more prone to die by necrosis compared with U87MG cells, thus ruling out that U87MG cells are in general more susceptible to necrosis. This observation indicates that cells can activate different necrotic responses.

G5 triggers the upregulation of wild-type p53 and downregulation of Bcl-xL in U87MG cells. However, neither of these two proteins can modulate the necrotic response to G5.

Combining expressional profile studies and functional studies has permitted to disclose that differences in the necrotic responsiveness could arise from diversity in the GSH detoxification system and in the microenvironment and, in particular, in the type of ECM proteins.

U87MG and T98G cells differ profoundly for the classes of GST enzymes expressed. *GSTM3* is abundantly expressed in T98G cells, and also, the γ-glutamylcysteine synthetase is expressed at higher levels in this cell line. Depletion experiments have indicated that GSH can modulate at least two events: (*a*) the rate of cell death in response to G5, possibly by G5 detoxification, (*b*) the decision about the particular type of death in response to G5, necrosis versus apoptosis.

Depending on the cellular context and the death insult, GSH depletion can synergize to induce apoptosis, necrosis, or can also switch the mode of death versus necrosis (20, 31, 32). GSH depletion can generate reactive oxygen species, increase the irreversible oxidation of cysteine residues,

[3] C. Foti, unpublished observation.

and can also influence the formation of protein-GSH mixed disulphides (*S*-glutathionylation; ref. 23). However, because the cotreatment with BSO and G5 failed to elicit oxidative damage in T98G cells (Supplementary Fig. S2C), something different from ROS generation should be evoked to explain the shift toward necrosis.

Interestingly, recent data have shown that *S*-glutathionylation of Fas increases its accumulation in lipid rafts and strengthens the death signal (33). Because G5 engages the extrinsic pathway to induce apoptosis (8, 11), we hypothesize that a reduction in *S*-glutathionylation of Fas could promote the appearance of necrosis in T98G cells treated with G5.

We also found that the microenvironment, as generated through the secretion of ECM components, differs profoundly between T98G and U87MG cells.

Interestingly, gene expression profile studies in brain tumors in comparison with normal brain tissue have revealed that GBMs overexpress genes of the microenvironment, including growth factor–related and structural/ECM-related genes (34–36). Differences in the microenvironment mark also different subtypes of GBMs. Primary GBMs with respect to secondary GBMs express genes characteristic of mesenchymal-derived tissues and stromal response (36, 37).

Among ECM genes highly expressed in the necrosis-resistant T98G cells, a consistent group was also identified as more expressed in primary GBM compared with normal brain tissue (38). This list includes *COL3A1*, *COL4A1*, *POSTN*, *COL4A2*, *LAMB1*, and *MGP* (38). *COL4A1* and *COL4A2* were also more expressed in primary GBMs with respect to secondary GBMs (36, 37). On the contrary, this list was extremely reduced in U87MG cells including only *TNC* and *TIMP1* genes.

Protection from G5-induced necrosis can be elicited in U87MG cells after adhesion to ECM. Adhesion to collagen IV, which is more expressed in T98G cells or to exogenous-added fibronectin, significantly rescued cells from death. It

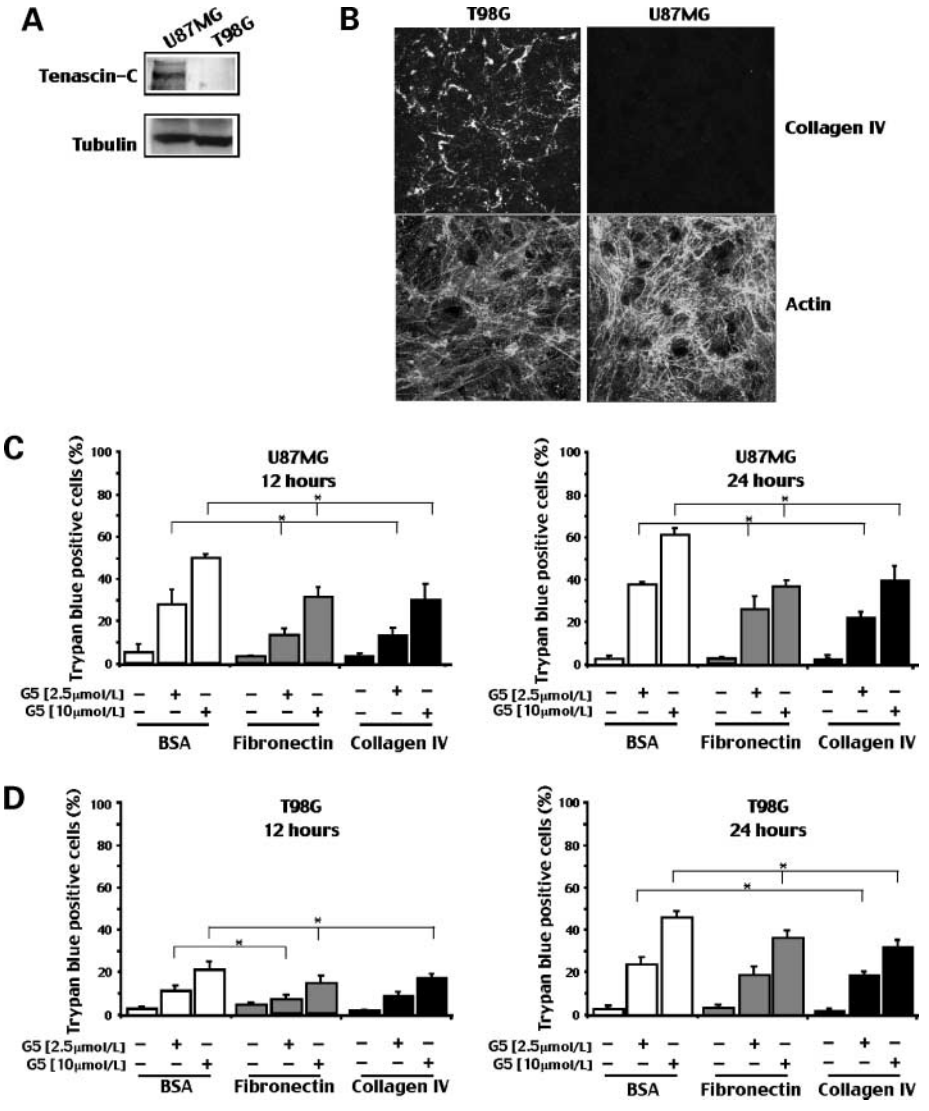

Figure 5. The microenvironment regulates the susceptibility to G5-induced necrosis. **A,** lysates from U87MG and T98G cells were prepared and subjected to immunoblot analysis using anti–tenascin-C antibody. Anti-tubulin was used as loading control. **B,** confocal microscopic analysis of U87MG and T98G cells 96 h after plating using rabbit anti–collagen IV antibody. The immunocomplexes were visualized with an anti-rabbit FITC-conjugated antibody and actin filaments with phalloidin-TRITC. Deposition of collagen IV can be visualized only in T98G cells. **C,** U87MG or (**D**) T98G cells were grown on fibronectin, collagen IV, or bovine serum albumin (*BSA*) as indicated. Six hours after seeding, cells were incubated with G5 (2.5 or 10 μmol/L) for 12 or 24 h. Cell death was scored by trypan blue staining [*columns*, means ($n = 3$); *bars*, SD]. *, $P < 0.05$.

is important to note that, although tenascin C (Tnc) enhances proliferation of glioma cells, it also inhibits cell spreading on fibronectin (39). This effect explains the antinecrotic role of exogenously added fibronectin, which can compete with the high levels of Tnc secreted by U87MG cells to promote adhesion. A role confirmed after the downregulation of Tnc expression by siRNA transfection, which, similarly to fibronectin addition, reduced G5-induced necrosis in U87MG cells (Supplementary Fig. S3).

We have recently shown that G5 can trigger necrosis in apoptotic-resistant cells (11). This necrotic death was likewise inhibited by adhesion to ECM. G5-induced necrosis was independent from common necrotic regulators such as oxidative stress, calcium, c-Jun-NH_2-kinase, and RIP1. Instead, it is characterized by an early and dramatic reorganization of actin cytoskeleton. We have similarly noted that G5 triggers dramatic changes in actin organization in U87MG but not in T98G cells. Before the appearances of necrotic markers, cells reduce actin projections, become polygonal, and next, with time, they eventually round up and detach (see Supplementary Fig. S4). The impact of G5 on actin dynamics and cell adhesion was corroborated by the diminished random migration scored in U87MG cells treated with low doses of G5 (see Supplementary Fig. S5). In the future, to define this necrotic pathway in more detail, it will be important to exclude off-target effects of G5, possibly through the development of more specific isopeptidase inhibitors.

Necrotic deaths that rely on microfilament/adhesion changes, as in the case of G5, have been recently observed (40). Necrotic death of lymphocytes, in response to mycophenolic, which involves Rho-GTPase Cdc42 activity and actin polymerization, shares some features with G5. In fact, it is Bcl-2, c-Jun-NH_2-kinase, and RIP independent (41).

Despite aggressive approaches, treatment of GBM patients represents an ongoing challenge (1, 2). Characterization of new necrotic pathways is important to overcome the resistance to apoptosis typical of GBMs. In addition, considering the necrotic propensity of GBMs, understanding the molecular mechanisms that govern necrosis is instrumental to design new therapeutic treatments. By characterizing the death response of GBM cell lines to G5 and bortezomib, we have provided a contribution to these important issues.

Disclosure of Potential Conflicts of Interest

No potential conflicts of interest were disclosed.

Acknowledgments

We thank S. Fulda (Ulm Germany) for GBM cell lines, and A. Colombatti (Aviano Italy) and P. Bonaldo (Padova Italy) for antibodies.

References

1. Furnari FB, Fenton T, Bachoo RM, et al. Malignant astrocytic glioma: genetics, biology, and paths to treatment. Genes Dev 2007;21:2683–710.

2. Zhu Y, Parada LF. The molecular and genetic basis of neurological tumours. Nat Rev Cancer 2002;2:616–26.

3. Demarchi F, Brancolini C. Altering protein turnover in tumor cells: new opportunities for anti-cancer therapies. Drug Resist Updat 2005; 8:359–68.

4. Brancolini C. Inhibitors of the ubiquitin-proteasome system and the cell death machinery: how many pathways are activated? Curr Mol Pharm 2008;1:24–37.

5. Love KR, Catic A, Schlieker C, Ploegh HL. Mechanisms, biology and inhibitors of deubiquitinating enzymes. Nat Chem Biol 2007;3: 697–705.

6. Amerik AY, Hochstrasser M. Mechanism and function of deubiquitinating enzymes. Biochim. Biophys Acta 2004;1695:189–207.

7. Kirkin V, Dikic I. Role of ubiquitin- and Ubl-binding proteins in cell signaling. Curr Opin Cell Biol 2007;19:199–205.

8. Aleo E, Henderson CJ, Fontanini A, Solazzo B, Brancolini C. Identification of new compounds that trigger apoptosome-independent caspase activation and apoptosis. Cancer Res 2006;66:9235–44.

9. Mullally JE, Fitzpatrick FA. Pharmacophore model for novel inhibitors of ubiquitin isopeptidases that induce p53-independent cell death. Mol Pharmacol 2002;62:351–8.

10. Nicholson B, Leach CA, Goldenberg SJ, et al. Characterization of ubiquitin and ubiquitin-like-protein isopeptidase activities. Protein Sci 2008; 17:1035–43.

11. Fontanini A, Foti C, Potu H, et al. The isopeptidase inhibitor G5 triggers a caspase-independent necrotic death in cells resistant to apoptosis: a comparative study with the proteasome inhibitor bortezomib. J Biol Chem 2009;284:8369–81.

12. Henderson CJ, Aleo E, Fontanini A, Maestro R, Paroni G, Brancolini C. Caspase activation and apoptosis in response to proteasome inhibitors. Cell Death Differ 2005;12:1240–54.

13. Opel D, Westhoff MA, Bender A, Braun V, Debatin KM, Fulda S. Phosphatidylinositol 3-kinase inhibition broadly sensitizes glioblastoma cells to death receptor- and drug-induced apoptosis. Cancer Res 2008; 68:6271–80.

14. Fischer U, Janicke RU, Schulze-Osthoff K. Many cuts to ruin: a comprehensive update of caspase substrates. Cell Death Differ 2003; 10:76–100.

15. Batista LF, Roos WP, Christmann M, Menck CF, Kaina B. Differential sensitivity of malignant glioma cells to methylating and chloroethylating anticancer drugs: p53 determines the switch by regulating xpc, ddb2, and DNA double-strand breaks. Cancer Res 2007;67:11886–95.

16. Li A, Walling J, Kotliarov Y, et al. Genomic changes and gene expression profiles reveal that established glioma cell lines are poorly representative of primary human gliomas. Mol Cancer Res 2008;6:21–30.

17. Olopade OI, Jenkins RB, Ransom DT, et al. Molecular analysis of deletions of the short arm of chromosome 9 in human gliomas. Cancer Res 1992;52:2523–9.

18. Hayes JD, Flanagan JU, Jowsey IR. Glutathione transferases. Annu Rev Pharmacol Toxicol 2005;45:51–88.

19. Dickinson DA, Levonen AL, Moellering DR, et al. Human glutamate cysteine ligase gene regulation through the electrophile response element. Free Radic Biol Med 2004;37:1152–9.

20. Troyano A, Fernández C, Sancho P, De Blas E, Aller P. Effect of glutathione depletion on antitumor drug toxicity (apoptosis and necrosis) in U-937 human promonocytic cells. The role of intracellular oxidation. J Biol Chem 2001;276:47107–15.

21. Syng-Ai C, Kumari AL, Khar A. Effect of curcumin on normal and tumor cells: role of glutathione and bcl-2. Mol Cancer Ther 2004;3:1101–8.

22. Griffith OW, Meister A. Potent and specific inhibition of glutathione synthesis by buthionine sulfoximine (S-n-butyl homocysteine sulfoximine). J Biol Chem 1979;254:7558–60.

23. Di Stefano A, Frosali S, Leonini A, et al. GSH depletion, protein S-glutathionylation and mitochondrial transmembrane potential hyperpolarization are early events in initiation of cell death induced by a mixture of isothiazolinones in HL60 cells. Biochim Biophys Acta 2006;1763:214–25.

24. Vercammen D, Beyaert R, Denecker G, et al. Inhibition of caspases increases the sensitivity of L929 cells to necrosis mediated by tumor necrosis factor. J Exp Med 1998;187:1477–85.

25. Wu YT, Tan HL, Huang Q, et al. Autophagy plays a protective role during zVAD-induced necrotic cell death. Autophagy 2008;4:457–66.

26. Golstein P, Kroemer G. Cell death by necrosis: towards a molecular definition. Trends Biochem Sci 2007;32:37–43.

27. Zong WX, Thompson CB. Necrotic death as a cell fate. Genes Dev 2006;20:1–15.

28. Hitomi J, Christofferson DE, Ng A, et al. Identification of a molecular signaling network that regulates a cellular necrotic cell death pathway. Cell 2008;135:1311–23.

29. Yin D, Zhou H, Kumagai T, et al. Proteasome inhibitor PS-341 causes cell growth arrest and apoptosis in human glioblastoma multiforme (GBM). Oncogene 2005;24:344–54.

30. La Ferla-Bruhl K, Westhoff MA, Karl S, et al. NF-kB-independent sensitization of glioblastoma cells for TRAIL-induced apoptosis by proteasome inhibition. Oncogene 2007;26:571–82.

31. Fernandes RS, Cotter TG. Apoptosis or necrosis: intracellular levels of glutathione influence the mode of cell death. Biochem. Pharmacol 1994; 48:675–81.

32. Chen D, Chan R, Waxman S, Jing Y. Buthionine sulfoximine enhancement of arsenic trioxide-induced apoptosis in leukemia and lymphoma cells is mediated via activation of c-Jun NH2-terminal kinase and up-regulation of death receptors. Cancer Res 2006;66:11416–23.

33. Anathy V, Aesif SW, Guala AS, et al. Redox amplification of apoptosis by caspase-dependent cleavage of glutaredoxin 1 and S-glutathionylation of Fas. J Cell Biol 2009;184:241–52.

34. Ljubimova JY, Lakhter AJ, Loksh A, et al. Overexpression of α4 chain-containing laminins in human glial tumors identified by gene microarray analysis. Cancer Res 2001;61:5601–10.

35. Freije WA, Castro-Vargas FE, Fang Z, et al. Gene expression profiling of gliomas strongly predicts survival. Cancer Res 2004;64:6503–10.

36. Phillips HS, Kharbanda S, Chen R, et al. Molecular subclasses of high-grade glioma predict prognosis, delineate a pattern of disease progression, and resemble stages in neurogenesis. Cancer Cell 2006;9:157–73.

37. Tso CL, Freije WA, Day A, et al. Distinct transcription profiles of primary and secondary glioblastoma subgroups. Cancer Res 2006;66:159–67.

38. Tso CL, Shintaku P, Chen J, et al. Primary glioblastomas express mesenchymal stem-like properties. Mol Cancer Res 2006;4:607–19.

39. Huang W, Chiquet-Ehrismann R, Moyano JV, Garcia-Pardo A, Orend G. Interference of tenascin-C with syndecan-4 binding to fibronectin blocks cell adhesion and stimulates tumor cell proliferation. Cancer Res 2001;61:8586–94.

40. Belkaid A, Fortier S, Cao J, Borhane A. Necrosis induction in glioblastoma cells reveals a new "bioswitch" function for the MT1-MMP/G6PT signaling axis in proMMP-2 activation versus cell death decision. Neoplasia 2007;9:332–40.

41. Chaigne-Delalande B, Guidicelli G, Couzi L, et al. The immunosuppressor mycophenolic acid kills activated lymphocytes by inducing a nonclassical actin-dependent necrotic signal. J Immunol 2008;181:7630–8.

Apoptosis (2011) 16:1229–1244
DOI 10.1007/s10495-011-0639-4

ORIGINAL PAPER

Type I IFNs signaling and apoptosis resistance in glioblastoma cells

Andrea Sgorbissa · Andrea Tomasella · Harish Potu · Ivana Manini · Claudio Brancolini

Published online: 21 August 2011

Abstract Deletion of type I IFN genes and resistance to apoptosis induced by type I IFNs are common in glioblastoma. Here we have investigated the importance of the constitutive weak IFN-signaling in the apoptotic response to IFN-α in glioblastoma cells. U87MG cells hold a deletion of type I IFN genes, whereas in T98G cells the spontaneous IFN signaling is intact. In response to IFN-α U87MG cells produce much less TRAIL, while other IFN-inducible genes were efficiently up-regulated. Alterations in TRAIL promoter sequence and activity were not observed. DNA methylation can influence TRAIL transcription but without overt differences between the two cell lines. We also discovered that TRAIL mRNA stability is influenced by IFN-α, but again no differences can be appreciated between the two cell lines. By silencing IFNAR1 we provide evidences that the spontaneous IFN signaling loop is required to sustain elevated levels of TRAIL expression, possibly through the regulation of IRF-1. Despite the presence/absence of the constitutive IFN signaling, both cell lines were resistant to IFN-α induced apoptosis. Targeting the deisgylase USP18 can overcome resistance to IFN-induced apoptosis only in T98G cells. Alterations in elements of the extrinsic apoptotic pathway, such as Bid and c-FLIP contribute to apoptotic resistance of U87MG cells. Down-regulation of USP18 expression together with the induction of ER-stress efficiently restored apoptosis in U87MG cells. Finally, we demonstrated that the BH3-only protein Noxa provides an important contribution in the apoptotic response to ER-stress in USP18 silenced cells.

Keywords USP18 · Spontaneous · Glioma · Caspase · TRAIL · Apoptosis · Noxa · IRF1 · PML · ER-stress · Interferon · DR5

Introduction

Type I IFNs are in clinical use for biotherapy against various malignancies. This family of cytokines influences several cellular responses including: differentiation, proliferation and apoptosis [1]. The anti-tumor activity of type I IFNs can be accomplished directly, by promoting growth arrest and apoptosis of neoplastic cells; or indirectly, by stimulating the host immune response [2]. Unfortunately, a substantial number of patients fail to respond to IFN therapy. Resistance commonly appears because cancer cells accumulate mutations in signaling elements of the IFN pathway or, in regulators of the apoptotic program [1, 2].

Glioblastoma multiforme (GBM) is among the most aggressive human cancers. After surgical resection, chemotherapeutic treatments show limited effect and relapse generally appears. Glioblastoma cells show a stubborn apoptotic resistance to several treatments, as well as to IFNs [3, 4]. Clinical studies have demonstrated only marginal benefits of type I IFNs in GBM treatment [5, 6]. Unfortunately, also in those tumors, where IFNs exert good clinical outcomes, a large proportion of patients fails to

Electronic supplementary material The online version of this article (doi:10.1007/s10495-011-0639-4) contains supplementary material, which is available to authorized users.

A. Sgorbissa · A. Tomasella · H. Potu · I. Manini · C. Brancolini (✉)
Dipartimento di Scienze Mediche e Biologiche and MATI Center of Excellence, Università degli Studi di Udine, P. le Kolbe 4, 33100 Udine, Italy
e-mail: claudio.brancolini@uniud.it

respond [1]. Hence, defining the mechanisms of IFNs resistance is pivotal to improve their use in vivo.

Homozygous deletions of the *IFNα/ω* genes are frequently observed in GBM [7–9], thus underlining an important suppressive role of these cytokines in glioblastoma development. In this respect, it is important to remember that although expression of type I IFNs is dramatically induced in response to viral and non-viral pathogens [1], cells constitutively secrete low levels of these cytokines [10]. It has been proposed that the constitutive IFNs signaling is essential for an efficient and timely response to pathogens [11]. Whether or not this constitutive signaling contributes to the apoptotic responsiveness of cancer cells to IFNs, is not defined.

USP18 is an IFN-responsive gene, which encodes for an isopeptidase involved in the deconjugation of the ubiquitin-like protein ISG15, from target proteins. In response to IFNs cells produce the whole enzymatic machinery controlling protein isgylation/deisgylation [12]. In addition, USP18 is a negative regulator of the IFN response in a catalytic-independent manner [13, 14]. USP18 can compete with Janus-activated kinase (JAK) for the binding to the cytosolic domain of the IFNAR2, a subunit of type I IFNs receptor. This association mitigates the IFN signaling [14].

In this study we have evaluated the contribution of the autocrine IFN loop in the apoptotic response to IFN-α. Since U87MG glioblastoma cells harbour a homozygous deletion of the entire *IFNα/IFNω* gene cluster and of the *IFNβ* gene, they were selected for these studies. U87MG were compared to T98G cells in which, as we demonstrate, the spontaneous IFN signaling is active. We have also investigated the rational of targeting USP18 to overcame apoptosis resistance in the two glioblastoma cell lines.

Materials and methods

Cell culture, drug treatments and apoptosis

T98G and U87MG cell lines were propagated as previously described [15]. Drugs used were IFN-α 2a (1,000 units/ml; Jena Bioscience), Actinomycin D (5 μg/ml; Sigma), 2′-Deoxy-5-azacytidine (Decitabine) (2.2 μM; Sigma), Tunicamycin (2 μg/ml, Sigma) and G5 (0.2 μM) [15]. For Decitabine experiments, cells were grown for 5 days in the presence of the drug before further treatments. For trypan blue exclusion assays, 400 cells from three independent experiments were counted for each data point. The DEVDase activity was evaluated using the Apo-ONE Assay (Promega). Recombinant histidine 6-tagged $TRAIL_{(114-281)}$ was purified by affinity chromatography [16].

Quantitative reverse transcription-PCR

cDNAs were synthesized from 1 μg of total RNA, obtained by Trizol (Invitrogen) extraction, using the First-Strand cDNA Synthesis kit (Invitrogen). Real-time PCR was performed using the KAPA SYBR® FAST Master Mix (Kapabiosytems) on a CFX96 Real-Time System (Bio-Rad). The obtained data were analyzed using the ΔΔCt method. The geometric average of HPRT1 (hypoxanthine phosphoribosyltransferase 1) and ACTB (*β*-actin) was used for normalization. Data were expressed as fold change from the untreated sample, when a single cell line was analyzed, or as fold change from the untreated sample of U87MG cells, when gene expression levels were compared between T98G and U87MG cells.

DNA cloning and sequencing

For cloning TRAIL promoters of U87MG and T98G cells, PCRs were made using the relative genomic DNAs, as templates. The resulting fragments were cloned in the pGL3 vector (Promega). All constructs were sequenced with the kit Big Dye® Terminator Sequencing RR-100 on ABI PRISM™ 310 Genetic Analyzer platform (Applied Biosystem).

siRNA, transfection and luciferase assay

siRNAs (Invitrogen) were transfected using Lipofectamine 2000 (Invitrogen). In the case of promoter reporter experiments cells were transfected with the Luc Reporter constructs for 24 h and then treated with interferon for further 16 h. Firefly luciferase activity in cell lysates was measured and normalized for *Renilla* luciferase activity using the Dual-Luciferase Reporter Assay System according to the vendor's instructions (Promega).

Immunofluorescence and immunoblotting

Cells grown directly onto coverslips were fixed in 3% paraformaldehyde. After washes with PBS/0.1 mol/l glycine, pH 7.5, cells were permeabilized with 0.1% Triton-X100 in PBS for 5 min. Next coverslips were treated with the anti-USP18 antibody and biotinylated WGA (Boehringer). Finally they were then washed twice with PBS and incubated with 488-Alexa conjugated secondary antibodies (Molecular Probes) and Streptavidin TRITC (Molecular Probes). Cells were examined with a Leica SP confocal microscope equipped with a 488 *λ* argon laser and a 543 *λ* helium neon. Immunoblotting was done as described previously [15]. Blots were developed with SuperSignal West Dura (Pierce). Antibodies used in this work were anti: TRAIL (Imgenex), Bid (BD Biosciences), FLIP (mouse,

Alexis) USP18 [17], Noxa (Calbiochem), Ran (BD Biosciences), USP33 (Millipore).

Oncomine data analysis

Genes co-expressed with TRAIL in glioblastoma tumors and in several cancer cell lines [18] were analyzed using the Oncomine database and gene microarray analysis tool [19]. Details of standardized normalization techniques and statistical calculations can be found on the Oncomine web site (https://www.oncomine.com/).

Results

Analysis of the IFN-α response in U87MG and T98G glioblastoma cells

U87MG cells harbour a deletion of type I IFN genes [9]. Hence, this cell line represents a useful model to explore the importance of the spontaneous IFN signaling in the apoptotic response to IFN-α. We used microarray analysis [15] to evaluate the existence of the spontaneous IFN-response in T98G cells. Several interferon responsive genes were highly expressed in T98G compared to U87MG cells, thus demonstrating the presence of the spontaneous IFN signaling (Supplementary Table S1).

Next we decided to analyze the activation of the IFN response in the two cell lines, as engaged by IFN-α. As similarly observed for IFN-β [20], U87MG and T98G cells were both resistant to IFN-α induced apoptosis (data not shown and Fig. 5a). To evaluate the response to IFN-α the kinetics of up-regulation of the transcription factors, *IRF-7* and *IRF-9* (Interferon Regulatory Factors) and of the IFNs inducible genes *USP18, PML* and *TRAIL* [21] were analyzed, by qRT-PCR (Fig. 1a).

Overall *IRF-7*, *IRF-9* and *PML* were similarly up-regulated in the two cell lines. A divergence was apparent at longer times, in particular for *IRF-7*. In U87MG cells *IRF-7* expression declined 24 h after stimulation, whereas in T98G cells, *IRF-7* expression augmented over the time and its level was still high, 24 h after IFN-α addition. Surprisingly, *TRAIL* induction was overtly impaired in U87MG cells. Although the pattern of up-regulation was comparable, with a rapid and transient rise of TRAIL mRNA, this response was much more pronounced in T98G cells. By contrast, USP18 transcripts showed an opposite behaviour, being induced at higher levels in U87MG cells as compared to T98G cells (Fig. 1a).

Next we decided to verify the differential induction of TRAIL and USP18 by immunoblot analysis. Figure 1b confirms that T98G cells express higher levels of TRAIL and that they accumulate higher amounts of the death ligand after IFN treatment. Despite differences in terms of mRNA expression, accumulation of USP18 protein, in response to IFN-α was comparable between the two cell lines. Finally, we also analyzed USP18 up-regulation and localization by immunofluorescence. The increase of USP18 levels after IFN-α addition can be appreciated in Fig. 1c. USP18 shows a diffuse cytosolic staining, which is dramatically increased in both cell lines, upon IFN-α treatment.

Transcription from the TRAIL promoter in U87MG and T98G cells

Our data indicate that certain IFN-inducible genes were similarly turned-on in the two cell lines in response to IFN-α. By contrast, up-regulation of TRAIL was less pronounced in U87MG cells. To comprehend at which step TRAIL induction in response to IFN-α was impaired in this cell line, we analyzed the transcriptional activity of TRAIL promoter [22]. Cells were transfected with a luciferase reporter gene driven by TRAIL promoter and next treated or not with IFN-α. In the absence of IFN-α, transcription from TRAIL promoter was similar in the two cell lines (Fig. 2a). Addition of IFN sustained luciferase transcription in both cell lines and, paradoxically, more strongly in U87MG cells.

Transcription from TRAIL promoter does not emulate the difference in TRAIL levels observed in the two cell lines. It is possible that genomic mutations, accumulated within the TRAIL promoter of U87MG cells, could be responsible for the observed defects in TRAIL expression. Hence, we decided to clone the TRAIL promoters from T98G and U87MG genomic DNA to monitor their relative transcriptional activities. Figure 2b illustrates that TRAIL promoters, isolated from U87MG and T98G cells, and transfected in both cell lines were indistinguishable in terms of basal and IFN-induced transcriptional activity. Furthermore, DNA sequencing analysis of the TRAIL promoters isolated from T98G and U87MG cells has not revealed overt alterations (Fig. 3), thus confirming the luciferase experiments.

We have also sequenced part of the first intron in which a new putative ISRE motif has been identified. Alignment with the previous published sequence of TRAIL promoter [22] has showed four bases substitutions and a single base insertion (−825/−824), in T98G cells. On the other side, five bases substitutions and two single base insertions (−1191/−1190 and +69/+70) were found in U87MG cells. Not surprisingly, different repetitions numbers of the polymorphic tetranucleotide repeat, (AAAG) were discovered in the three promoters. Among all these changes only the G/A (−76 and −11) substitutions in the U87MG promoter are placed within putative transcription factor cores (SP1 and IRF-E respectively).

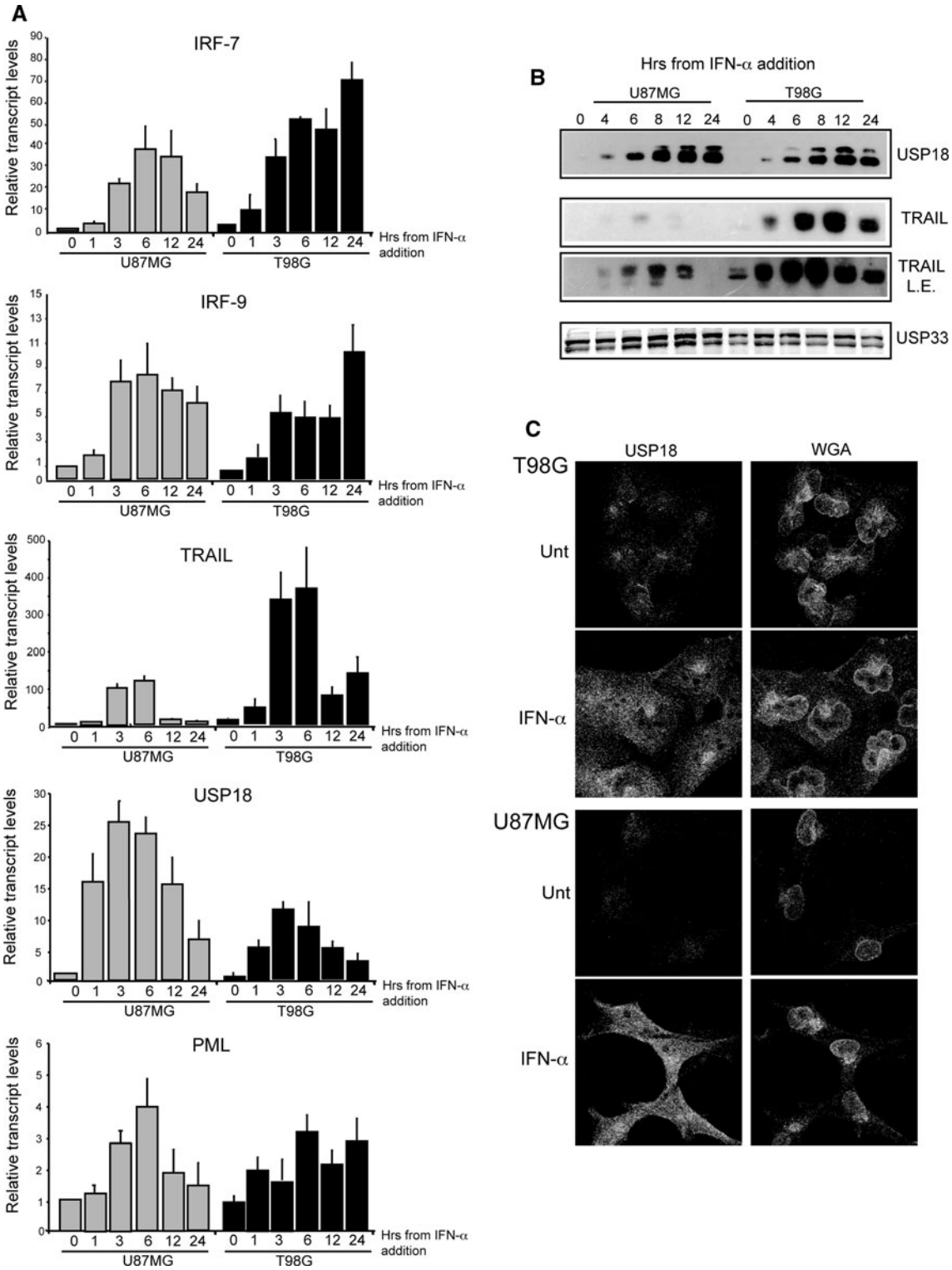

Fig. 1 The interferon response in U87MG and T98G glioblastoma cells. **a** Regulation of *IRF-7, IRF-9, TRAIL, PML* and *USP18* mRNAs expression by IFN-α in glioblastoma cells. qRT-PCR analysis was performed to quantify *IRF-1, IRF-2, IRF-3, IRF-7, IRF-9, TRAIL, PML* and *USP18* mRNAs. T98G and U87MG cells treated for the indicated times with IFN-α were lysed and mRNAs extracted. Samples were normalized as described in MM. (means ± SD, $n = 4$). **b** Time course analysis of TRAIL and USP18 induction in U87MG and T98G cells by immunoblots using the specific antibodies. Lysates were generated from U87MG and T98G cells treated for the indicated times with IFN-α. USP33 was used as loading control. A long exposure of TRAIL immunoblot is shown (L.E). **c** Immunofluorescence analysis investigating USP18 induction and subcellular localization in T98G and U87MG cells. WGA (wheat germ agglutinin) was used to stain plasma membrane and Golgi apparatus

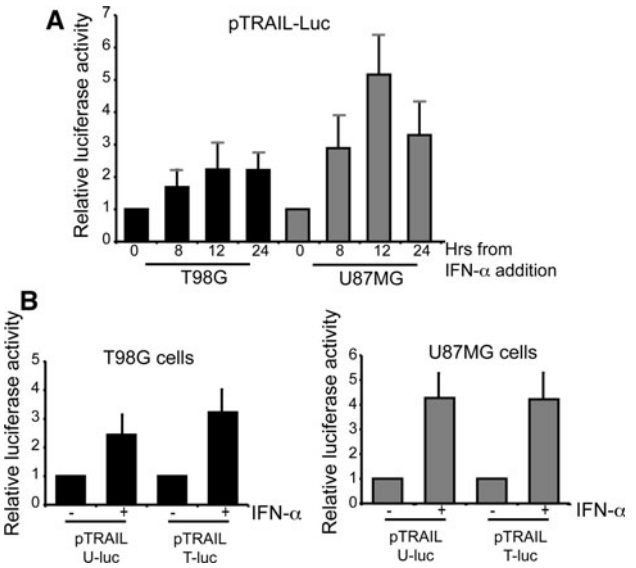

Fig. 2 TRAIL transcription in the glioblastoma cells. **a** Relative luciferase activity from co-transfection of the reporter plasmid pTRAIL-luc (−1523/+55) in T98G and U87MG cells, treated with IFN-α for the indicated times. The *renilla* luciferase plasmid was used as internal control (means ± SD, $n = 3$). **b** Relative luciferase activity from co-transfection of the reporter plasmids pTRAIL-U-luc containing the *TRAIL* promoter (−1508/+55) isolated from U87MG cells and pTRAIL-T-luc isolated from T98G cells (−1496/+55). The two glioblastoma cell lines were transfected with the indicated plasmids and next treated or not with IFN-α for 12 h. The *renilla* luciferase plasmid was used as internal control (means ±SD, $n = 3$)

Having excluded that mutations in the promoter sequence could be responsible for TRAIL defective expression in U87MG cells, we decided to investigate the contribution of epigenetic modifications.

Several studies have shown that DNA methylation can influence the IFN response and TRAIL up-regulation [23]. Furthermore there are several CpG sites within the TRAIL promoter (Fig. 3). Therefore we assessed the capability of the demethylating agent 5-aza-2′-deoxycytidine (5-AzadC) to influence TRAIL expression in glioblastoma cells (Fig. 4a). 5-AzadC augmented the expression of TRAIL ($p < 0.05$) and IRF-7 ($p < 0.05$) in U87MG cells stimulated with IFN. However, TRAIL levels remained far below those observed in IFN-treated T98G cells. Surprisingly, in IFN-treated T98G cells 5-AzadC sustained IRF-7 transcription ($p < 0.01$) but diminished TRAIL expression ($p < 0.05$).

In conclusion our studies indicate that, although DNA methylation influences TRAIL expression and IFN signaling in glioblastoma cells, additional mechanisms are responsible for the TRAIL deficit observed in U87MG cells.

TRAIL mRNA stability

Having excluded explicit alterations in TRAIL transcription, we investigated whether differences in mRNA stability could account for its defective expression in U87MG cells. To explore this possibility the two glioblastoma cell lines were treated for 3 h with IFN-α and next actinomycin-D (Act-D) was added to block transcription. qRT-PCR was used to compare the stability of TRAIL mRNA in the two cell lines (Fig. 4b).

When the analysis was performed 3 h after IFN-α addition the mRNA for TRAIL appeared to be stable, with a half-life longer than 12 h. By contrast, in the absence of IFN-α TRAIL mRNA was unstable, with a half-life of less than 3 h. This behaviour was analogous in the two cell lines.

The long half-life of TRAIL mRNA in IFN-treated cells was unexpected. In fact, after a rapid induction with a peak at 6 h, TRAIL mRNA rapidly drops down, 12 h after stimulation (Fig. 1a). This result clearly suggests a rapid decay of TRAIL mRNA stability also in the presence of IFN. Hence, to clarify this point we decided to evaluate the stability of TRAIL mRNA 10 h after IFN-α stimulation. Figure 4c demonstrates that 10 h after IFN-α stimulation TRAIL transcript showed a reduced stability, thus indicating that IFN-α stabilization of TRAIL mRNA is a transient event. In conclusion these data suggest that also the regulation of mRNA stability is under IFN control. Nevertheless, differences in TRAIL mRNA stability cannot be appreciated between the two cell lines.

The spontaneous IFN-signaling supports TRAIL expression in T98G cells

Our studies indicate that despite the huge difference in the amount of TRAIL protein between T98G and U87MG cells, differences in TRAIL transcription and TRAIL mRNA stability cannot be observed. Looking more carefully at the time-course showed in Fig. 1a, we noted that the strongest discrepancy in terms of TRAIL mRNA levels, between the two cell lines can be observed in the absence of IFN (see also the microarray data in Supplementary Table S2). This data can be more clearly illustrated, when the levels of TRAIL transcripts were represented as a ratio between the two cell lines (Fig. 5a). At time 0 TRAIL was 24 fold less expressed in U87MG compared to T98G cells.

This dramatic difference of TRAIL levels in untreated cells could be the result of the absence of the spontaneous interferon response in U87MG cells. To evaluate this hypothesis we decided to switch-off type I IFNs signaling in T98G cells by silencing the expression of IFNAR1, a subunit of the receptor for type I IFNs. Levels of *TRAIL, IRF-1*, *IRF-7* and *IRF-9* mRNAs were evaluated and compared to the levels present in U87MG cells. Figure 5b proves that switching off the constitutive type I IFN signaling has profound effects on the expression of *TRAIL, IRF-1, IRF-7* and *IRF-9*. In T98G cells silenced for

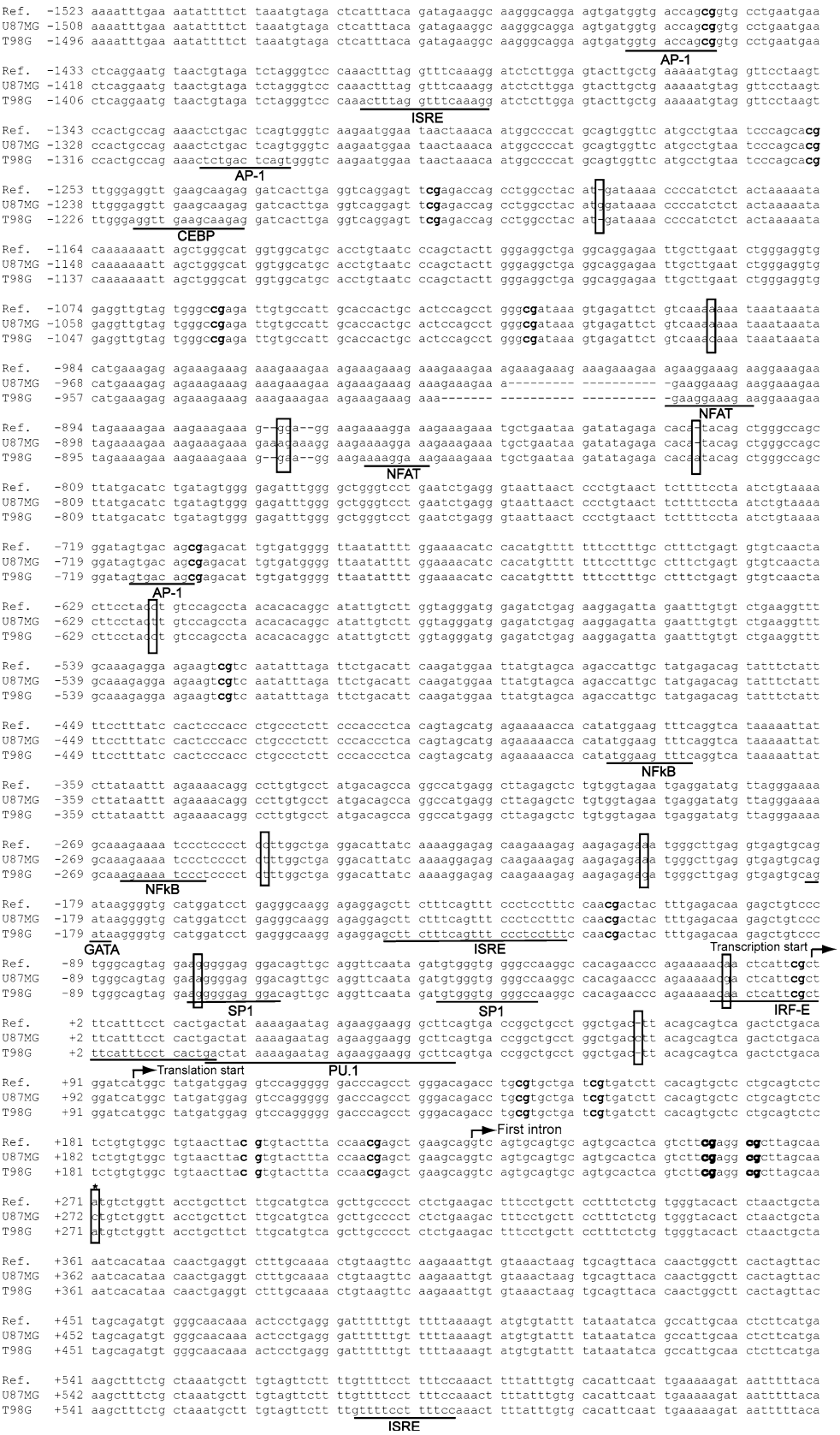

Fig. 3 Nucleotide sequence analysis of the human *TNSF10(TRAIL)* promoter region from glioblastoma cell lines U87MG and T98G. The reference sequence of the TRAIL promoter region is based on the sequences published on NCBI (AF178756.1) [21] as well as on sequences published in Ensembl (ENSG00000121858). Putative and verified binding sites for transcription factors are *underlined*, as previously described [21, 23]. *Boxes* evidence the identified mutations. Putative CG methylation sites are represented in *bold*. *Arrows* highlight transcription/translation start sites and the onset of the first intron, as predicted by Ensembl. The alignments, carried out with blast nucleotide algorithm on NCBI site, show regions of deletion/insertion present in U87MG and T98G promoter regions of hTRAIL. The nucleotide sequence of the first transcribed 541 bp region is included. We have also identified another putative ISRE sequence inside the first intron

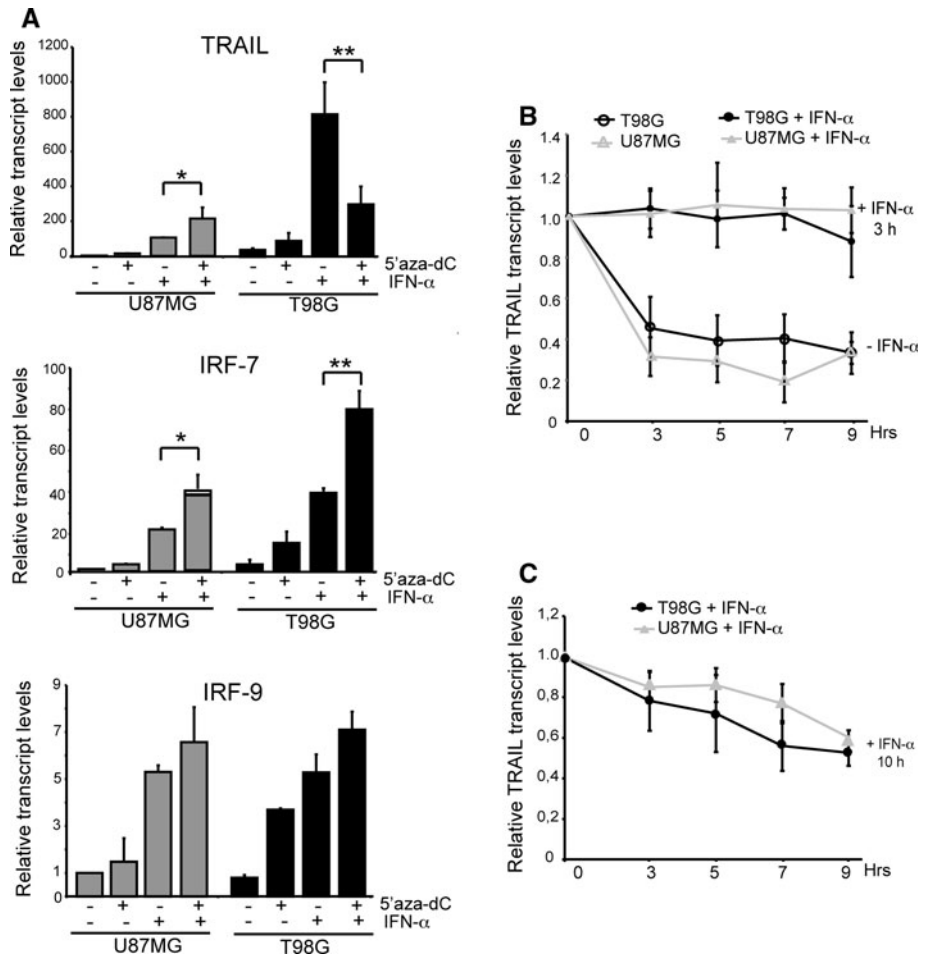

Fig. 4 Analysis of TRAIL mRNA stability in T98G and U87MG cells. **a** Regulation of *IRF-7* and *TRAIL* mRNAs expression by IFN-α in glioblastoma cells pre-treated with 5-AzadC. Before IFN-α addition cells were grown for 5 days in the presence of 5-AzadC (2.2 μM). qRT-PCR analysis was performed to quantify *IRF-7* and *TRAIL* mRNAs. T98G and U87MG cells treated or not for 12 h with IFN-α were lysed and mRNAs extracted. Samples were normalized as described in MM. (means ± SD, $n = 4$). $^{*}P < 0.05$; $^{**}P < 0.01$. **b** Act-D (5 μg/ml) was added to cells pre-treated or not for 3 h with IFN-α. RNA was extracted at the different times, as indicated. qRT-PCR analysis was performed to quantify *TRAIL* mRNA. Samples were normalized as described in MM. (means ± SD, $n = 3$). **c** Act-D (5 μg/ml) was added to cells pre-treated for 10 h with IFN-α. RNA was extracted at the different times, as indicated. qRT-PCR analysis was performed to quantify *TRAIL* mRNA. Samples were normalized as described in MM. (means ± SD, $n = 3$)

IFNAR1 mRNAs levels of *IRF-1, IRF-7* and *TRAIL* were similar to those observed in U87MG cells. Curiously IRF-9 mRNA levels were higher in U87MG cells, possibly highlighting an IFN-independent regulation of its expression.

IRF-1 is an important regulator of TRAIL transcription [24]. Having identified that IRF-1 expression is highly susceptible to the spontaneous IFN signaling we decided to compare its up-regulation in response to IFN-α in the two cell lines. As shown in Fig. 5c, the pattern of IRF-1 mRNA in response to IFN-α, in both cell lines, is very similar to those of TRAIL mRNA (Fig. 1a). IRF-1 up-regulation, similarly to TRAIL is largely impaired in U87MG cells (Fig. 5c).

Next, to prove the contribution of IRF-1 to the spontaneous interferon signaling and to the control of TRAIL expression we transfected T98G cells with a siRNA against IRF-1. The experiments were also performed in cells treated with IFN-α. In T98G cells silenced for IRF-1 there was a reduction of TRAIL levels (Fig. 5d). However this reduction was less pronounced compared to cells silenced for IFNAR1. These results indicate that IRF-1 plays a role in the regulation of TRAIL expression but also indicate that additional interferon-regulated factors are implicated. Similarly, in cells silenced for IRF-1 and treated with IFN-α, TRAIL up-regulation was partially impaired (Fig. 5d).

To understand whether the relationship between IRF-1 and TRAIL expression was not limited to the examined glioblastoma cells, we took advantage of the oncomine database [19]. Initially we analyzed the TCGA Brain data, which include the analysis of mRNA expression for 144 glioblastoma and an anaplastic astrocytoma, using the human genome U133A array. Results of the analysis are

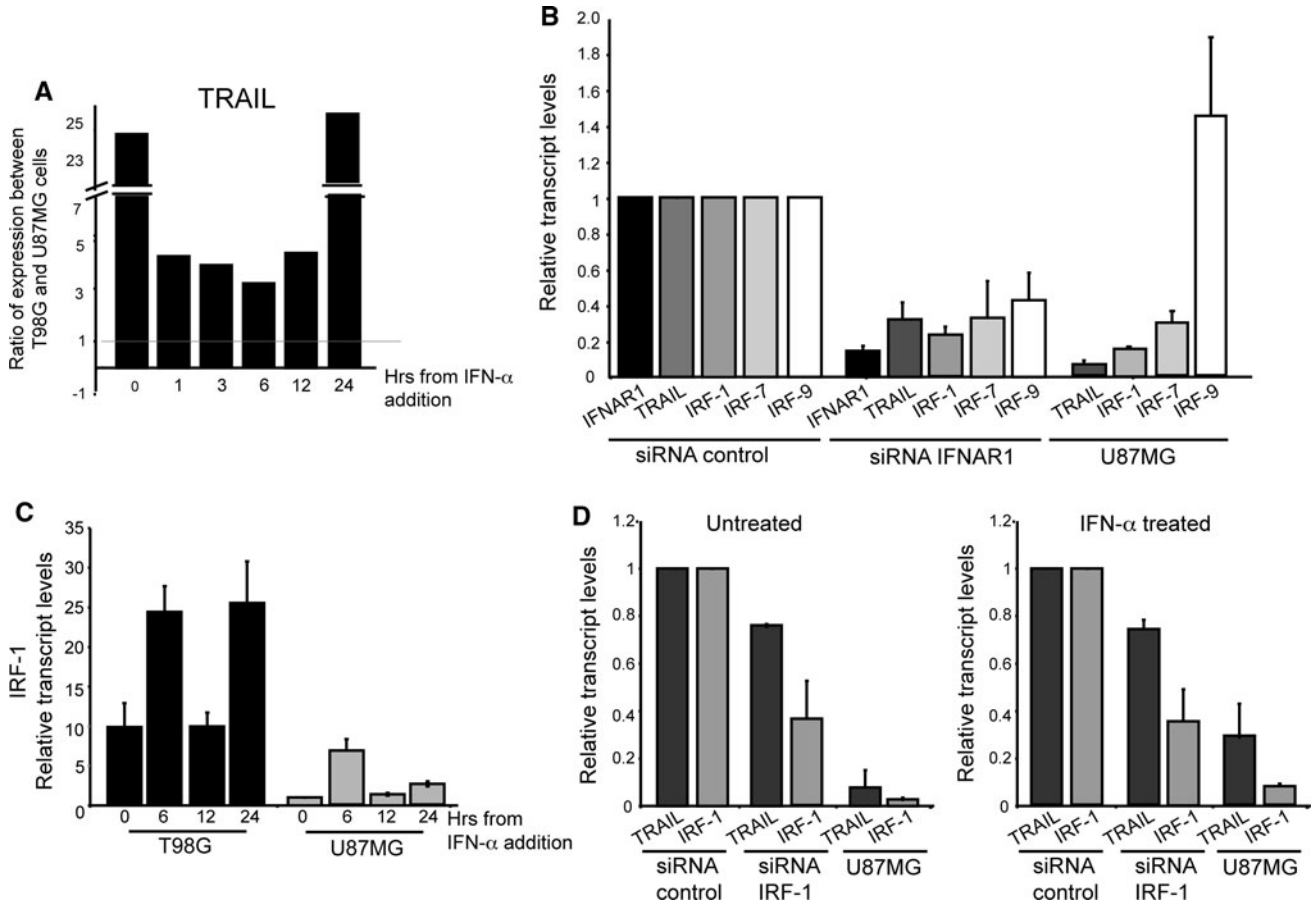

Fig. 5 The spontaneous IFN signaling is required to sustain TRAIL expression in T98G cells. **a** Cells were incubated with IFN-α for the indicated times. qRT-PCR analysis was performed to quantify *TRAIL* mRNA. Samples were normalized as described in MM. (means ± SD, $n = 4$). Data are reported as the ratio of TRAIL mRNAs levels between T98G and U87MG cells. **b** *IRF-1, IRF-7, IRF-9* and *TRAIL* mRNAs levels in T98G cells after silencing of *IFNAR1*. mRNAs levels are shown relative to those of T98G cells transfected with control siRNA. mRNA levels of the same genes in U87MG cells are included for comparison. Levels of *IFNAR1* mRNA were investigated to prove silencing effectiveness. **c** Regulation of *IRF-1* mRNAs expression by IFN-α in T98G and U87MG cells. qRT-PCR analysis was performed to quantify *IRF-1* mRNAs. Cells treated for the indicated times with IFN-α were lysed and mRNAs extracted. Samples were normalized as described in MM. (means ± SD, $n = 4$). **d** *TRAIL* mRNAs levels in T98G cells after silencing of *IRF-1*. 44 h after transfection cells were treated or not for further 6 h with IFN-α. *TRAIL and IRF-1* mRNAs levels are shown relative to those of T98G cells transfected with control siRNA. mRNA levels of the two genes in U87MG cells are included for comparison. Samples were normalized as described in MM (means ± SD, $n = 3$)

shown in Table 1 and expressed as co-expression values. We have reported the absolute best score and the best scores for genes regulated by IFNs. The IFN-inducible gene *IL15RA* (IL-15 receptor alpha-chain) showed the greatest co-expression value with *TRAIL*. *IRF-1* was the third hit of the list. In general, there were several correlations with genes of the IFN response (*USP18, ISG20, ISG15*) thus possibly indicating that in the selected tumors an inflammatory response was engaged [25].

To restrict the co-expression analysis to conditions where only the spontaneous IFN signalling should be active, we selected the Wagner cell lines data, which comprise the expression profiles of 119 different cancer cell lines [18]. In this case the best score, in terms of co-expression with *TRAIL,* was for *SMAD6* and among the IFNs inducible genes *IRF-1* was the second best score after *IL15*. In the analyzed cancer cell lines several IFN-inducible genes such *ISG15, XAF1, PML* and *UBA7* did not evidenced significant co-expression values with *TRAIL*.

In conclusion these studies suggest that the spontaneous IFN signaling, possibly through the regulation of IRF-1 levels could contribute to sustain TRAIL expression in glioblastoma cells.

Down-regulation of USP18 sensitizes T98G but not U87MG cells to IFN-α induced apoptosis

Despite TRAIL was highly induced in T98G compared to U87MG cells, IFN was incapable of eliciting apoptosis in both cell lines (Fig. 6a, b). USP18, a negative regulator of

Table 1 TCGA BRAIN 145 samples: 144 Glioblastoma and 1 Anaplastic Astrocytoma, Wagner cell lines 119 samples

Gene	Co-expression value*	Gene	Co-expression value*
TRAIL/TNFSF10	1.00	*TRAIL/TNFSF10*	1.00
IL15RA	0.698	*SMAD6*	0.588
UBA7	0.619	*IL-15*	0.449
IRF-1	0.549	*IRF-1*	0.402
CASP1	0.549	*IRF-6*	0.378
CASP4	0.549	*IRF-8*	0.261
ISG20	0.502	*ISG20*	0.202
USP18	0.467	*OAS1*	0.202
ISG15	0.467	*PML*	−0.062
XAF1	0.467	*UBA7*	−0.062
IRF-9	0.467	*XAF1*	−0.062
STAT-1	0.328	*ISG15*	−0.062

* The coexpression value is derived from average linkage hierarchical clustering and represents the correlation value of the node that includes the query gene and at least 10 other reporters

the IFN response can increase the susceptibility to IFN-induced apoptosis [17]. Hence, we investigated whether down-regulation of USP18 was sufficient to sensitize U87MG and T98G cells to apoptosis in response to IFN treatment. Silencing of USP18 efficiently promoted IFN-α induced apoptosis and caspase activation in T98G, but not in U87MG cells (Fig. 6a, b). This apoptotic response was largely dependent on TRAIL. In fact, silencing of TRAIL impaired IFN-α induced apoptosis and caspase activation, in T98G cells with down-regulated USP18 expression (Fig. 6c).

To evaluate TRAIL levels after USP18 down-regulation, immunoblot analysis was performed at 8 and 24 h from IFN-α addition. In T98G cells, USP18 down-regulation augmented TRAIL expression already after 8 h from IFN treatment. Furthermore, silencing of USP18 dramatically sustained TRAIL levels at 24 h from stimulation (Fig. 6d). Similarly, in U87MG cells silencing of USP18 endorsed TRAIL expression. After 8 h from IFN-α treatment, its level was comparable to those observed in T98G cells transfected with the control siRNA. However, in these cells, down-regulation of USP18 was insufficient to maintain TRAIL expression at later time from IFN-α addition. 24 h after treatment expression of TRAIL was almost undetectable, irrespectively from the presence or not of USP18 (Fig. 6d).

To exclude that the limited up-regulation of TRAIL in U87MG cells, following USP18 silencing, could be the consequence of its shedding from the plasma membrane as provoked by proteases [21], we also analyzed the accumulation of TRAIL in the medium of the two cell lines (Fig. 6d lower panel). TRAIL was detected in the SN of T98G cells silenced for USP18 and treated with IFN-α, whereas only a faint band was visualized in the SN of U87MG cells silenced for USP18 and treated with IFN-α. Hence, shedding from the PM is not responsible for the partial effect of USP18 silencing on TRAIL levels in U87MG cells.

ER stress sensitizes U87MG cells to TRAIL induced apoptosis

Targeting USP18 can efficiently sensitize T98G cells to IFN induced apoptosis, whereas it was ineffective in U87MG cells. Resistance of U87MG cells could be the result of the imperfect up-regulation of TRAIL but also of an intrinsic resistance to TRAIL apoptotic signaling. Hence, we evaluated the response to TRAIL-induced apoptosis in these cell lines. Figure 7a and b demonstrate that T98G cells are sensitive to TRAIL induced apoptosis, whereas U87MG cells are resistant, as previously observed in certain studies [26]. This behaviour could be the consequence of alterations in elements of the extrinsic pathway, such as Bid and $FLIP_L$ as highlighted by immunoblot (Fig. 7c) and microarray analysis (supplementary table S2).

Having proved an intrinsic resistance to TRAIL signaling in U87MG cells we decided to evaluate the ability of different compounds, well-known TRAIL sensitizers, of rendering these cells responsive to TRAIL-induced apoptosis. Since TRAIL is an important element of the apoptotic response to IFN, these compounds should also synergize with IFNs to trigger apoptosis.

We observed that the isopeptidase inhibitor G5 [15] and tunicamycin, an inducer of ER-stress could sensitize U87MG cells to TRAIL-induced apoptosis (Fig. 7d, e). Since also G5 can induce ER-stress we focused our attention on tunicamycin. USP18 was depleted by RNAi in U87MG cells and next, tunicamycin was added for 24 or 48 h. Cells were also treated or not with IFN-α for 24 or 48 h. Appearance of cell death was scored by trypan blue staining. Figure 7f demonstrates that in U87MG cells IFN-α did not influence ER-stress induced cell death. However, silencing of USP18 greatly increased cell death, in cells grown for 48 h in the presence of tunicamycin. This effect was not influenced by the addition of IFN-α.

Several studies have shown that ER-stress can sustain TRAIL induced apoptosis through different mechanisms [27]. It is well known that expression of the TRAIL receptor DR5/TRAIL-R2 and of the BH3-only protein Noxa is increased in response to ER-stress [28]. Hence, DR5/TRAIL-R2 and Noxa induction in response to tunicamycin treatment was evaluated in U87MG cells. Figure 7g shows that expression of both proteins was augmented after

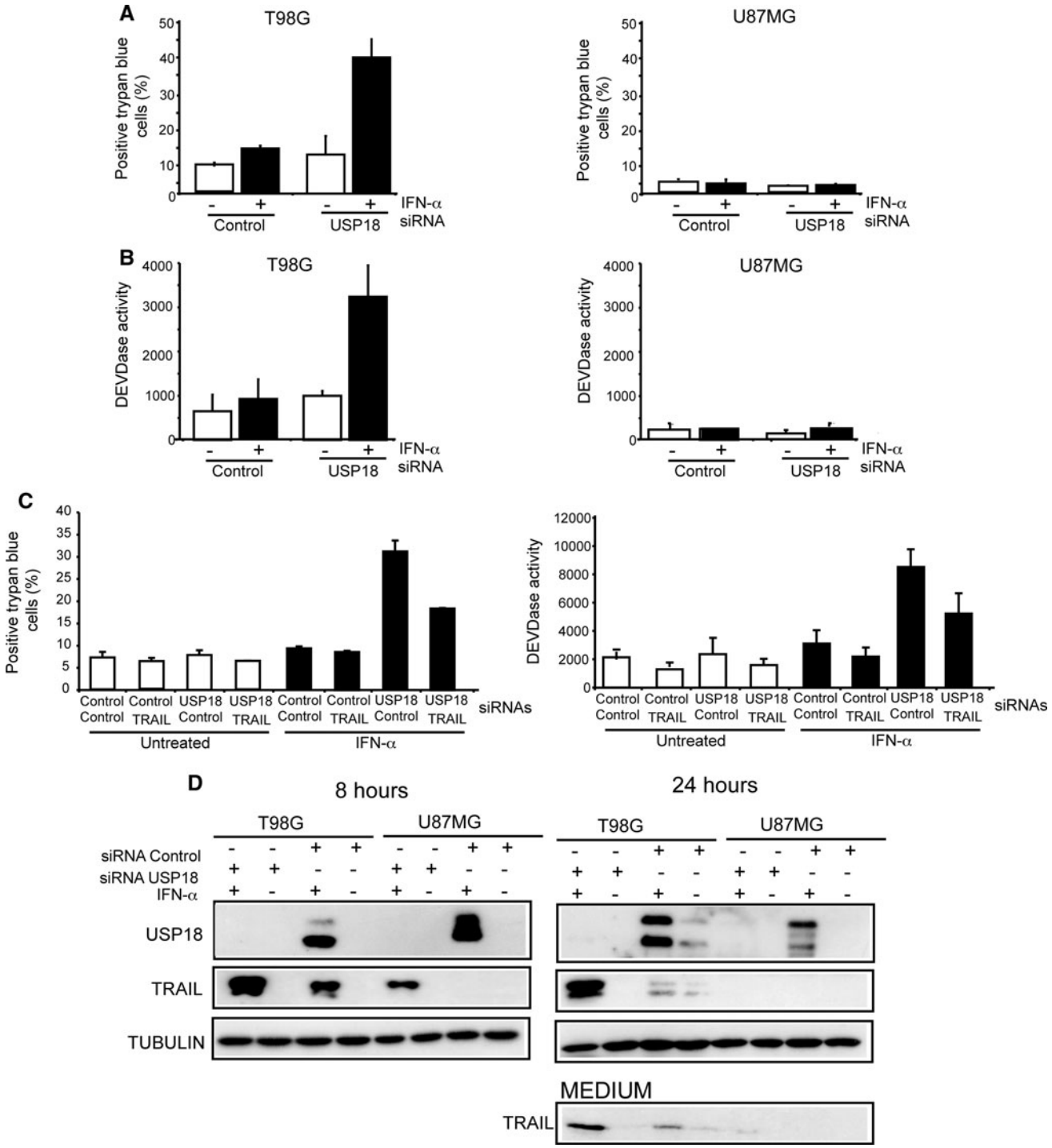

Fig. 6 USP18 down-regulation promotes TRAIL induction and apoptosis in response to IFN-α in T98G but not in U87MG cells. **a** T98G and U87MG cells were transfected with the siRNAs specific for USP18 or the control siRNA as indicated. 24 h after transfection cells were treated or not, for further 24 h with IFN-α. Cell death was evaluated by trypan blue staining (means ± SD, $n = 3$). **b** T98G and U87MG cells were transfected with the siRNAs specific for USP18 or the control siRNA as indicated. 24 h after transfection cells were treated or not, for further 24 h with IFN-α. Apoptosis was evaluated by scoring caspase activity (DEVDase activity). **c** T98G cells were transfected with combinations of the two different siRNAs as indicated. 24 h after transfection cells were treated or not, for further 24 h with IFN-α. Cell death was scored after trypan blue staining and by Caspase-3/7 (DEVDase) activity (means ± SD, $n = 3$). **d** Analysis of the expression levels of USP18 and TRAIL in U87MG and T98G cells down-regulated for USP18 expression. Lysates from T98G and U87MG cells silenced as indicated and treated for 8 or 24 h with IFN-α were prepared and subjected to immunoblot analysis using the specific antibodies. Tubulin was used as loading control. Culture media of the same experiment were analysed by immunoblotting to detect the soluble form of TRAIL (*lower panel*)

induction of ER-stress. By contrast TRAIL expression was not induced after tunicamycin treatment (Supplementary Fig. S1).

Finally we decided to analyse the contribution of Noxa and TRAIL-signaling during apoptosis elicited by the combination of ER-stress and USP18 down-regulation. Cells were double silenced for USP18 and TRAIL or Noxa and the induction of cell death, following tunicamycin treatment was evaluated. Silencing of TRAIL poorly attenuated the pro-death effect of USP18 down-regulation. Abrogation of Noxa caused a more effective reduction of cell death in USP18 silenced U87MG cells (Fig. 7h). Hence both TRAIL signaling and Noxa activities are involved in the death response of glioblastoma cells, as elicited by ER-stress in the absence of USP18.

Discussion

Type I IFNs can elicit apoptosis in neoplastic cells, however the pro-death effect of these cytokines is indirect and mainly depends on the transcriptional modulation of a set of pro-apoptotic genes. Several ISGs with pro-apoptotic functions have been characterized and a central role is played by the death ligand TRAIL [1, 2].

Cancer cells frequently acquire resistance to IFN treatment. Resistance to IFN can arise from defects in the IFN signaling pathway or from alterations in the apoptotic circuits. Defects in IRF-9 and STAT2 expression or epigenetic changes are responsible for resistance to IFN-mediated anti-tumor activity and for apoptotic insensitivity [29–33]. On the other side, up-regulation of anti-apoptotic Bcl-2 family members and activation of the NF-kB pathway can also confer resistance to IFN-mediated cell death [34–36].

In this work we hypothesized that deletions of the type I IFN genes, which abrogate the spontaneous IFN signaling and frequently occur in glioblastoma could endorse apoptotic resistance to IFN treatment. It is well known that type I IFNs can exert biological effects at low, constitutive levels of expression [11]. For example, the weak IFN-β-mediated signaling augments IFN-α/β induction in response to virus, through a positive feedback, involving autocrine/paracrine up-regulation of IRF-7 [37]. The constitutive IFN signaling can also prevent oncogenic transformation [38] and it is abrogated during spontaneous cellular transformation [39]. Also apoptosis in serum deprived macrophage depends on the autocrine secretion of type I IFNs [40].

We have demonstrated that glioblastoma cells deleted for type I IFN genes are defective for TRAIL up-regulation in response to IFN-α compared to glioblastoma cells, in which the autocrine loop is active. Other IFN-inducible genes such as IRF-9, USP18 and PML were similarly up-regulated in the two cell lines.

We have excluded that the defect observed in U87MG cells could stem from alterations in TRAIL promoter, or from differences in TRAIL mRNA stability. Interestingly, we have demonstrated that also the stability of TRAIL mRNA is under the influence of the IFN signaling.

Epigenetic changes, such as DNA methylation can influence TRAIL expression in certain cancer cell lines [39]. The TRAIL promoter contains several CG motifs but treatments with 5-AzadC slightly up-regulated TRAIL expression in U87MG cells in response to IFN. Although DNA methylation can influence TRAIL expression, it is not the sole responsible for the reduced and temporally restricted gene transcription, observed in U87MG cells.

We provide evidences that TRAIL levels are highly susceptible to the spontaneous IFN signaling. Abrogation of this autocrine loop has a profound effect on TRAIL levels. IRF-1 expression, similarly to TRAIL is impaired in U87MG cells following IFN-α treatment and is dependent on the spontaneous IFN signaling. Previous studies have indicated that IRF-1 is an important regulator of TRAIL transcription [24, 41, 42]. Clarke and co-authors have suggested that complex interactive structures, resembling the IFNβ enhanceosome [43] could be organized at the TRAIL promoter.

We have showed that in T98G cells IRF-1 is required for an efficient TRAIL expression, both in the presence and absence of IFN-α. However, switching-off the spontaneous IFN signalling, through the silencing of IFNAR1 has a more profound effect on TRAIL, compared to the silencing of IRF-1. These results indicate that additional interferon-regulated factors are implicated in TRAIL transcription. In U87MG cells the limited availability of IRF-1 and of additional factors could contribute to temporally restrict the robust up-regulation of TRAIL in response to IFN-α.

IRF-1 expression is under the control of both type I and II IFNs [44] and subjected to multiple mechanisms of regulation, including interaction with MyD88 [45] or SUMOylation [46]. IRF-1 is a bona-fine tumor suppressor gene controlling apoptosis, and inactivating mutations have been identified in tumors [47–49]. Using the publicly available Oncomine microarray database [19, 50] we have observed a significant correlation between the levels of expression of IRF-1 and TRAIL in several cancer cell lines and glioblastoma tumors. Hence, the correlation between TRAIL and IRF-1, emerging from our data could be of broader significance than a simple difference between two glioblastoma cell lines.

Curiously, experiments using the transfected TRAIL promoter in the two cell lines failed to recapitulate the defect in TRAIL up-regulation. We do not have an explanation for this apparent contradictory result. It is

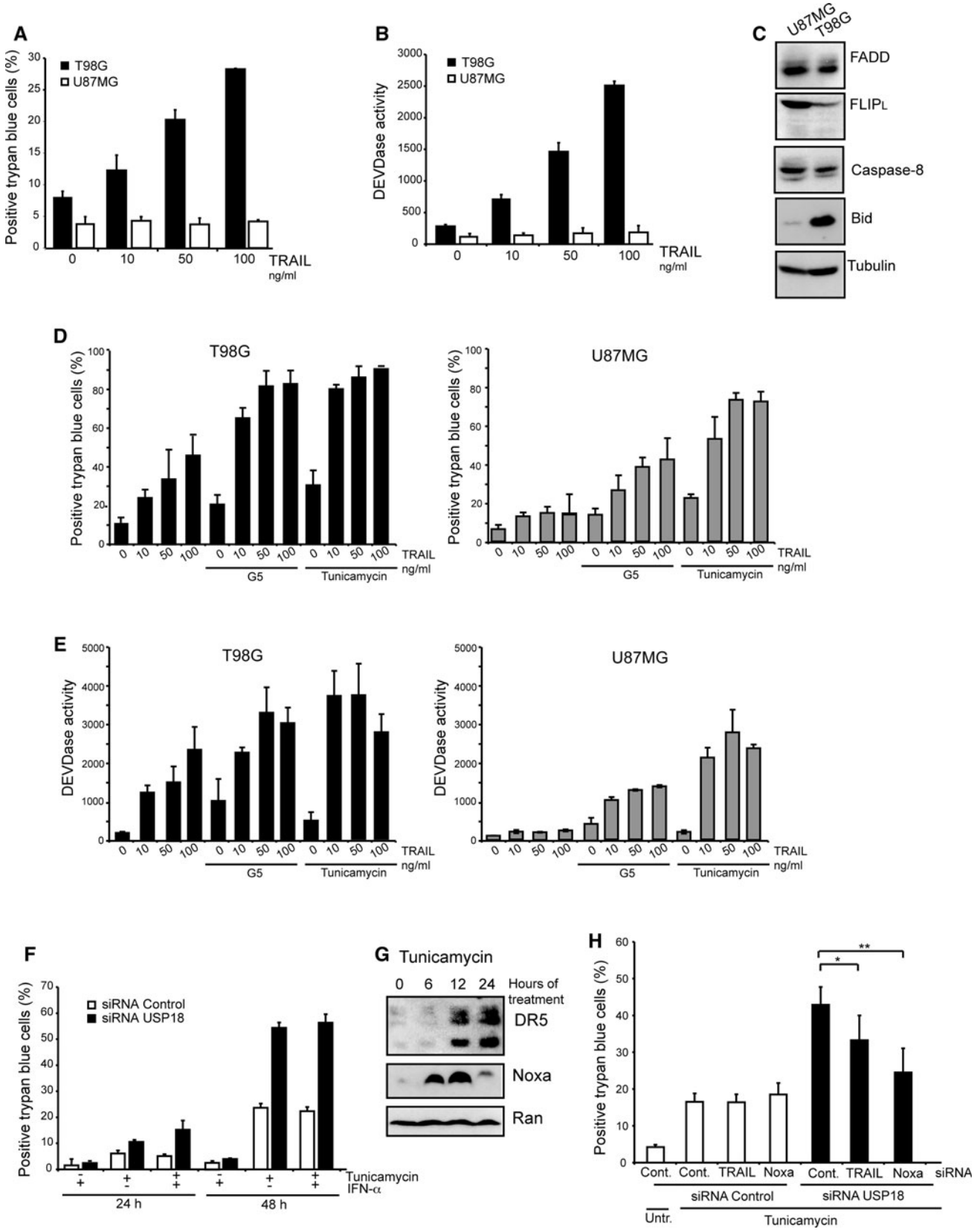

◀ **Fig. 7** USP18 influence ER-stress induced cell death in U87MG cells. **a** Glioblastoma cell lines were treated or not for 24 h, with the indicated amounts of rTRAIL. Cell death was scored by trypan blue staining (means ± SD, $n = 3$). **b** Glioblastoma cell lines were treated or not for 24 h, with the indicated amounts of rTRAIL. Caspase activity (DEVDase) was evaluated using a fluorogenic assay (means ± SD, $n = 3$). **c** Expression levels of some components of extrinsic pathway by immunoblot analysis. Lysates were generated from U87MG and T98G cells and used for the immunoblot. Tubulin was used ad loading control. **d** T98G and U87MG cells were treated or not for 24 h with G5 (20 nM) or with tunicamycin (2 μg/ml). Next, indicated amounts of rTRAIL were added and incubation was prolonged for further 24 h. Cell death was scored by trypan blue staining (means ±SD, $n = 3$). **e**) T98G and U87MG cells were treated or not for 24 h with G5 (20 nM) or with tunicamycin (2 μg/ml). Next indicated amounts of rTRAIL were added and incubation was prolonged for further 12 h. Caspase activity (DEVDase) was evaluated using a fluorogenic assay (means ± SD, $n = 3$). **f** U87MG cells were transfected with the siRNAs specific for USP18 or the control siRNA as indicated. 24 h after transfection cells were treated or not, for further 24 or 48 h with tunicamycin, IFN-α, or a combination of both molecules, as indicated. Cell death was evaluated by trypan blue staining (means ± SD, $n = 3$). **g** Analysis of the expression levels of DR5/TRAIL-R2 and Noxa in U87MG cells treated with tunicamycin. Cellular lysates were prepared at different times from tunicamycin addition and subjected to immunoblot analysis using the specific antibodies. Ran was used as loading control. **h** U87MG cells were transfected with combinations of the two different siRNAs as indicated. 24 h after transfection cells were treated or not, for further 48 h with tunicamycin. Cell death was scored after trypan blue staining (means ±SD, $n = 4$)

possible that the limited amount of transcription factors cannot promote transcriptional difference from transient transfected TRAIL promoter or other factors, such as epigenetic changes, could also influence transcription from transiently transfected promoters [51]. It is evident that our knowledge of the temporal assembling of transcriptional regulators, at the TRAIL promoter is limited and further studies are necessary. Therefore, it is unclear if the ectopically expressed TRAIL promoters faithfully recapitulate all the fine regulative changes that operate on the endogenous promoter.

In conclusion we suggest that turning off the spontaneous IFN signaling provide an additional advantage to cancer cells conferring resistance to the pro-apoptotic effect of type I IFNs. Resistance, that largely stems from the limited up-regulation of the death ligand TRAIL.

Irrespective from the presence or absence of the spontaneous IFN signaling, both cell lines were resistant to IFN-α induced apoptosis. However, the autocrine IFN loop could be responsible also for overcoming the apoptotic resistance to IFNs. In fact, silencing of USP18 was sufficient to allow entrance in apoptosis only in T98G cells. This apoptotic response was largely dependent on TRAIL (Fig. 8). USP18 plays a critical role in limiting temporally and quantitatively TRAIL up-regulation. This negative function of USP18 is evident in both glioblastoma cell

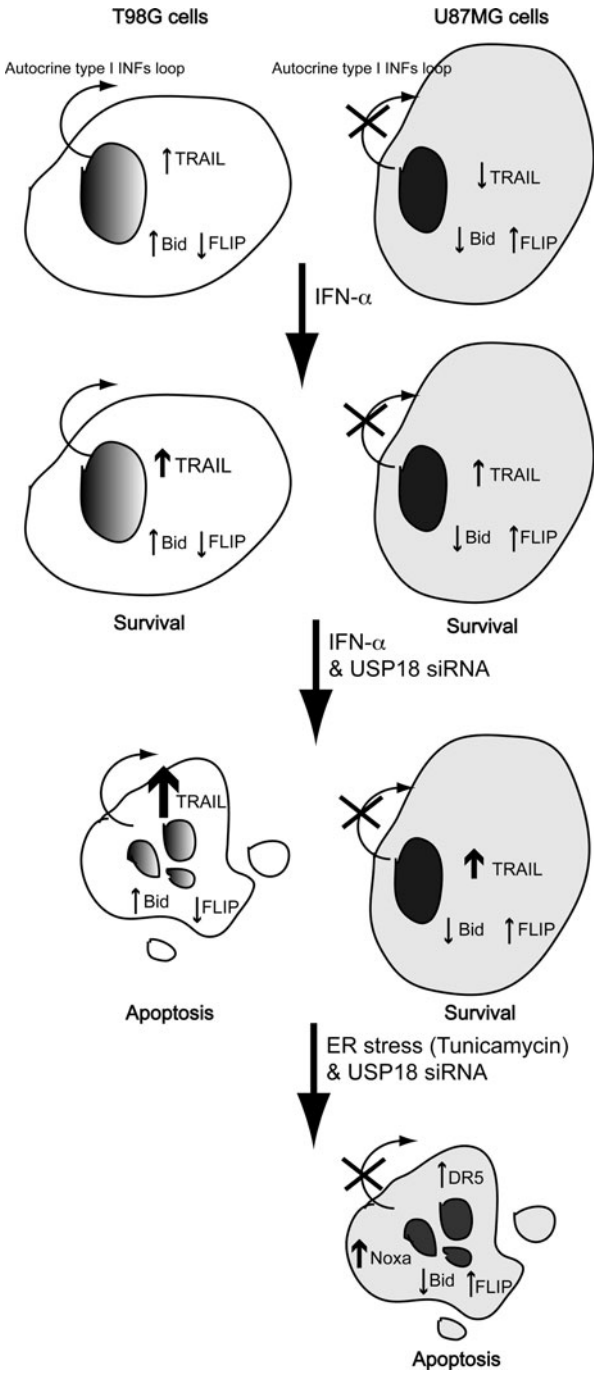

Fig. 8 Summary of the differences in terms of TRAIL up-regulation and responsiveness, between T98G and U87MG glioblastoma cells. T98G cells express higher levels of Bid and TRAIL, whereas U87MG cells show increased amounts of FLIP (*see arrows*). The autocrine loop is defective in U87MG cells. Following IFN-α treatment TRAIL expression is augmented, but at higher levels in T98G cells (*compare arrows*). This increase is insufficient to elicit apoptosis. Combining USP18 silencing and IFN-α treatment raises TRAIL levels to a greater extent, particularly in T98G cells (*larger arrow*) that now die by apoptosis. The increase in TRAIL observed in U87MG cells is insufficient to trigger apoptosis, also because of the low Bid levels and the high FLIP expression. ER stress, as induced by tunicamycin promotes Noxa and DR5 up-regulation, which, in combination with USP18 down-regulation, efficiently promote apoptosis in U87MG cells

lines. However, in U87MG cells TRAIL up-regulation, elicited by the removal of USP18 is less pronounced and insufficient to sustain apoptosis.

In addition to the limited up-regulation of TRAIL, U87MG cells have accumulated alterations in some elements of the extrinsic pathway, including Bid and $FLIP_L$ (Fig. 8). Resistance to TRAIL–induced apoptosis is frequent in glioblastoma [52]. Different studies have evaluated the ability of several treatments and drugs to synergize with TRAIL to kill glioblastoma cells [53–56]. We have identified two compounds: the isopeptidase inhibitor G5 and the inducer of ER-stress tunicamycin, capable of restoring apoptotic sensitivity to TRAIL in U87MG cells.

As previously shown in other models [57, 58], tunicamycin promoted the up-regulation of DR5/TRAIL-R2 and Noxa, which possibly facilitate the induction of apoptosis in response to TRAIL. Up-regulation of DR5/TRAIL-R2 is also the mechanism through which arsenic trioxide abrogates the resistance to TRAIL induced apoptosis in glioblastoma [56].

When tunicamycin was tested in combination with IFN-α, additive effects were not observed. Surprisingly, when USP18 expression was down-regulated tunicamycin alone potently promoted apoptosis but again, addition of IFN-α was irrelevant. It is possible that in a context of activation of the UPR (unfolded protein response), solely the removal of USP18 is sufficient to sustain a full apoptotic response [58].

In conclusion our data provide some explanations for the different apoptotic susceptibility of glioblastoma cells to IFN-α treatment. Moreover, they also establish USP18, as an important target to boost the pro-apoptotic effect of type I IFNs in glioblastoma. Targeting USP18 could be an interesting approach also in glioblastoma showing a stubborn apoptotic resistance, as exemplified by U87MG cells.

Acknowledgments We thank Dr. Zauli and Dr. Secchiero for TRAIL cDNA. This work was supported by grant from AIRC (Associazione Italiana Ricerca sul Cancro IG-10437), MIUR and Regione FVG (AITT-LR25/07). IM is a CIB (Consorzio Interuniversitario Biotecnologie) fellow.

Conflict of interest None.

References

1. Borden EC, Sen GC, Uze G, Silverman RH, Ransohoff RM, Foster GR, Stark GR (2007) Interferons at age 50: past, current and future impact on biomedicine. Nat Rev Drug Discov 6(12):975–990
2. Chawla-Sarkar M, Lindner DJ, Liu YF, Williams BR, Sen GC, Silverman RH, Borden EC (2003) Apoptosis and interferons: role of interferon-stimulated genes as mediators of apoptosis. Apoptosis 8(3):237–249
3. Furnari FB, Fenton T, Bachoo RM, Mukasa A, Stommel JM, Stegh A, Hahn WC, Ligon KL, Louis DN, Brennan C, Chin L, DePinho RA, Cavenee WK (2007) Malignant astrocytic glioma: genetics, biology, and paths to treatment. Genes Dev 21(21): 2683–2710
4. Stewart LA (2002) Chemotherapy in adult high-grade glioma: a systematic review and meta-analysis of individual patient data from 12 randomised trials. Lancet 359(9311):1011–1018
5. Yung WK, Prados M, Levin VA, Fetell MR, Bennett J, Mahaley MS, Salcman M, Etcubanas E (1991) Intravenous recombinant interferon beta in patients with recurrent malignant gliomas: a phase I/II study. J Clin Oncol 9(11):1945–1949
6. Fine HA, Wen PY, Robertson M, O'Neill A, Kowal J, Loeffler JS, Black PM (1997) A phase I trial of a new recombinant human beta-interferon (BG9015) for the treatment of patients with recurrent gliomas. Clin Cancer Res 3(3):381–387
7. Ichimura K, Schmidt EE, Yamaguchi N, James CD, Collins VP (1994) A common region of homozygous deletion in malignant human gliomas lies between the IFN alpha/omega gene cluster and the D9S171 locus. Cancer Res 54(12):3127–3130
8. Dreyling MH, Bohlander SK, Adeyanju MO, Olopade OI (1995) Detection of CDKN2 deletions in tumor cell lines and primary glioma by interphase fluorescence in situ hybridization. Cancer Res 55(5):984–988
9. Olopade OI, Jenkins RB, Ransom DT, Malik K, Pomykala H, Nobori T, Cowan JM, Rowley JD, Diaz MO (1992) Molecular analysis of deletions of the short arm of chromosome 9 in human gliomas. Cancer Res 52(9):2523–2529
10. Lienenklaus S, Cornitescu M, Zietara N, Lyszkiewicz M, Gekara N, Jablonska J, Edenhofer F, Rajewsky K, Bruder D, Hafner M, Staeheli P, Weiss S (2009) Novel reporter mouse reveals constitutive and inflammatory expression of IFN-beta in vivo. J Immunol 183(5):3229–3236
11. Taniguchi T, Takaoka A (2001) A weak signal for strong responses: interferon-alpha/beta revisited. Nat Rev Mol Cell Biol 2(5):378–386
12. Sadler AJ, Williams BR (2008) Interferon-inducible antiviral effectors. Nat Rev Immunol 8(7):559–568
13. Knobeloch KP, Utermohlen O, Kisser A, Prinz M, Horak I (2005) Reexamination of the role of ubiquitin-like modifier ISG15 in the phenotype of UBP43-deficient mice. Mol Cell Biol 25(24): 11030–11034
14. Malakhova OA, Kim KI, Luo JK, Zou W, Kumar KG, Fuchs SY, Shuai K, Zhang DE (2006) UBP43 is a novel regulator of interferon signaling independent of its ISG15 isopeptidase activity. EMBO J 25(11):2358–2367
15. Foti C, Florean C, Pezzutto A, Roncaglia P, Tomasella A, Gustincich S, Brancolini C (2009) Characterization of caspase-dependent and caspase-independent deaths in glioblastoma cells treated with inhibitors of the ubiquitin-proteasome system. Mol Cancer Ther 8(11):3140–3150
16. MacFarlane M, Ahmad M, Srinivasula SM, Fernandes-Alnemri T, Cohen GM, Alnemri ES (1997) Identification and molecular cloning of two novel receptors for the cytotoxic ligand TRAIL. J Biol Chem 272(41):25417–25420
17. Potu H, Sgorbissa A, Brancolini C (2010) Identification of USP18 as an important regulator of the susceptibility to IFN-alpha and drug-induced apoptosis. Cancer Res 70(2):655–665
18. Wagner KW, Punnoose EA, Januario T, Lawrence DA, Pitti RM, Lancaster K, Lee D, von Goetz M, Yee SF, Totpal K, Huw L, Katta V, Cavet G, Hymowitz SG, Amler L, Ashkenazi A (2007) Death-receptor O-glycosylation controls tumor-cell sensitivity to the proapoptotic ligand Apo2L/TRAIL. Nat Med 13(9): 1070–1077
19. Rhodes DR, Kalyana-Sundaram S, Mahavisno V, Varambally R, Yu J, Briggs BB, Barrette TR, Anstet MJ, Kincead-Beal C,

Kulkarni P, Varambally S, Ghosh D, Chinnaiyan AM (2007) Oncomine 3.0: genes, pathways, and networks in a collection of 18, 000 cancer gene expression profiles. Neoplasia 9(2):166–180
20. Saito R, Mizuno M, Hatano M, Kumabe T, Yoshimoto T, Yoshida J (2004) Two different mechanisms of apoptosis resistance observed in interferon-beta induced apoptosis of human glioma cells. J Neurooncol 67(3):273–280
21. Papenfuss K, Cordier SM, Walczak H (2008) Death receptors as targets for anti-cancer therapy. J Cell Mol Med 12(6B):2566–2585
22. Wang Q, Ji Y, Wang X, Evers BM (2000) Isolation and molecular characterization of the 5′-upstream region of the human TRAIL gene. Biochem Biophys Res Commun 276(2):466–471
23. Borden EC (2007) Augmentation of effects of interferon-stimulated genes by reversal of epigenetic silencing: potential application to melanoma. Cytokine Growth Factor Rev 18(5–6):491–501
24. Clarke N, Jimenez-Lara AM, Voltz E, Gronemeyer H (2004) Tumor suppressor IRF-1 mediates retinoid and interferon anticancer signaling to death ligand TRAIL. EMBO J 23(15): 3051–3060
25. Reynes G, Vila V, Martin M, Parada A, Fleitas T, Reganon E, Martinez-Sales V (2011) Circulating markers of angiogenesis, inflammation, and coagulation in patients with glioblastoma. J Neurooncol 102(1):35–41
26. La Ferla-Bruhl K, Westhoff MA, Karl S, Kasperczyk H, Zwacka RM, Debatin KM, Fulda S (2007) NF-kappaB-independent sensitization of glioblastoma cells for TRAIL-induced apoptosis by proteasome inhibition. Oncogene 26(4):571–582
27. Zou W, Yue P, Khuri FR, Sun SY (2008) Coupling of endoplasmic reticulum stress to CDDO-Me-induced up-regulation of death receptor 5 via a CHOP-dependent mechanism involving JNK activation. Cancer Res 68(18):7484–7492
28. Li J, Lee B, Lee AS (2006) Endoplasmic reticulum stress-induced apoptosis: multiple pathways and activation of p53-up-regulated modulator of apoptosis (PUMA) and NOXA by p53. J Biol Chem 281(11):7260–7270
29. Matin SF, Rackley RR, Sadhukhan PC, Kim MS, Novick AC, Bandyopadhyay SK (2001) Impaired alpha-interferon signaling in transitional cell carcinoma: lack of p48 expression in 5637 cells. Cancer Res 61(5):2261–2266
30. Romero-Weaver AL, Wang HW, Steen HC, Scarzello AJ, Hall VL, Sheikh F, Donnelly RP, Gamero AM (2010) Resistance to IFN-alpha-induced apoptosis is linked to a loss of STAT2. Mol Cancer Res 8(1):80–92
31. Du Z, Fan M, Kim JG, Eckerle D, Lothstein L, Wei L, Pfeffer LM (2009) Interferon-resistant Daudi cell line with a Stat2 defect is resistant to apoptosis induced by chemotherapeutic agents. J Biol Chem 284(41):27808–27815
32. Reu FJ, Bae SI, Cherkassky L, Leaman DW, Lindner D, Beaulieu N, MacLeod AR, Borden EC (2006) Overcoming resistance to interferon-induced apoptosis of renal carcinoma and melanoma cells by DNA demethylation. J Clin Oncol 24(23):3771–3779
33. Reu FJ, Leaman DW, Maitra RR, Bae SI, Cherkassky L, Fox MW, Rempinski DR, Beaulieu N, MacLeod AR, Borden EC (2006) Expression of RASSF1A, an epigenetically silenced tumor suppressor, overcomes resistance to apoptosis induction by interferons. Cancer Res 66(5):2785–2793
34. Lesinski GB, Raig ET, Guenterberg K, Brown L, Go MR, Shah NN, Lewis A, Quimper M, Hade E, Young G, Chaudhury AR, Ladner KJ, Guttridge DC, Bouchard P, Carson WE 3rd (2008) IFN-alpha and bortezomib overcome Bcl-2 and Mcl-1 overexpression in melanoma cells by stimulating the extrinsic pathway of apoptosis. Cancer Res 68(20):8351–8360
35. Tracey L, Streck CJ, Du Z, Williams RF, Pfeffer LM, Nathwani AC, Davidoff AM (2010) NF-kappaB activation mediates resistance to IFN beta in MLL-rearranged acute lymphoblastic leukemia. Leukemia 24(4):806–812
36. Sheng Z, Li L, Zhu LJ, Smith TW, Demers A, Ross AH, Moser RP, Green MR (2010) A genome-wide RNA interference screen reveals an essential CREB3L2-ATF5-MCL1 survival pathway in malignant glioma with therapeutic implications. Nat Med 16(6): 671–677
37. Hata N, Sato M, Takaoka A, Asagiri M, Tanaka N, Taniguchi T (2001) Constitutive IFN-alpha/beta signal for efficient IFN-alpha/beta gene induction by virus. Biochem Biophys Res Commun 285(2):518–525
38. Chen HM, Tanaka N, Mitani Y, Oda E, Nozawa H, Chen JZ, Yanai H, Negishi H, Choi MK, Iwasaki T, Yamamoto H, Taniguchi T, Takaoka A (2009) Critical role for constitutive type I interferon signaling in the prevention of cellular transformation. Cancer Sci 100(3):449–456
39. Kulaeva OI, Draghici S, Tang L, Kraniak JM, Land SJ, Tainsky MA (2003) Epigenetic silencing of multiple interferon pathway genes after cellular immortalization. Oncogene 22(26):4118–4127
40. Wei J, Sun Z, Chen Q, Gu J (2006) Serum deprivation induced apoptosis in macrophage is mediated by autocrine secretion of type I IFNs. Apoptosis 11(4):545–554
41. Park SY, Seol JW, Lee YJ, Cho JH, Kang HS, Kim IS, Park SH, Kim TH, Yim JH, Kim M, Billiar TR, Seol DW (2004) IFN-gamma enhances TRAIL-induced apoptosis through IRF-1. Eur J Biochem 271(21):4222–4228
42. Huang Y, Walstrom A, Zhang L, Zhao Y, Cui M, Ye L, Zheng JC (2009) Type I interferons and interferon regulatory factors regulate TNF-related apoptosis-inducing ligand (TRAIL) in HIV-1-infected macrophages. PLoS One 4(4):e5397
43. Ford E, Thanos D (2010) The transcriptional code of human IFN-beta gene expression. Biochim Biophys Acta 1799(3–4):328–336
44. Taniguchi T, Ogasawara K, Takaoka A, Tanaka N (2001) IRF family of transcription factors as regulators of host defense. Annu Rev Immunol 19:623–655
45. Negishi H, Fujita Y, Yanai H, Sakaguchi S, Ouyang X, Shinohara M, Takayanagi H, Ohba Y, Taniguchi T, Honda K (2006) Evidence for licensing of IFN-gamma-induced IFN regulatory factor 1 transcription factor by MyD88 in Toll-like receptor-dependent gene induction program. Proc Natl Acad Sci USA 103(41): 15136–15141
46. Park J, Kim K, Lee EJ, Seo YJ, Lim SN, Park K, Rho SB, Lee SH, Lee JH (2007) Elevated level of SUMOylated IRF-1 in tumor cells interferes with IRF-1-mediated apoptosis. Proc Natl Acad Sci USA 104(43):17028–17033
47. Nozawa H, Oda E, Nakao K, Ishihara M, Ueda S, Yokochi T, Ogasawara K, Nakatsuru Y, Shimizu S, Ohira Y, Hioki K, Aizawa S, Ishikawa T, Katsuki M, Muto T, Taniguchi T, Tanaka N (1999) Loss of transcription factor IRF-1 affects tumor susceptibility in mice carrying the Ha-ras transgene or nullizygosity for p53. Genes Dev 13(10):1240–1245
48. Gao J, Senthil M, Ren B, Yan J, Xing Q, Yu J, Zhang L, Yim JH (2010) IRF-1 transcriptionally upregulates PUMA, which mediates the mitochondrial apoptotic pathway in IRF-1-induced apoptosis in cancer cells. Cell Death Differ 17(4):699–709
49. Nozawa H, Oda E, Ueda S, Tamura G, Maesawa C, Muto T, Taniguchi T, Tanaka N (1998) Functionally inactivating point mutation in the tumor-suppressor IRF-1 gene identified in human gastric cancer. Int J Cancer 77(4):522–527
50. Rhodes DR, Yu J, Shanker K, Deshpande N, Varambally R, Ghosh D, Barrette T, Pandey A, Chinnaiyan AM (2004) ONCOMINE: a cancer microarray database and integrated data-mining platform. Neoplasia 6(1):1–6
51. Smith CL, Hager GL (1997) Transcriptional regulation of mammalian genes in vivo. A tale of two templates. J Biol Chem 272(44):27493–27496
52. Bellail AC, Tse MC, Song JH, Phuphanich S, Olson JJ, Sun SY, Hao C (2010) DR5-mediated DISC controls caspase-8 cleavage

and initiation of apoptosis in human glioblastomas. J Cell Mol Med 14(6A):1303–1317
53. Opel D, Westhoff MA, Bender A, Braun V, Debatin KM, Fulda S (2008) Phosphatidylinositol 3-kinase inhibition broadly sensitizes glioblastoma cells to death receptor- and drug-induced apoptosis. Cancer Res 68(15):6271–6280
54. Fulda S, Wick W, Weller M, Debatin KM (2002) Smac agonists sensitize for Apo2L/TRAIL- or anticancer drug-induced apoptosis and induce regression of malignant glioma in vivo. Nat Med 8(8):808–815
55. Li J, Anderson MG, Tucker LA, Shen Y, Glaser KB, Shah OJ (2009) Inhibition of Aurora B kinase sensitizes a subset of human glioma cells to TRAIL concomitant with induction of TRAIL-R2. Cell Death Differ 16(3):498–511
56. Kim EH, Yoon MJ, Kim SU, Kwon TK, Sohn S, Choi KS (2008) Arsenic trioxide sensitizes human glioma cells, but not normal astrocytes, to TRAIL-induced apoptosis via CCAAT/enhancer-binding protein homologous protein-dependent DR5 up-regulation. Cancer Res 68(1):266–275
57. Jiang CC, Chen LH, Gillespie S, Kiejda KA, Mhaidat N, Wang YF, Thorne R, Zhang XD, Hersey P (2007) Tunicamycin sensitizes human melanoma cells to tumor necrosis factor-related apoptosis-inducing ligand-induced apoptosis by up-regulation of TRAIL-R2 via the unfolded protein response. Cancer Res 67(12): 5880–5888
58. Sun Y, Leaman DW (2005) Involvement of Noxa in cellular apoptotic responses to interferon, double-stranded RNA, and virus infection. J Biol Chem 280(16):15561–15568

RESEARCH PAPER

Cancer Biology & Therapy 14:12, 1–9; December 2013; © 2013 Landes Bioscience

The DeISGylase USP18 limits TRAIL-induced apoptosis through the regulation of TRAIL levels

Cellular levels of TRAIL influences responsiveness to TRAIL-induced apoptosis

Ivana Manini†, Andrea Sgorbissa†, Harish Potu, Andrea Tomasella, and Claudio Brancolini*

Dipartimento di Scienze Mediche e Biologiche and MATI Center of Excellence; Università degli Studi di Udine; Udine, Italy

†These authors contributed equally to this work.

Keywords: IFN-α, TRAIL, USP18, autocrine loop, IFNAR, TRAIL-R2

Tumor necrosis factor (TNF)-related apoptosis-inducing ligand (TRAIL) is a promising molecule for anti-cancer therapies. Unfortunately, cancer cells frequently acquire resistance to rhTRAIL. Various co-treatments have been proposed to overcome apoptosis resistance to TRAIL. Here we show that downregulation of the deISGylase USP18 sensitizes cancer cells to rhTRAIL, whereas, elevate levels of USP18 inhibit TRAIL-induced apoptosis, in a deISGylase independent manner. USP18 influences TRAIL signaling through the control of the IFN autocrine loop. In fact, cells with downregulated USP18 expression augment the expression of cellular TRAIL. Downregulation of cellular TRAIL abrogates the synergism between TRAIL and USP18 siRNA and also limits cell death induced by rhTRAIL. By comparing the apoptotic responsiveness to TRAIL in a panel of cancer cell lines, we have discovered a correlation between TRAIL levels and the apoptotic susceptibility to rhTRAIL, In cells expressing high levels of TRAIL-R2 susceptibility to rhTRAIL correlates with TRAIL expression. In conclusion, we propose that cellular TRAIL is an additional factor that can influence the apoptotic response to rhTRAIL.

Introduction

Tumor necrosis factor (TNF)-related apoptosis-inducing ligand (TRAIL) belongs to the TNF superfamily of extracellular signals. TRAIL has been subjected of intense research because of its specific pro-apoptotic activity against transformed cells.[1] TRAIL is exposed at the surface of many cell types and its expression is stimulated by IFNs.[2,3] Five TRAIL receptors have been identified, of which only two: DR4/TRAIL-R1 and DR5/TRAIL-R2 can engage the extrinsic apoptotic pathway.[4-6]

The resistance to TRAIL induced apoptosis, frequently acquired by cancer cells has limited the therapeutic possibilities of recombinant human TRAIL (rhTRAIL), or agonistic antibodies against its receptors.[1,7] Neoplastic cells adapt different strategies to limit the apoptotic influence of TRAIL including increased expression of: decoy receptors,[8] cFLIP,[9] X-linked inhibitor of apoptosis (XIAP) and of anti-apoptotic Bcl-2 family members.[10-12] Also the engagement of different signaling pathways such as the NFκB and the PI3K/Akt can influence the responsiveness to TRAIL.[13,14]

Several research groups have explored the use of different compounds or treatments to overcome resistance to TRAIL induced apoptosis. A combined approach could represent an ideal therapy to elicit apoptosis in resistant cells.[1,7] Histone deacetylase inhibitors, the proteasome inhibitor bortezomib, or compounds that trigger ER-stress can synergize with TRAIL to kill resistant cells.[15-17] Bortezomib, for example can sustain TRAIL induced apoptosis through multiple mechanisms. In several cancer cells bortezomib can elicit ER-stress, Noxa and DR5 accumulation,[18,19] in glioblastoma cells bortezomib stabilizes the cleaved form of Bid (tBid)[20] and inhibits the NFκB pathway.[21] In malignant B cells it can suppress Bax degradation.[22]

Also interferons can sensitize neoplastic cells to the pro-apoptotic efforts of TRAIL.[23] Moreover, TRAIL is an ISG (interferon stimulated gene), which plays a key role in the apoptotic response to IFNs.[24,25] Hence cells treated with IFN express higher amounts of TRAIL and are more prone to die in response to TRAIL. However, it is unclear whether the boost of TRAIL production sensitizes cells to treatments with exogenous TRAIL.

ISGs production, including TRAIL, in response to IFNs is a timely regulated process that operates through negative feedback loops. The ISG USP18 is an important element of these negative feed-back loops. USP18 is a component of the molecular machinery that modifies protein through the addition of the Ubl protein ISG15.[26] Viral infection and the interferon response elicit

*Correspondence to: Claudio Brancolini; Email: claudio.brancolini@uniud.it
Submitted: 06/28/2013; Revised: 09/17/2013; Accepted: 09/18/2013
http://dx.doi.org/10.4161/cbt.26525

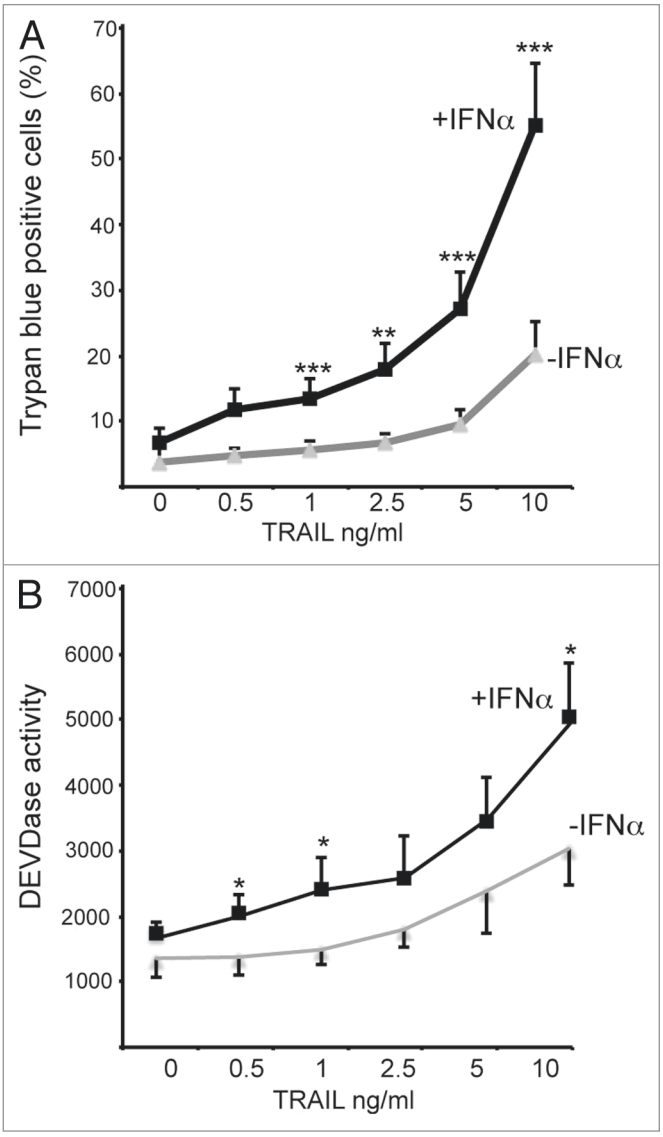

Figure 1. IFN-α pretreatment sensitizes T98G glioblastoma cells to TRAIL-induced apoptosis. (**A**) T98G cells were pre-treated with IFN-α (1000 units/ml). Twelve hours later cells were treated or not, for further 24 h with increasing doses of rhTRAIL as indicated. Cell death was evaluated by trypan blue staining. Columns, mean ($n = 3$); bars, ± SD (**B**) T98G cells were pre-treated with IFN-α. Twelve hours later cells were treated or not, for further 24 h with increasing doses of rhTRAIL as indicated. Apoptosis was evaluated by scoring caspase activity (DEVDase activity).

protein ISGylation through an enzymatic cascade similar to the system for poly-ubiquitination, with dedicated E1, E2, and E3 enzymes.[27] This response is an important piece of the antiviral defense system. USP18 reverse protein ISGylation by removing the conjugated ISG15 from target proteins.[26] In addition to the deISGylase function, USP18 acts as negative regulator of IFN-signaling by suppressing STAT activation.[28]

We have recently identified in USP18 an important regulator of the apoptotic response to interferons and to other pro-death stimuli such as proteasome inhibitors and genotoxic stresses.[29] The pro-survival function of USP18 depends on its ability to buffer the spontaneous interferon signaling. In this manuscript we have investigated the ability of USP18 to modulate TRAIL-induced apoptosis in the glioblastoma cell line T98G. Our data indicate that USP18 limits the apoptotic influence of rhTRAIL.

Results

INF-α pretreatment sensitizes T98G glioblastoma cells to TRAIL-induced apoptosis

T98G glioblastoma cells are susceptible to TRAIL-induced apoptosis and in this cell line is active the spontaneous interferon response.[30] Hence, they represent a good model to investigate the synergisms between TRAIL ad the IFN signaling. To evaluate the effect of the IFN-α treatment on apoptosis responsiveness to TRAIL, T98G cells were treated with IFN-α and next incubated with increasing amounts of rhTRAIL. Cell death was scored by trypan blue staining 24 h later. **Figure 1A** illustrates that pre-treatment with IFN-α sensitizes T98G cells to cell death induced by rhTRAIL. To prove that cell death under the described experimental conditions assumed the characteristic of apoptosis, we also evaluated caspase-3/-7 activation. Also in this case caspase activity in response to TRAIL was augmented in cells pre-incubated with IFN-α (**Fig. 1B**).

USP18 downregulation increases the responsiveness to TRAIL-induced apoptosis

USP18 is a negative regulator of the IFN signaling. Downregulation of USP18 increases apoptosis in response to different stimuli including: DNA damage, inhibition of protein degradation and ER-stress. The pro-survival effect of USP18 is correlated with its function as inhibitor of the spontaneous interferon signaling.[29]

To evaluate whether USP18 can influence TRAIL induced apoptosis we generated T98G cells stably expressing a shRNA specific for USP18. Clones were isolated and treated with IFN-α to evaluate the robustness of silencing. In the isolated clones sh#3 and sh#12, upregulation of USP18 was impaired compared with a clone expressing the control shRNA (**Fig. 2A**). Next we evaluated the apoptotic response to IFN-α treatment. T98G cells with impaired USP18 expression entered cell death after IFN-α treatment, whereas the control cell line was resistant (**Fig. 2B**). Finally we explored whether impaired USP18 expression could augment apoptosis in response to TRAIL treatment. The different cell lines were incubated with increasing amounts of rhTRAIL and cell death was scored 24 h later. **Figure 2C** shows that TRAIL-induced cell death was increased in cells with reduced levels of USP18. The observed cell death assumed the characteristic of apoptosis, as testified by the caspase assay in **Figure 2D**.

USP18 suppresses TRAIL induced apoptosis with a catalysis independent mechanism

USP18 is a cysteine-protease that removes the Ubl protein ISG15, from target proteins. To confirm the influence of USP18 to TRAIL-induced apoptosis and to clarify whether the enzymatic activity of USP18 is required for this outcome, we generated T98G cells stably expressing USP18-wt or the catalytic inactive mutant C64S. After retroviral infection T98G

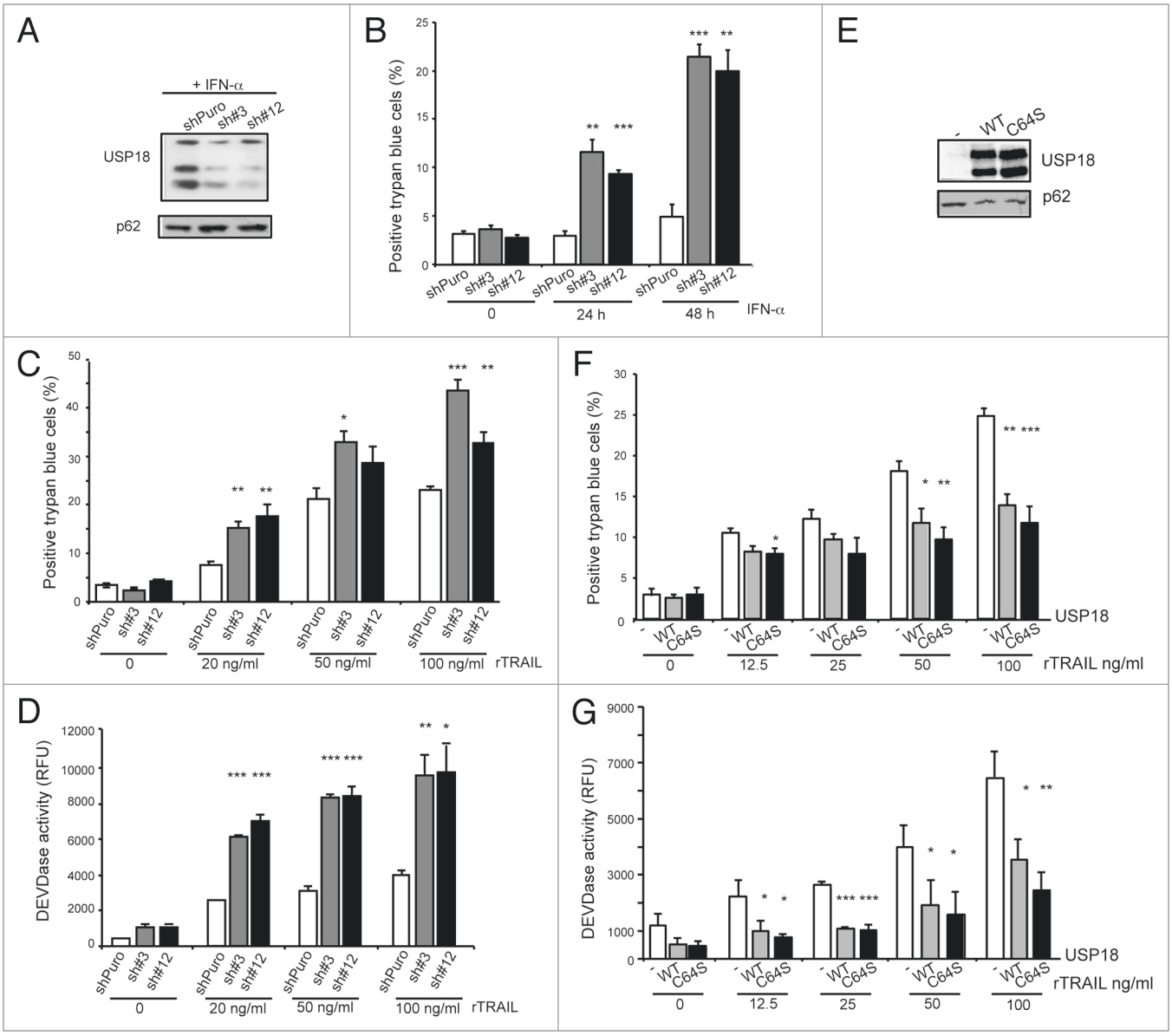

Figure 2. USP18 downregulation increases the responsiveness to TRAIL-induced apoptosis. (**A**) Analysis of the expression levels of USP18 in T98G cells expressing a shRNA against USP18 or a control shRNA (shPuro). Lysates from T98G clones silenced as indicated and treated for 24 h with IFN-α were prepared and subjected to immunoblot analysis using the anti-USP18 antibody. Nucleoporin p62 was used as loading control. (**B**) T98G clones expressing a shRNA against USP18 or a control shRNA (shPuro) were treated or not, for 24 h with IFN-α. Cell death was evaluated by trypan blue staining. (**C**) T98G clones expressing a shRNA against USP18 or a control shRNA (shPuro) were treated or not for 24 h with increasing doses of rhTRAIL. Cell death was evaluated by trypan blue staining. (**D**) T98G clones expressing a shRNA against USP18 or a control shRNA (shPuro) were treated or not for 24 h with increasing doses of rhTRAIL. Apoptosis was evaluated by scoring caspase activity (DEVDase activity). Columns, mean ($n = 3$); bars, ± SD (**E**) Analysis of the expression levels of USP18 in T98G cells expressing USP18-wt, its catalytic inactive mutant USP18-C64S or the resistance gene. Lysates from T98G clones were prepared and subjected to immunoblot analysis using the anti-USP18 antibody. Nucleoporin p62 was used as loading control. (**F**) T98G cells expressing USP18-wt, its catalytic inactive mutant USP18-C64S or the resistance gene were treated or not, for 24 h with increasing doses of rhTRAIL. Cell death was evaluated by trypan blue staining. (**G**) T98G cells expressing USP18-wt, its catalytic inactive mutant USP18-C64S or the resistance gene were treated or not, for 24 h with increasing doses of rhTRAIL. Apoptosis was evaluated by scoring caspase activity (DEVDase activity).

cell lines expressing USP18-wt, its catalytic mutant C64S or the hygromicin resistance gene were isolated (**Fig. 2E**). To evaluate the apoptotic response to rhTRAIL cells were treated with increasing doses of the death ligand (**Fig. 2F**). USP18 was able to limit the apoptotic response to rhTRAIL. Furthermore T98G cells overexpressing USP18 or the C64S mutant were equally resistant to TRAIL induced apoptosis, both in terms of trypan blue assay and of DEVDase activity (**Fig. 2G**). Hence these results confirm that USP18 influences TRAIL induced apoptosis and evidence a deISGylase independent activity.

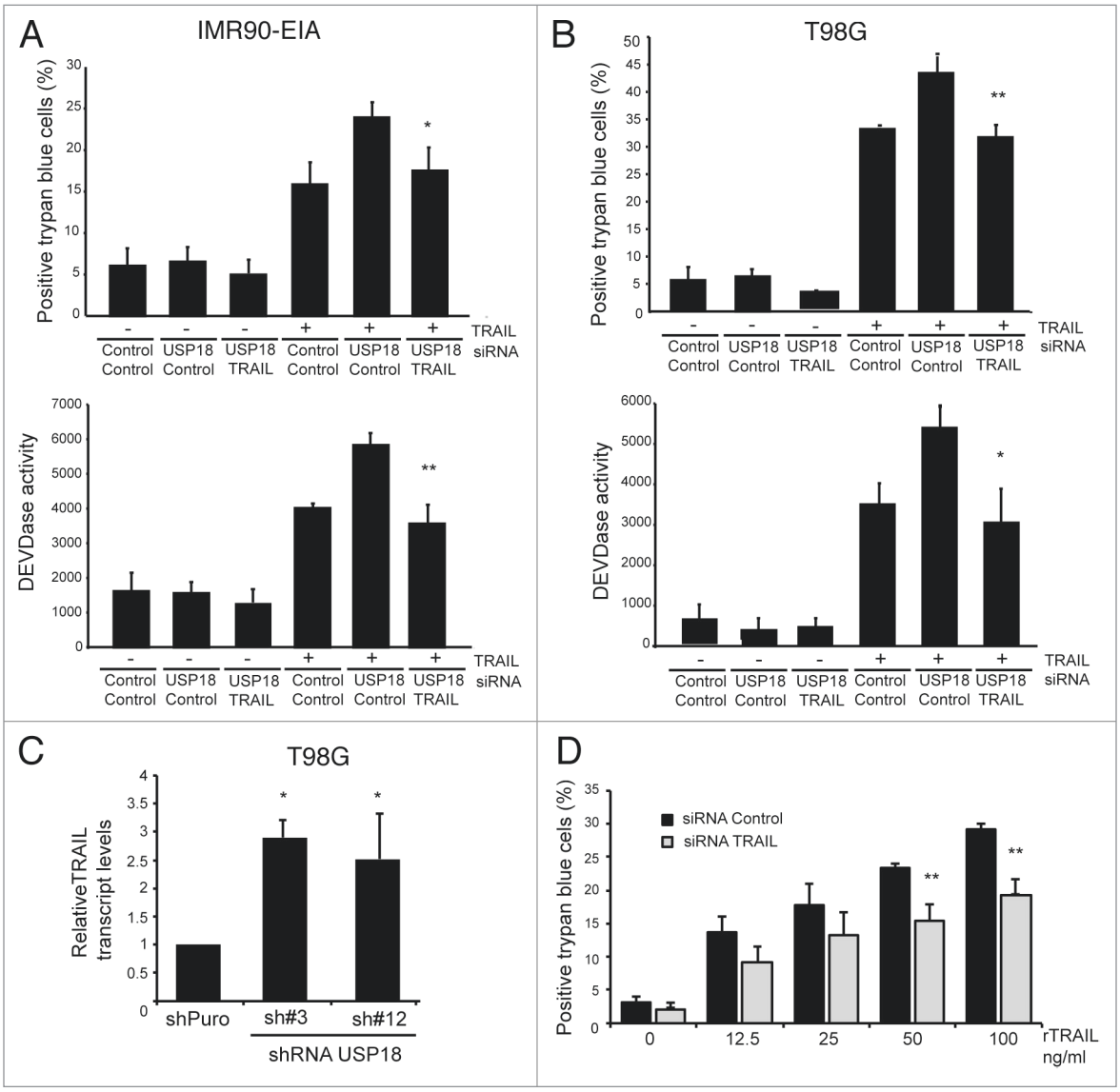

Figure 3. Cellular TRAIL is required to augment the apoptotic response to rhTRAIL in USP18 silenced cells. (**A**) IMR90-E1A cells were transfected with combinations of the three different siRNAs as indicated. Twenty-four hours after transfection, cells were treated or not, for a further 20 h, with rhTRAIL (100 ng/ml). Cell death was scored by trypan blue staining and DEVDase assay. (**B**) T98G cells were transfected with combinations of the three different siRNAs as indicated. Twenty-four hours after transfection, cells were treated or not, for a further 20 h, with rhTRAIL (100 ng/ml). Cell death was scored by trypan blue staining and DEVDase assay. (**C**) USP18-dependent regulation of *TRAIL* mRNAs expression in glioblastoma cells. qRT-PCR analysis was performed to quantify *TRAIL* mRNA in T98G clones expressing the shRNA against USP18 or the control shRNA. Cells were lysed and mRNAs extracted. Samples were normalized as described in MM. (**D**) T98G cells were transfected with a siRNA against TRAIL or a control. Twenty-four hours later cells were treated or not, for 24 h with increasing doses of rhTRAIL. Cell death was evaluated by trypan blue staining.

Cellular TRAIL is required to augment the apoptotic response to rhTRAIL in USP18 silenced cells

In fibroblasts transformed with the oncogene E1A, USP18 can increase the apoptotic susceptibility to different apoptotic stimuli in a TRAIL-dependent manner, by augmenting the spontaneous interferon response.[29] Hence, we decided to explore whether also the improved apoptotic response to rhTRAIL, observed in cells with reduced USP18 expression was dependent on cellular TRAIL. E1A-transformed fibroblasts were co-transfected with two different RNAi specific for USP18 and for TRAIL, or the relative controls (**Fig. 3**).

Downregulation of USP18 augmented cell death and caspase activity in response to rhTRAIL in E1A cells. The simultaneous downregulation of TRAIL abrogated the sensitizing effect of USP18 silencing (**Fig. 3A**).

Similarly, a TRAIL-dependent effect of USP18 downregulation on rhTRAIL-dependent apoptosis was also observed when T98G glioblastoma cells were transiently co-transfected with RNAi specific for USP18 and TRAIL (**Fig. 3B**).

Having confirmed that TRAIL levels can influence rhTRAIL-induced apoptosis we analyzed whether, in T98G cells with downregulated USP18 expression, cellular TRAIL levels were

augmented. qRT-PCR analysis was performed and, as illustrated in **Figure 3C**, expression of TRAIL was increased in cells (sh#3 and sh#12) with reduced USP18 expression.

If the cellular levels of TRAIL, as modulated by USP18 play an important role in sensitizing cells to TRAIL-induced apoptosis, similarly TRAIL-induced apoptosis should be influenced by siRNA against TRAIL, also independently form USP18. Hence, we again took advantage from T98G cells, which express a detectable level of TRAIL and, after downregulating its expression using the specific siRNA (**Fig. 4**), we evaluated the activation of apoptosis in response to rhTRAIL. **Figure 3D** illustrates that downregulation of cellular TRAIL levels impairs apoptosis when is induced by incubation with rhTRAIL.

As a first step to understand how cellular TRAIL can influence TRAIL responsiveness, we analyzed the expression levels of different DISC elements in T98G cells with downregulated TRAIL expression, as obtained by the specific siRNA. **Figure 4** shows that the level of cellular TRAIL does not influence the expression of the tested DISC components.

TRAIL levels correlates with the responsiveness to TRAIL-induced apoptosis

Cancer cells frequently accumulate mutations in pro-apoptotic genes to acquire resistance in the tumor microenvironment. Since our studies have discovered that cellular levels of TRAIL affect the apoptotic response to TRAIL, a correlation between TRAIL expression and resistance to TRAIL-induced cell death should be noted in cancer cell lines.

To explore this possibility, we took advantage from microarray experiments performed by Wagner and co-authors.[31] In their studies cancer cell lines of various origin were clustered on the basis of TRAIL sensitivity, in resistant and sensitive. Next gene expression profiles were acquired in order to unveil the genetic origins of the resistance.[31]

To test for a correlation between TRAIL sensitivity and TRAIL expression levels, we used the robust non-parametric Wilcoxon rank sum test. As is shown in **Figure 5A** the test failed in identifying a correlation between the expression levels of TRAIL and the responsiveness to TRAIL induced apoptosis (**Fig. 5A**). Since the cancer cell lines used in the study are of heterogeneous origin, we also analyzed the data according to the different tissue origin. As shown in **Figure 5B**, when cancer cells were subdivided considering the tissue of origin, there is a slight increase, although not statistically significant, of TRAIL levels in the sensitive compared with the resistant cells. The only exception was noted in the lung cancer cells.

It is well known that alterations in specific elements of the death signaling pathway can confer resistance to TRAIL.[1,7,32] Hence, we reasoned that, being TRAIL the upstream element of the pathway, a correlation between cellular TRAIL levels and the apoptotic susceptibility to rhTRAIL could emerge only when alterations in downstream elements of the extrinsic pathway are not present.

To address this matter, we first analyzed the correlation between the expression levels of several components of the extrinsic apoptotic pathway: TRAIL-R1, TRAIL-R2, TRAIL-R3, TRAIL-R4, OPG, CASP-8, FADD, FLIP, BID,

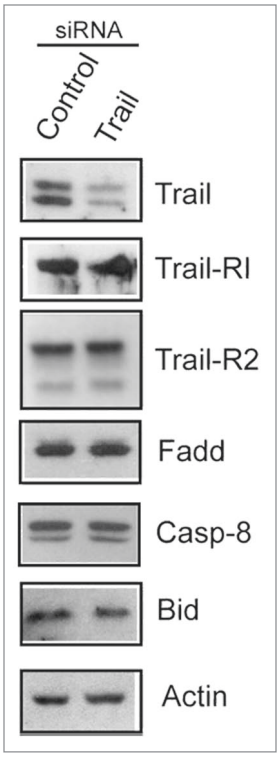

Figure 4. Comparative analysis of DISC components expression in cells silenced for TRAIL. Analysis of the expression levels of the indicated DISC elements in T98G cells transfected with RNAi against TRAIL or control. Lysates were prepared and subjected to immunoblot analysis using the indicated antibodies. Actin was used as loading control.

XIAP, and resistance/sensitivity to TRAIL treatment. We found that only TRAIL-R1, TRAIL-R2, CASP-8, and BID expression correlate significantly with TRAIL sensitivity (**Fig. 5C**).

To explore our assumption, next we focused the attention to cancer cell lines expressing high levels of genes correlated with TRAIL responsiveness (TRAIL-R1, TRAIL-R2, CASP-8, and BID). As a cut-off we selected cancer cells in which the expression levels of these genes were above the median value reached in the susceptible cell lines. The selected cell lines were again subdivided between resistant and susceptible to TRAIL-induced apoptosis.

After these selections, we found that specifically in cells expressing elevated TRAIL-R2 levels, TRAIL expression correlates with sensitivity to rhTRAIL treatment (**Fig. 5D**). This correlation was not observed in cells where the expression of the other critical elements of the extrinsic pathway, namely TRAIL-R1, CASP-8, and BID was above the median of the susceptible sub-population.

Cells expressing high levels of USP18 disconnected from the IFN response show resistance to rhTRAIL induced apoptosis with higher frequency

Finally we decided to evaluate the correlation between USP18 expression levels and the susceptibility to rhTRAIL induced apoptosis in the 111 cell lines of the Wagner data set. Since the IFN response can strengthen TRAIL induced apoptosis, before evaluating the correlation between USP18 and TRAIL sensitivity, it was necessary to explore whether a positive correlation with the

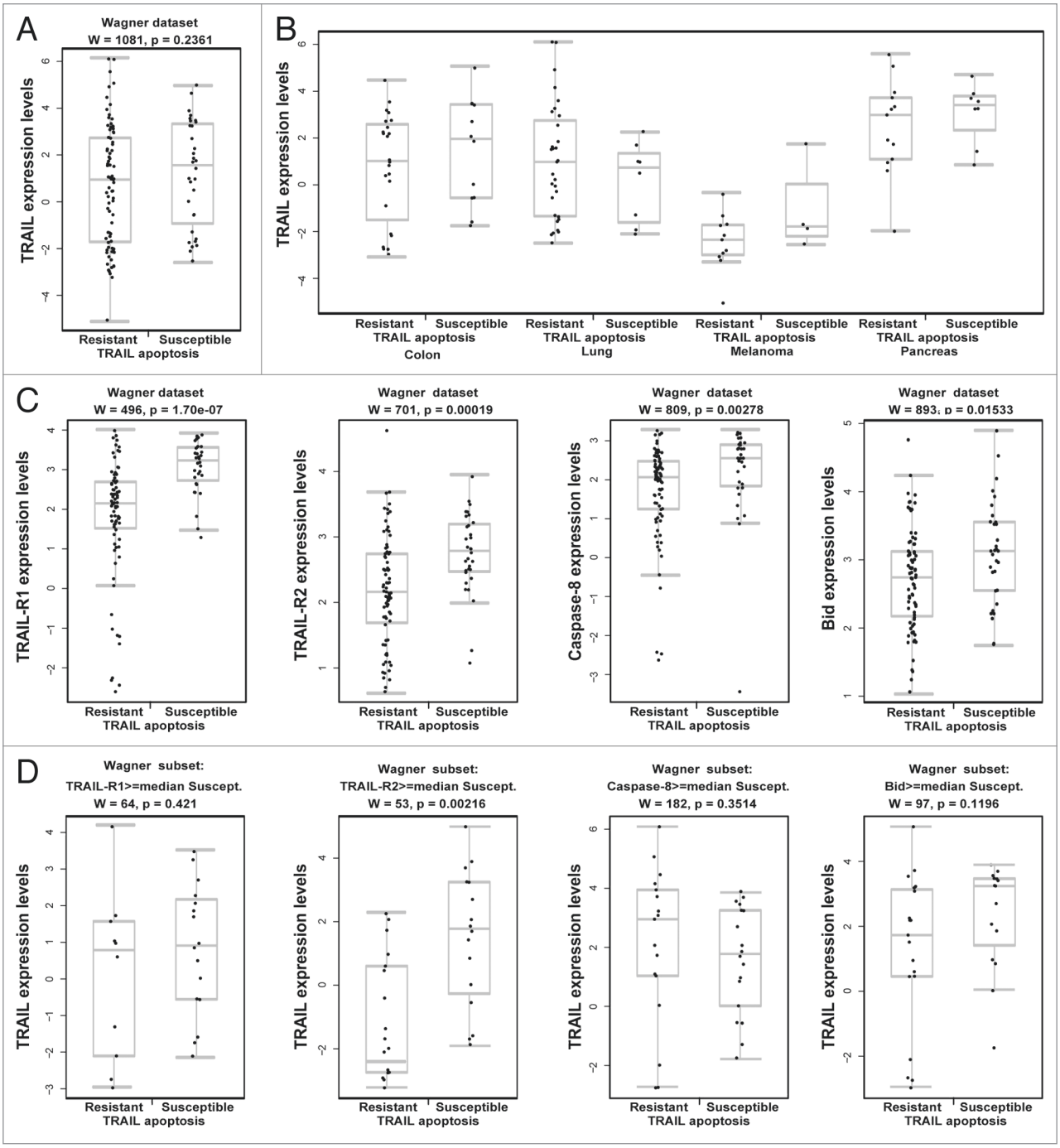

Figure 5. Correlation studies between TRAIL expression and resistance to TRAIL-induced apoptosis. (**A**) Boxplots/stripchart of TRAIL expression levels in cells resistant or susceptible to rhTRAIL induced apoptosis. Data are from the Wagner data set ($n = 111$) excluding the intermediate susceptible cell lines ($n = 8$). (**B**) Same analysis as in (**A**) but data are stratified for cancer tissue origin. Single dots in the stripchart represent individual observations (single cell line array experiments). Dark horizontal lines represent the median, with the box representing the first and third quartiles, the whiskers the maximum and minimum. Values below 1.5 IQR (interquartile range) of the first quartile or above 1.5 IQR of the third quartile are represented as single dots above or below the whiskers. (**C**) Boxplots/stripchart of TRAIL-R1, TRAIL-R2, Caspase-8, and BID expression levels in cells resistant or susceptible to rhTRAIL induced apoptosis. Data are from the Wagner data set ($n = 111$). (**D**) The same as in (**A**) but the analysis was performed with a subset of the Wagner data set in which the expression levels of TRAIL-R1, TRAIL-R2, Caspase-8, and BID, were above or equal to the median of the susceptible sub-population. For every binary comparison resistant vs. susceptible, a Wilcoxon rank sum test was performed and the corresponding W statistic and *P* value were reported.

IFN response could be observed. To monitor the activation of the IFN response, in the different cell lines, we used a signature of 10 IFN-inducible genes, excluding USP18.

As expected, a significant correlation was scored between the expression levels of the IFN signature and apoptosis in response to rhTRAIL (**Fig. 6A**). By contrast USP18 levels in the tested

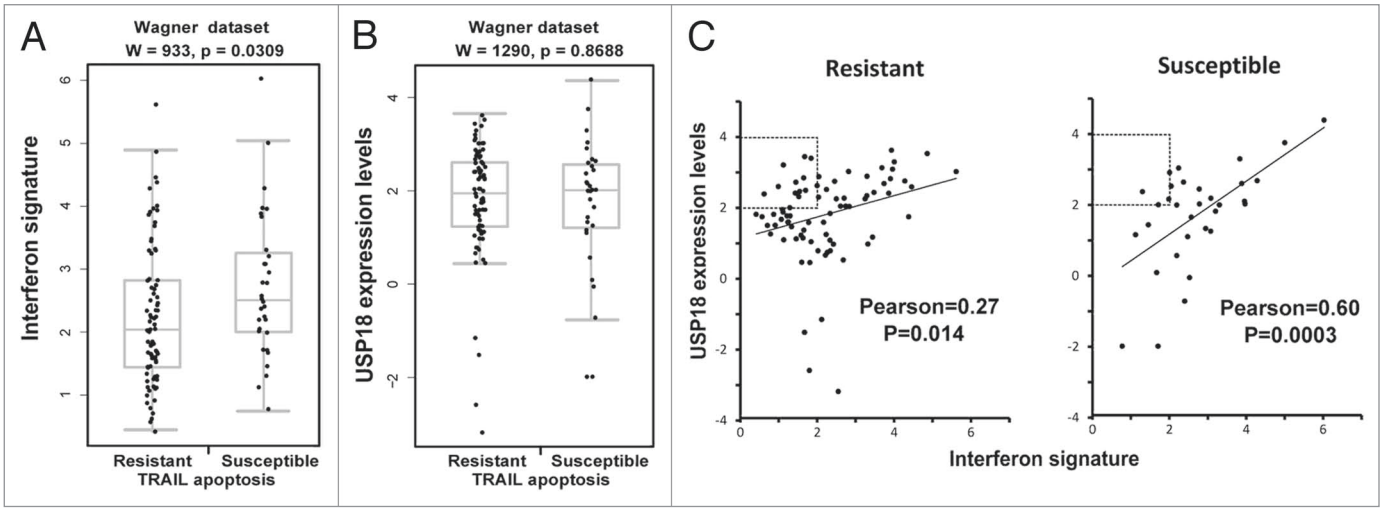

Figure 6. Correlation studies between the IFN response, USP18 expression and resistance to TRAIL-induced apoptosis. (**A**) Boxplots/stripchart of the IFN signature expression in cells resistant or susceptible to rhTRAIL induced apoptosis. The Interferon signature represents the average of the expression levels of 10 interferon-responsive genes (IRF9, ISG15, UBE2L6, UBA7, STAT1, MX1, OAS1, TRAIL, XAF1, and IRF7). Data are from the Wagner data set ($n = 111$). (**B**) Boxplots/stripchart of the USP18 expression levels in cells resistant or susceptible to rhTRAIL induced apoptosis. (**C**) Scatterplot of USP18 expression levels vs. the IFN signature in cell-resistant or -susceptible. The Pearson correlation index for USP18/IFN in the two subpopulations (resistant and susceptible) is reported. The area of the graph highlighted with dotted squares clusters cell lines with high USP18 expression levels and low IFN activation.

cell lines do not correlate with rhTRAIL susceptibility (**Fig. 6B**). This result suggests that in some cells USP18 expression could be disconnected from the IFN response.

Hence, we performed a correlation study between USP18 and the IFN signature in the different cell lines and in relation to rhTRAIL susceptibility. The dot-plot in **Figure 6C** illustrates such analysis and demonstrates that in the susceptible cell lines USP18 expression shows a good correlation with the IFN response (Pearson = 0.60, $P = 0.0003$), whereas in the resistant cells the correlation is much weaker (Pearson = 0.23, $P = 0.014$).

Next we focused our attention on those cell lines, which express high levels of USP18 (expression levels between 2 and 4), in the absence of a robust IFN response (expression levels of IFN signature from 0 to 2). Twelve cell lines (**Fig. 6C**) shared these features and only one entered apoptosis in response to rhTRAIL (8% of the cell lines). By contrast 29% of the 111 cell lines analyzed are responsive to TRAIL-induced apoptosis. Hence we can conclude that USP18 expression, when uncoupled with the IFN response correlates with resistance to rhTRAIL treatment.

Discussion

In this work, by investigating the ability of the deISGylase USP18 to influence rhTRAIL-induced apoptosis, we have discovered a role of the cellular TRAIL in influencing the apoptotic response to rhTRAIL.

It is well known that type I IFNs can sustain the pro-apoptotic activity of TRAIL.[23] We have confirmed this observation and also demonstrated that, through the downregulation of USP18, a negative regulator of the IFN signaling, it is possible to sustain the spontaneous interferon response[29] and to strengthen apoptosis induced by rhTRAIL. Analysis of gene expression profiles in several cancer cell lines corroborated that cells expressing high levels of USP18 exhibit resistance to rhTRAIL-induced apoptosis.

Several studies have proved that TRAIL is an important player of the apoptotic response to IFNs.[24,25] TRAIL itself is an interferon inducible gene.[2] Interestingly, analysis of gene expression signatures from several tumors has revealed that the interferon response is frequently upregulated in cancer. Under the same circumstances expression of TRAIL is instead downregulated, thus possibly limiting the anti-proliferative potency of IFNs.[27]

Surprisingly we have found that TRAIL expression, which is augmented in cells with downregulated USP18 is an important determinant also when apoptosis is triggered by ectopically added rhTRAIL. This conclusion is sustained by the observation that: (1) the simultaneous downregulation of USP18 and TRAIL abrogates the increase in apoptosis in response rhTRAIL, and (2) downregulation of TRAIL alone reduces apoptosis in response to rhTRAIL

By analyzing the gene expression profiles of cancer cells resistant or responsive to rhTRAIL, a statistic significant correlation between TRAIL levels and apoptosis can be evidenced only in cells with elevated levels of TRAIL-R2 expression. This result is not surprisingly since, being TRAIL the uppermost element of the signaling pathway, alterations in the downstream effectors could impair apoptosis also in the presence of elevated levels of cellular TRAIL. Surprisingly the correlation was not observed with TRAIL-R1. Although we cannot exclude that with an enlarged number of samples a correlation could be found also with this receptor. It is important to note that TRAIL-R1 and TRAIL-R2 show some peculiarities. For example for the mechanisms controlling the trafficking to the PM,[33] the recruitment to the membrane rafts[34] and their internalization.

Since TRAIL-R2, compared with TRAIL-R1 is internalized with lower frequency[32,35] it could be argued that a complex among cellular TRAIL and TRAIL-R2 could be more stable and could facilitate the activity of rhTRAIL.

Several additional hypotheses could be formulated about the mechanisms through which cellular TRAIL influences TRAIL-induced apoptosis. Cellular TRAIL could interact with and engage DRs that are not exposed at the cell surface[36] or it can promote with stronger potency the re-localization into the membrane rafts.[37] Certainly, we can exclude that cellular TRAIL can influence the expression levels of the major DISC components. Finally cellular TRAIL could engage additional signaling pathways thus influencing responsiveness to rhTRAIL.

In conclusion in this manuscript, by investigating the role of USP18 in the apoptotic response to TRAIL, we have discovered an important contribution of cellular TRAIL in the apoptotic response to rhTRAIL. Further studies are necessary to define the specific molecular events that are influenced by cellular TRAIL, which are responsible for increase apoptotic responsiveness.

Materials and Methods

Cell culture and apoptosis

T98G and IMR90-E1A were propagated in the Dulbecco's modified Eagle medium supplemented with L-glutamine (2 mM), penicillin (100 U/ml), streptomycin (100 µg/ml), and 10% fetal bovine serum at 37 °C in 5% CO_2, as previously described.[29,38] Stealth RNA interference RNAi for USP18, TRAIL, and non-targeting shRNA were purchased from Invitrogen. Cells were transfected 24 h after plating by adding the medium OptiMem, containing Lipofectamine 2000 (Invitrogen) plus the stealth RNAi oligos. IFN-α2a (Jena Bioscience) was used at 1000 units/ml, final concentration. In all trypan blue exclusion assays, 400 cells from three independent samples were counted for each data point. Data were represented as arithmetic mean ± SD for at least three independent experiments. The DEVDase activity was evaluated using the Apo-ONE assay (Promega). For experimental data the Student t-test was employed. $P < 0.05$ was chosen as statistical limit of significance. We marked with $^{*}P < 0.05$, $^{**}P < 0.01$, and $^{***}P < 0.001$. Unless otherwise indicated, all the data in the figures were represented as arithmetic mean ± SD of at least three independent experiments.

Generation of T98G cells stably expressing USP18-wt, USP18C64S or USP18shRNA

The USP18 point mutant C64S[29] was cloned into a pLPC retroviral vector. USP18shRNA and non-targeting control shRNA were obtained by cloning double stranded oligos into the pSUPER.retro puro, retroviral vector, purchased from OligoEngine. Retroviral supernatants were produced after transfection of 293T packaging cell line, using the calcium phosphate method. At 72 h after transfection, viral supernatants were collected, filtered by 0.45 µm filter and used as medium to infect target cells, after addition of 8 µg/ml polybrene. The infected cells were incubated at 32 °C for 24 h and selected with puromycin (1 µg/ml), until the formation of single clones.

Immunoblotting

Proteins obtained after an SDS denaturating lysis and sonication were transferred to a 0.2 µm pore sized nitro-cellulose membrane (Schleicher and Schuell) using a semidry blotting apparatus (Amersham Pharmacia Biotech) (transfer buffer: 20% methanol, 48 mM Tris, 39 mM glycine, and 0.0375% SDS). The nitrocellulose membranes were saturated for 1 h in Blotto-Tween 20 (50 mM Tris-HCl, pH 7.5, 200 mM NaCl, 5% nonfat dry milk, and 0.1% Tween 20) and incubated overnight at room temperature using the primary antibodies. Membranes were then rinsed three times with Blotto-Tween 20 and incubated with peroxidase-conjugated goat anti-rabbit (Sigma) or goat anti-mouse (Sigma) for 1 h at room temperature. After 4 washes by Blotto-Tween 20, the membranes were rinsed in phosphate buffered saline and developed with Super Signal West Pico, as recommended by the vendor (Pierce).

Quantitative reverse transcription-PCR

cDNAs were synthesized from 1 µg of total RNA, obtained by Trizol (Invitrogen) extraction, using the First-Strand cDNA Synthesis kit (Invitrogen). Real-time PCR was performed using the KAPA SYBR® FAST Master Mix (Kapabiosytems) on a CFX96 Real-Time System (Bio-Rad). The obtained data were analyzed using the ΔΔCt method. The geometric average of HPRT1 (hypoxanthine phosphoribosyltransferase 1) GAPDH and ACTB (β-actin) was used for normalization. Data were expressed as fold change from the T98G cells expressing the control shRNA.

Bioinformatic analysis

For gene arrays analysis the free software R with the GEOquery package for downloading gene expression data from Geo portal (http://www.ncbi.nlm.nih.gov/geo) was used. In the case of multiple probe set for a given gene the best probe set was selected using the PLANdbAffy database.[39] The calculation of the Wilcoxon test P values, the graphics, and all the following analysis were also performed with R.

Disclosure of Potential Conflicts of Interest

No potential conflicts of interest were disclosed.

Acknowledgments

This work was supported by AIRC (IG-10437) and FIRB (Progetto RBAP11S8C3_002). IM was supported by CIB and Talents (Area science park Trieste) fellowships.

References

1. Dimberg LY, Anderson CK, Camidge R, Behbakht K, Thorburn A, Ford HL. On the TRAIL to successful cancer therapy? Predicting and counteracting resistance against TRAIL-based therapeutics. Oncogene 2013; 32:1341-50; PMID:22580613; http://dx.doi.org/10.1038/onc.2012.164
2. Kayagaki N, Yamaguchi N, Nakayama M, Eto H, Okumura K, Yagita H. Type I interferons (IFNs) regulate tumor necrosis factor-related apoptosis-inducing ligand (TRAIL) expression on human T cells: A novel mechanism for the antitumor effects of type I IFNs. J Exp Med 1999; 189:1451-60; PMID:10224285; http://dx.doi.org/10.1084/jem.189.9.1451
3. Allen JE, El-Deiry WS. Regulation of the human TRAIL gene. Cancer Biol Ther 2012; 13:1143-51; PMID:22892844; http://dx.doi.org/10.4161/cbt.21354
4. Pan G, O'Rourke K, Chinnaiyan AM, Gentz R, Ebner R, Ni J, Dixit VM. The receptor for the cytotoxic ligand TRAIL. Science 1997; 276:111-3; PMID:9082980; http://dx.doi.org/10.1126/science.276.5309.111

5. MacFarlane M, Ahmad M, Srinivasula SM, Fernandes-Alnemri T, Cohen GM, Alnemri ES. Identification and molecular cloning of two novel receptors for the cytotoxic ligand TRAIL. J Biol Chem 1997; 272:25417-20; PMID:9325248; http://dx.doi.org/10.1074/jbc.272.41.25417
6. Walczak H, Degli-Esposti MA, Johnson RS, Smolak PJ, Waugh JY, Boiani N, Timour MS, Gerhart MJ, Schooley KA, Smith CA, et al. TRAIL-R2: a novel apoptosis-mediating receptor for TRAIL. EMBO J 1997; 16:5386-97; PMID:9311998; http://dx.doi.org/10.1093/emboj/16.17.5386
7. Pintzas A, Zhivotovsky B, Workman P, Clarke PA, Linardopoulos S, Martinou JC, Lacal JC, Robine S, Nasioulas G, Andera L. Sensitization of (colon) cancer cells to death receptor related therapies: a report from the FP6-ONCODEATH research consortium. Cancer Biol Ther 2012; 13:458-66; PMID:22406997; http://dx.doi.org/10.4161/cbt.19600
8. Pan G, Ni J, Wei YF, Yu G, Gentz R, Dixit VM. An antagonist decoy receptor and a death domain-containing receptor for TRAIL. Science 1997; 277:815-8; PMID:9242610; http://dx.doi.org/10.1126/science.277.5327.815
9. Irmler M, Thome M, Hahne M, Schneider P, Hofmann K, Steiner V, Bodmer JL, Schröter M, Burns K, Mattmann C, et al. Inhibition of death receptor signals by cellular FLIP. Nature 1997; 388:190-5; PMID:9217161; http://dx.doi.org/10.1038/40657
10. Cummins JM, Kohli M, Rago C, Kinzler KW, Vogelstein B, Bunz F. X-linked inhibitor of apoptosis protein (XIAP) is a nonredundant modulator of tumor necrosis factor-related apoptosis-inducing ligand (TRAIL)-mediated apoptosis in human cancer cells. Cancer Res 2004; 64:3006-8; PMID:15126334; http://dx.doi.org/10.1158/0008-5472.CAN-04-0046
11. Fulda S, Meyer E, Debatin KM. Inhibition of TRAIL-induced apoptosis by Bcl-2 overexpression. Oncogene 2002; 21:2283-94; PMID:11948412; http://dx.doi.org/10.1038/sj.onc.1205258
12. Sun SY, Yue P, Zhou JY, Wang Y, Choi Kim HR, Lotan R, Wu GS. Overexpression of BCL2 blocks TNF-related apoptosis-inducing ligand (TRAIL)-induced apoptosis in human lung cancer cells. Biochem Biophys Res Commun 2001; 280:788-97; PMID:11162590; http://dx.doi.org/10.1006/bbrc.2000.4218
13. Ehrhardt H, Fulda S, Schmid I, Hiscott J, Debatin KM, Jeremias I. TRAIL induced survival and proliferation in cancer cells resistant towards TRAIL-induced apoptosis mediated by NF-kappaB. Oncogene 2003; 22:3842-52; PMID:12813457; http://dx.doi.org/10.1038/sj.onc.1206520
14. Xu J, Zhou JY, Wei WZ, Wu GS. Activation of the Akt survival pathway contributes to TRAIL resistance in cancer cells. PLoS One 2010; 5:e10226; PMID:20419107; http://dx.doi.org/10.1371/journal.pone.0010226
15. Jiang CC, Chen LH, Gillespie S, Kiejda KA, Mhaidat N, Wang YF, Thorne R, Zhang XD, Hersey P. Tunicamycin sensitizes human melanoma cells to tumor necrosis factor-related apoptosis-inducing ligand-induced apoptosis by up-regulation of TRAIL-R2 via the unfolded protein response. Cancer Res 2007; 67:5880-8; PMID:17575157; http://dx.doi.org/10.1158/0008-5472.CAN-07-0213
16. Johnson TR, Stone K, Nikrad M, Yeh T, Zong WX, Thompson CB, Nesterov A, Kraft AS. The proteasome inhibitor PS-341 overcomes TRAIL resistance in Bax and caspase 9-negative or Bcl-xL overexpressing cells. Oncogene 2003; 22:4953-63; PMID:12902978; http://dx.doi.org/10.1038/sj.onc.1206656
17. Inoue H, Shiraki K, Ohmori S, Sakai T, Deguchi M, Yamanaka T, Okano H, Nakano T. Histone deacetylase inhibitors sensitize human colonic adenocarcinoma cell lines to TNF-related apoptosis inducing ligand-mediated apoptosis. Int J Mol Med 2002; 9:521-5; PMID:11956660
18. Aleo E, Henderson CJ, Fontanini A, Solazzo B, Brancolini C. Identification of new compounds that trigger apoptosome-independent caspase activation and apoptosis. Cancer Res 2006; 66:9235-44; PMID:16982768; http://dx.doi.org/10.1158/0008-5472.CAN-06-0702
19. Liu X, Yue P, Chen S, Hu L, Lonial S, Khuri FR, Sun SY. The proteasome inhibitor PS-341 (bortezomib) up-regulates DR5 expression leading to induction of apoptosis and enhancement of TRAIL-induced apoptosis despite up-regulation of c-FLIP and survivin expression in human NSCLC cells. Cancer Res 2007; 67:4981-8; PMID:17510429; http://dx.doi.org/10.1158/0008-5472.CAN-06-4274
20. Unterkircher T, Cristofanon S, Vellanki SH, Nonnenmacher L, Karpel-Massler G, Wirtz CR, Debatin KM, Fulda S. Bortezomib primes glioblastoma, including glioblastoma stem cells, for TRAIL by increasing tBid stability and mitochondrial apoptosis. Clin Cancer Res 2011; 17:4019-30; PMID:21525171; http://dx.doi.org/10.1158/1078-0432.CCR-11-0075
21. Jane EP, Premkumar DR, Pollack IF. Bortezomib sensitizes malignant human glioma cells to TRAIL, mediated by inhibition of the NF-kappaB signaling pathway. Mol Cancer Ther 2011; 10:198-208; PMID:21220502; http://dx.doi.org/10.1158/1535-7163.MCT-10-0725
22. Liu FT, Agrawal SG, Gribben JG, Ye H, Du MQ, Newland AC, Jia L. Bortezomib blocks Bax degradation in malignant B cells during treatment with TRAIL. Blood 2008; 111:2797-805; PMID:18160669; http://dx.doi.org/10.1182/blood-2007-08-110445
23. Chawla-Sarkar M, Leaman DW, Jacobs BS, Borden EC. IFN-beta pretreatment sensitizes human melanoma cells to TRAIL/Apo2 ligand-induced apoptosis. J Immunol 2002; 169:847-55; PMID:12097388
24. Borden EC, Sen GC, Uze G, Silverman RH, Ransohoff RM, Foster GR, Stark GR. Interferons at age 50: past, current and future impact on biomedicine. Nat Rev Drug Discov 2007; 6:975-90; PMID:18049472; http://dx.doi.org/10.1038/nrd2422
25. Chawla-Sarkar M, Lindner DJ, Liu YF, Williams BR, Sen GC, Silverman RH, Borden EC. Apoptosis and interferons: role of interferon-stimulated genes as mediators of apoptosis. Apoptosis 2003; 8:237-49; PMID:12766484; http://dx.doi.org/10.1023/A:1023668705040
26. Malakhov MP, Malakhova OA, Kim KI, Ritchie KJ, Zhang DE. UBP43 (USP18) specifically removes ISG15 from conjugated proteins. J Biol Chem 2002; 277:9976-81; PMID:11788588; http://dx.doi.org/10.1074/jbc.M109078200
27. Sgorbissa A, Brancolini C. IFNs, ISGylation and cancer: Cui prodest? Cytokine Growth Factor Rev 2012; 23:307-14; PMID:22906767; http://dx.doi.org/10.1016/j.cytogfr.2012.07.003
28. Malakhova OA, Kim KI, Luo JK, Zou W, Kumar KG, Fuchs SY, Shuai K, Zhang DE. UBP43 is a novel regulator of interferon signaling independent of its ISG15 isopeptidase activity. EMBO J 2006; 25:2358-67; PMID:16710296; http://dx.doi.org/10.1038/sj.emboj.7601149
29. Potu H, Sgorbissa A, Brancolini C. Identification of USP18 as an important regulator of the susceptibility to IFN-alpha and drug-induced apoptosis. Cancer Res 2010; 70:655-65; PMID:20068173; http://dx.doi.org/10.1158/0008-5472.CAN-09-1942
30. Foti C, Florean C, Pezzutto A, Roncaglia P, Tomasella A, Gustincich S, Brancolini C. Characterization of caspase-dependent and caspase-independent deaths in glioblastoma cells treated with inhibitors of the ubiquitin-proteasome system. Mol Cancer Ther 2009; 8:3140-50; PMID:19887551; http://dx.doi.org/10.1158/1535-7163.MCT-09-0431
31. Wagner KW, Punnoose EA, Januario T, Lawrence DA, Pitti RM, Lancaster K, Lee D, von Goetz M, Yee SF, Totpal K, et al. Death-receptor O-glycosylation controls tumor-cell sensitivity to the proapoptotic ligand Apo2L/TRAIL. Nat Med 2007; 13:1070-7; PMID:17767167; http://dx.doi.org/10.1038/nm1627
32. Pennarun B, Meijer A, de Vries EG, Kleibeuker JH, Kruyt F, de Jong S. Playing the DISC: turning on TRAIL death receptor-mediated apoptosis in cancer. Biochim Biophys Acta 2010; 1805:123-40; PMID:19961901
33. Oh Y, Jeon YJ, Hong GS, Kim I, Woo HN, Jung YK. Regulation in the targeting of TRAIL receptor 1 to cell surface via GODZ for TRAIL sensitivity in tumor cells. Cell Death Differ 2012; 19:1196-207; PMID:22240897; http://dx.doi.org/10.1038/cdd.2011.209
34. Xiao W, Ishdorj G, Sun J, Johnston JB, Gibson SB. Death receptor 4 is preferentially recruited to lipid rafts in chronic lymphocytic leukemia cells contributing to tumor necrosis related apoptosis inducing ligand-induced synergistic apoptotic responses. Leuk Lymphoma 2011; 52:1290-301; PMID:21699383; http://dx.doi.org/10.3109/10428194.2011.567317
35. Cheng J, Hylander BL, Baer MR, Chen X, Repasky EA. Multiple mechanisms underlie resistance of leukemia cells to Apo2 Ligand/TRAIL. Mol Cancer Ther 2006; 5:1844-53; PMID:16891471; http://dx.doi.org/10.1158/1535-7163.MCT-06-0050
36. Chen JJ, Shen HC, Rivera Rosado LA, Zhang Y, Di X, Zhang B. Mislocalization of death receptors correlates with cellular resistance to their cognate ligands in human breast cancer cells. Oncotarget 2012; 3:833-42; PMID:22909995
37. Song JH, Tse MC, Bellail A, Phuphanich S, Khuri F, Kneteman NM, Hao C. Lipid rafts and nonrafts mediate tumor necrosis factor related apoptosis-inducing ligand induced apoptotic and nonapoptotic signals in non small cell lung carcinoma cells. Cancer Res 2007; 67:6946-55; PMID:17638906; http://dx.doi.org/10.1158/0008-5472.CAN-06-3896
38. Sgorbissa A, Tomasella A, Potu H, Manini I, Brancolini C. Type I IFNs signaling and apoptosis resistance in glioblastoma cells. Apoptosis 2011; 16:1229-44; PMID:21858676; http://dx.doi.org/10.1007/s10495-011-0639-4
39. Nurtdinov RN, Vasiliev MO, Ershova AS, Lossev IS, Karyagina AS. PLANdbAffy: probe-level annotation database for Affymetrix expression microarrays. Nucleic Acids Res 2010; 38(Database issue):D726-30; PMID:19906711; http://dx.doi.org/10.1093/nar/gkp969